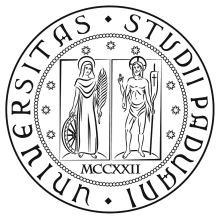

UNIVERSITÀ DEGLI STUDI DI PADOVA

DIPARTIMENTO DI INGEGNERIA INDUSTRIALE

CORSO DI LAUREA MAGISTRALE IN
INGEGNERIA CHIMICA E DEI PROCESSI INDUSTRIALI

Tesi di Laurea Magistrale in
Ingegneria Chimica e dei Processi Industriali

Development of an online model-based flow assurance application to operate subsea natural gas pipeline networks

Relatore: Prof. Fabrizio Bezzo
Correlatori: Dr. Apostolos Giovanoglou
Dr. Javier Rodriguez

Laureando: MATTEO TREVISAN

Anno accademico 2016/2017

"When a man is tired of London, he is tired of life;
for there is in London all that life can afford."
Dr. Samuel Johnson

Abstract

Natural gas is a hydrocarbon mixture which is usually found in nature in underground reservoirs, many of which are located offshore. The cheapest and most common way to transport the extracted gas is via a subsea pipeline network. Due to the impossibility to operate subsea measurement systems one has to rely on simulations, and therefore modelling accurately the fluctuating conditions of gas mixtures coming from different branches of the network is crucial to obtain a stable operation and avoid threats to the downstream processing facility. The use of a high-fidelity process simulator allows to simulate the network dynamically, thus obtaining meaningful information on the conditions of the fluid in each pipeline, and predicting its possible condensation, which undermines the stability of the whole network. The validation of the model has been done using data coming from an existing natural gas pipeline network. The results show a remarkable accuracy, and a significantly low computational time has been achieved. However, some trade-offs need to be considered in order to have an efficient model which can be applied online.

Process Systems Enterprise Ltd (London, UK) is gratefully acknowledged for the professional, financial and human support.

Riassunto

Il gas naturale è una miscela di idrocarburi, prevalentemente metano, che si trova in natura sotto diverse forme o può essere prodotta a partire da svariate materie prime organiche. Uno dei metodi più diffusi è l'estrazione da giacimenti sotterranei del gas, che può essere presente in miscela con petrolio o carbone. Altre forme non convenzionali di estrazione di gas naturale sono in continua espansione. In seguito all'estrazione il gas deve essere purificato in specifici impianti e trasportato all'utilizzatore. Il modo più economico di trasportare il gas naturale dal luogo di produzione all'impianto di purificazione è solitamente tramite tubazioni. In alternativa, il gas può essere liquefatto a basse temperature, e trasportato in apposite cisterne criogeniche.

Numerosi giacimenti di gas naturale sono sottomarini, a centinaia di chilometri dalla costa (dove solitamente si trova l'impianto di trattamento). Questo rappresenta un limite all'estrazione del gas, poichè aumenta le difficoltà e i costi operativi. Il gas estratto dal giacimento (il quale solitamente è sfruttato da diversi pozzi e piattaforme) può essere trasportato all'impianto di purificazione tramite reti (network) di tubazioni sottomarine, o utilizzando navi metaniere. La scelta tra queste due alternative è basata sul costo di trasporto, il quale dipende principalmente dalla distanza che il gas deve compiere, ma può coivolgere anche considerazioni di natura geopolitica.

Mentre il monitoraggio di tubazioni terrestri è relativamente facile, sistemi di misura sottomarini sono estremamente costosi e difficili da operare, perciò nella pratica non vengono mai utilizzati. Per questo motivo, l'unico modo per controllare un network sottomarino è di affidarsi ad un software che generi predizioni riguardo alle condizioni operative delle tubazioni. Modellare accuratamente le condizioni del network in tempo reale è fondamentale per ottenere dati significativi sulle condizioni con cui il gas arriva all'impianto di purificazione, in modo da evitare possibili minacce alla stabilità e sicurezza con cui esso deve operare. Questo ramo del settore Oil & Gas viene comunemente chiamato *flow assurance*.

gPROMS® ProcessBuilder è un simulatore di processo dinamico avanzato, sviluppato da *Process Systems Enterprise Ltd*, il quale grazie alla propria versatilità ha le potenzialità per modellare accuratamente un network di tubazioni. Il modello di tubazione utilizzato è *Pipeline single-phase gML*, nel quale sono implementati i bilanci dinamici di materia, energia e quantità di moto per un fluido multicomponente monofasico. Il modello è distribuito nella direzione assiale, e considera perciò le variazioni delle proprietà con l'avanzamento nella tubazione. Esso include una *flag* che segnala il possibile moto multifasico (cioè la condensazione parziale del liquido), senza però modellarne accuratamente il regime. Il modello termodinamico scelto dopo un'accurata validazione e analisi di sensitività sui

tempi computazionali è l'equazione di stato di Peng-Robinson, sebbene sia meno accurata se comparata ad altri modelli quale l'equazione di stato GERG-2008. Per questo motivo durante tutto lo svolgimento del progetto si è sempre considerata la possibilità di utilizzare la GERG-2008 qualora i suoi tempi computazionali risultino accettabili e tali da poter considerare l'applicazione *online* (avente quindi risultati analizzabili in tempo reale durante l'operazione del network).

Il modello è stato validato utilizzando dati provenienti da un network esistente. Le simulazioni mostrano risultati soddisfacenti in termini di accuratezza e tempi computazionali. Tuttavia, alcuni compromessi che ne diminuiscono l'accuratezza devono essere utilizzati al fine di considerare la possibilità di un'applicazione *online*.

Contents

Introduction **1**

1 Literature review **3**
1.1 Natural gas . . . 3
1.1.1 Background . . . 3
1.1.2 Transport . . . 4
1.1.3 Forecasts . . . 6
1.2 Flow assurance and pipeline modelling . . . 8
1.2.1 Different approaches . . . 8
1.2.2 The company's choices . . . 9
1.2.3 Single-phase dynamic pipeline model . . . 10

2 Software and tools **15**
2.1 gPROMS® ProcessBuilder . . . 15
2.1.1 Equation-oriented approach . . . 15
2.1.2 Dynamic simulations and pressure-driven mode . . . 16
2.1.3 gML models . . . 17
2.2 The *Pipeline single-phase gML* model . . . 18
2.2.1 Conservation equations . . . 18
2.2.2 Heat transfer modelling . . . 19
2.2.3 Discretisation and other features . . . 22

3 Natural gas thermodynamics **25**
3.1 Phase behaviour and definitions . . . 25
3.1.1 Phase diagram . . . 25
3.1.2 Retrograde condensation . . . 27
3.2 Thermodynamic models . . . 28
3.2.1 Soave-Redlich-Kwong Equation of State . . . 28
3.2.2 Peng-Robinson Equation of State . . . 29
3.2.3 GERG-2008 Equation of State . . . 30
3.3 Choice of the thermodynamic model . . . 31
3.3.1 Thermodynamic validation . . . 31
3.3.2 Thermodynamic model in dynamic simulations . . . 34

4 Single pipeline simulations and sensitivity analyses **37**
4.1 Dynamic response . . . 37
4.1.1 Composition step change . . . 38
4.1.2 Flowrate step change . . . 42

4.1.3 Consistency of the dynamic response 45
4.2 Sensitivity analyses 46
4.2.1 Heat exchange 46
4.2.2 Dynamic and convective terms of the momentum balance . 49
4.2.3 Discretisation points 51
4.2.4 Reporting interval 52

5 Whole network simulation **55**
5.1 The network flowsheet and test simulations 56
5.1.1 Sensitivity analyses 58
5.2 Making the simulations meaningful 61
5.2.1 Packing the network 61
5.2.2 *Save* and *Restore* tasks 63
5.2.3 Predicting the arrival conditions 65
5.3 Results validation 66
5.4 Predicting condensation in the network 70

Conclusions **73**

Bibliography **77**

Acknowledgments **81**

List of Figures

1.1 Gas transportation costs as function of the distance to cover (Wood et al., 2007). 5

1.2 (a) Natural gas production recent growth per geographical region in Bcm; (b) Natural gas consumption recent growth per geographical region in Bcm (BP, 2016). 6

1.3 (a) NG production growth forecast per geographical region; (b) NG consumption growth forecast per geographical region (CEDIGAZ, 2016). 7

1.4 Global natural gas production forecasts per different NG kinds (CEDIGAZ, 2016). 7

1.5 Prospects for net inter-regional trade of NG via (a) pipeline networks and (b) LNG (CEDIGAZ, 2015). 7

1.6 Parameters affecting complexity in simulating pipeline flow (Adapted from Bratland, 2013). 8

2.1 Modelling of the heat transport phenomena in a model not supporting multilayer walls. Heat is conduced radially and axially in the pipe wall and by forced convection at the inner and outer surfaces. 20

2.2 Modelling of the conduction through the multilayer wall by finding an overall wall thermal resistance (Adapted from Cengel, 2006). . 21

2.3 Modelling of the conduction through the multilayer wall by neglecting the epoxy and steel resistance and modifying the external thermal resistance (Adapted from Cengel, 2006). 21

3.1 Typical phase envelope of a natural gas mixture with main definitions. The arrows and points explain the retrograde condensation phenomenon. Source: Multiflash™ calculation with custom natural gas mixture. 26

3.2 PVT software interpretation of a natural gas phase envelope. Source: Multiflash™ calculation with custom natural gas mixture. 27

3.3 Experimental points and predicted phase envelopes for the mixture Gas 1. Source: Multiflash™. 32

3.4 Experimental points and predicted phase envelopes for the mixture Gas 2. Source: Multiflash™. 33

3.5 'Test Pipeline' flowsheet. Source: gPROMS® ProcessBuilder. . . . 34

4.1 Profile over time of the pressure at axial position 0.1 in the *Heavier* case study, 'Test Pipeline' flowsheet. Source: gPROMS® ProcessBuilder. 39

4.2 Profile over time of the density at axial position 0.1 in the *Heavier* case study, 'Test Pipeline' flowsheet. Source: gPROMS® ProcessBuilder. 39

4.3 Profile over time of the molar flowrate at the sink in the *Heavier* case study, 'Test Pipeline' flowsheet. Source: gPROMS® ProcessBuilder. 40

4.4 Profile over time of the mass flowrate at the sink in the *Heavier* case study, 'Test Pipeline' flowsheet. Source: gPROMS® ProcessBuilder. 40

4.5 Profile over time of the methane molar fraction at the sink in the *Heavier* case study, 'Test Pipeline' flowsheet. Source: gPROMS® ProcessBuilder. 41

4.6 Profile over time of the mass flowrate at the sink in the *Lighter* case study, 'Test Pipeline' flowsheet. Source: gPROMS® ProcessBuilder. 41

4.7 Axial profile of the methane molar fraction after 30 000 seconds in the *Heavier* case study, 'Test Pipeline' flowsheet. Source: gPROMS® ProcessBuilder. 42

4.8 Profile of the pressure at axial position 0.1 over the first 10 000 seconds of simulation in the *More* case study, 'Test Pipeline' flowsheet. Source: gPROMS® ProcessBuilder. 43

4.9 Profile of the molar flowrate at the sink over the first 10 000 seconds of simulation in the *More* case study, 'Test Pipeline' flowsheet. Source: gPROMS® ProcessBuilder. 43

4.10 Profile of the mass flowrate at the sink over the first 10 000 seconds of simulation in the *More* case study, 'Test Pipeline' flowsheet. Source: gPROMS® ProcessBuilder. 44

4.11 Profile of the molar flowrate at the sink over the first 10 000 seconds of simulation in the *Less* case study, 'Test Pipeline' flowsheet. Source: gPROMS® ProcessBuilder. 44

4.12 a) gFLARE®'s pipeline flowsheet; b) Custom flowsheet built with the alternation of 19 *Pipe gML* and *Junction gML* models in gPROMS® ProcessBuilder. 45

4.13 Profiles of the mass flowrate at half pipe over the first 10 000 seconds of simulation using the gPROMS® *Pipeline single-phase gML* model, the gFLARE® model and the custom model. Sources: gPROMS® ProcessBuilder and gFLARE®. 46

4.14 Profile of the mass flowrate at the sink over the first 30 000 seconds of simulation in the *More* case study, 'Test Pipeline' flowsheet, with calculated heat transfer coefficients, fixed heat transfer coefficient and no heat exchanged (adiabatic pipeline). Calculated HTC and Fixed HTC curves are perfectly overlapping. Source: gPROMS® ProcessBuilder. 47

4.15 Axial profile of the temperature in the *More* case study, 'Test Pipeline' flowsheet, with calculated heat transfer coefficients, fixed heat transfer coefficient and no heat exchanged (adiabatic pipeline). The profiles are plotted at the end of the simualation, after 100 000 seconds, but they do not depend on time. Calculated HTC and Fixed HTC curves are perfectly overlapping. Source: gPROMS® ProcessBuilder. 48
4.16 Profiles of the molar flowrate at the sink over the entire simulation time in the *Heavier* case study, 'Test Pipeline' flowsheet, with dynamic and convective term both included (Terms On) or excluded (Terms Off) from the momentum balance. Source: gPROMS® ProcessBuilder. 49
4.17 Profile of the molar flowrate at the sink and at axial position 0.1 ($1/10^{\text{th}}$ of pipeline) over the first 200 seconds of simulation in the *Heavier* case study, 'Test Pipeline' flowsheet, with dynamic term included (Dynamic Term On) or excluded (Dynamic Term Off) from the momentum balance. The profiles are independent on the convective term. Source: gPROMS® ProcessBuilder. 50
4.18 Profiles over time of the molar flowrate at the sink in the *Heavier* case study, 'Test Pipeline' flowsheet, with different numbers of discretisation points. Source: gPROMS® ProcessBuilder. 51
4.19 Profiles over time of the molar flowrate at the sink in the *Heavier* case study, 'Test Pipeline' flowsheet, with different values of the reporting interval. Source: gPROMS® ProcessBuilder. 52

5.1 'Network' flowsheet. Source: gPROMS® ProcessBuilder. 56
5.2 Profile over time of the methane molar fraction at the terminal in the *Step* case study, 'Network' flowsheet. Source: gPROMS® ProcessBuilder. 57
5.3 Profile over time of the molar flowrate at the terminal in the *Step* case study, 'Network' flowsheet, with calculated heat transfer coefficients, fixed heat transfer coefficients and no heat exchanged (adiabatic pipelines). Source: gPROMS® ProcessBuilder. 59
5.4 Profile over time of the propane molar fraction at the terminal in the *Step* case study, 'Network' flowsheet, with different discretisation schemes. 60
5.5 Rationale of the procedure to make the simulations meaningful and have an efficient online flow assurance application. Step 1 simulation consists on the *packing* procedure. It starts from steady-state initial conditions and covers a period at least equal to the total residence time, after which the pipeline is packed. Then, if needed, further specifications can be simulated in order to validate the results. Step 2 simulation is the one to be performed during online monitoring of the network. It starts from a steady-state calculation, which needs to be erased, after which the new specifications are simulated dynamically (as ramps). Then, the system settles to a new steady-state in order to predict the arrival conditions at the terminal. 62

5.6 Schematic of the connection of the *Source linear interpolated gML* and *Set signal to bus gML* models to the *Sink gML* model to ramp the pressure at the terminal. Source: gPROMS® ProcessBuilder. . 63
5.7 'Network' flowsheet modified to model ramp changes instead of step changes. Each *Source gML* model has 16 *Source linear interpolated gML* models (the boxes) and 16 *Set signal to bus gML* models (which are hidden from the flowsheet, so the connecting lines are hidden as well). See Figure 5.6 for comparisons on each *Source gML* connectivity. Source: gPROMS® ProcessBuilder. . . 64
5.8 Profile of the propane molar fraction at the terminal in the divided simulation (Step 1 and Step 2), and in the continuous simulation. 66
5.9 Profile over time of the propane molar fraction at the terminal with the different discretisation schemes, and actual data. 67
5.10 Profile over time of the CO_2 molar fraction at the terminal with the different discretisation schemes, and actual data. 67
5.11 Profile over time of the H_2S molar fraction at the terminal with the different discretisation schemes, and actual data. 68
5.12 Profile over time of the molar flowrate at the terminal with the different discretisation schemes, and actual data. The calculated profiles (Scheme A, Scheme B and Scheme C) are perfectly overlapping. 68
5.13 Execution output of the *Condensation* case study, 'Network' flowsheet, using the GERG-2008 EoS. The red *Pipeline single-phase gML* models (Pipe 4, Pipe 5, Pipe 6, Pipe 9 and Pipe 17) are the ones in which there is multi-phase flow. Source: gPROMS® ProcessBuilder. 70
5.14 Predicted phase envelope of the mixture at the terminal in the *Condensation* case study, using the Peng-Robinson EoS and the GERG-2008 EoS. The operating conditions are depicted by the point. Source: Multiflash™. 71

List of Tables

1.1 Typical molar composition ranges (percent) of each component in raw natural gas (Häring, 2008). 4

3.1 Code names and compositions (molar fraction) for natural gas experimental mixtures. Both mixtures from Avila et. al. (2002). . . 32
3.2 Specifications of the 'Test Pipeline' flowsheet. 34
3.3 Computational times of the 'Test Pipeline' simulations with different number of discretisation points and thermodynamic models (Soave-Redlich-Kwong, Peng-Robinson and GERG-2008 EoSs). The simulations involve a composition step change. 35

4.1 Mixtures A, B and C used in the *Heavier* case study (step change from composition A to B) and in the *Lighter* case study (step change from composition A to C). 38
4.2 Computational times of the *More* case study with calculated heat transfer coefficient, fixed heat transfer coefficient and no heat exchanged (adiabatic pipeline). 47
4.3 Computational times of the *Heavier* case study, including and excluding the dynamic and convective terms individually. 49
4.4 Computational times of the *Heavier* case study with different numbers of discretisation points. 51
4.5 Computational times of the *Heavier* case study with different reporting intervals. 53

5.1 Computational times of the *Step* case study with calculated heat transfer coefficient, fixed heat transfer coefficient and no heat exchanged (adiabatic pipelines). 59
5.2 Number of discretisation points used in schemes A, B and C. . . 60
5.3 Computational times of the *Step* case study with different discretisation schemes. 61
5.4 Computational times of Step 1 and Step 2 simulations using different discretisation schemes and thermodynamic models. 69

Introduction

Natural gas is a mixture of hydrocarbons, mainly methane, which is usually found in nature or could be produced from different organic raw materials. One of the most diffused way to obtain natural gas is to extract it from underground reservoirs, where it can be also mixed with oil and coal, and purify it in specific processing facilities. Then, the treated natural gas must be transported to the user. The cheapest way to transport natural gas is usually via pipeline networks. Alternatively, the gas could be liquefied at low temperature and transported in cryogenic tanks.

Many natural gas reservoirs are offshore, far from the coast and deep under the seabed. Extraction of the gas from these reservoirs is feasible, but more difficult than from onshore reservoirs, hence leading to higher capital and operating costs. The gas could then be transported to the onshore processing facility using subsea pipelines, or it could be condensed to Liquefied Natural Gas (LNG) and transported in adequate carriers (tank ships). This choice is based on economic reasons, which basically depend on the distance the gas has to cover, but could imply geopolitical considerations (e.g. crossing borders or unsafe areas).

While monitoring the behaviour of land pipelines is relatively easy, underwater measurement systems are extremely difficult to build and operate, and therefore they are practically never used. For this reason, in order to control subsea pipeline networks the only possibility is to use simulators for predicting their behaviour. Modelling accurately in real time (online) the fluctuating flow conditions of the gas due to mixing of the fluids from different platforms across the network is key in controlling the arrival conditions to the terminal, in order to ensure stable operation. In particular, predicting the condensation of the gas is critical to avoid threats to the terminal.

The software used in this project is gPROMS® ProcessBuilder, an advanced dynamic process simulator developed by *Process Systems Enterprise Ltd.* The project itself has been developed at the *Process Systems Enterprise*'s headquarters in London. With its many flow transport models (such as pipelines and junctions), ProcessBuilder has the potential to accurately simulate a natural gas pipeline network, in order to control its behaviour in the so-called *flow assurance* issue. The goals of the project are to (i) assess if ProcessBuilder single-phase one-dimensionally distributed model of pipe (*Pipeline single-phase gML*) is complete and accurate enough for the control of a network, (ii) assess if the computational time is small enough for the application to be considered as online, and (iii) determine the best thermodynamic model to describe natural gas behaviour accurately. A case study on an existing pipeline network has been used for validations purposes.

This thesis consists of five chapters. Chapter 1 presents a background on natural gas, focused on its actual market importance, its ways of transport and some forecasts, in order to understand why the flow assurance topic is important and this project needs to be developed accurately. Then, pipeline modelling is discussed, with an introduction to the different approaches, the features needed by *Process Systems Enterprise* for their flow assurance application, and some mathematical details about the chosen way of modelling.

The main software used in the project, gPROMS® ProcessBuilder, is presented in Chapter 2, and its features and models of interest are exposed. A particular focus is put on the *Pipeline single-phase gML* model, which has been chosen to describe the flow of the gas in the pipelines of the network.

In the third Chapter natural gas thermodynamics is explained, starting from basic definitions to some characteristic phenomena. Then, thermodynamic models to predict natural gas properties are presented, and the methods and results of the thermodynamic validation are reported. Furthermore, some simple tests are carried out to understand how the thermodynamic models affects the dynamic simulations, in particular in terms of computational time.

In Chapter 4 the simpler case studies are reported, which have been run to understand the behaviour of the natural gas in pipelines and its mixing in junctions in dynamic simulations. For each level of complexity some sensitivity analyses have been carried out, in order to have important information on how to run properly the complete network simulations.

The network simulations are reported in Chapter 5, focusing on the ways to decrease the computational time in order for the model to be effective for online applications, and to achieve a good accuracy. Modelling results are validated against actual data coming from the network. Then, some tests simulations are reported to assess the importance of using an accurate thermodynamic model to efficiently predict condensation in the pipeline network.

Chapter 1

Literature review

The first chapter of this thesis reports the literature review performed at the beginning of the project in order to obtain a solid background on natural gas, its transport and market, and the modelling of its flow in pipelines. In particular, it has been crucially important to understand what the process simulation market has to offer in terms of pipeline modelling and *flow assurance*.

1.1 Natural gas

In this section a brief introduction to natural gas will be followed by some market insights, the forecasts on its production and demand in the world, and an explanation of the principal ways of transport (including some forecasts on the transport itself), which represent the basic reasons why it is worth investing resources in pipeline modelling.

1.1.1 Background

Natural gas is a mixture of light hydrocarbons (mainly methane with decreasing quantities of ethane, propane, etc.) and small quantities of non-hydrocarbon gases (such as CO_2, N_2, H_2S and rare gases) which is found in deep underground rock formations or reservoirs, or could be produced from different organic raw materials. It is a fossil non-renewable resource used as fuel for cooking, heating, electricity generation, transport fuel and as a raw material in the production of plastics and organic chemicals.

Natural gas forms naturally when decomposing organic matter stays buried for millions of years under the Earth's surface, and it can be either biogenic (created by methanogenic organisms) or thermogenic (created by high pressure and temperature). It is labelled as 'associated' if found in oil fields, or 'non-associated' if isolated in natural gas fields. Natural gas is usually labelled as 'conventional' if found in underground reservoirs composed of sandstone, while 'unconventional' mixtures can be found in coal beds (coalbed methane), shale formations (shale gas), or in reservoir rocks with extremely low permeability (tight gas).

Raw natural gas composition depends on the geology of the geographical area it is extracted from, as well as on the type and depth of the reservoir. Water is almost always present in the extracted natural gas, so it is common practice to

assume that, unless the gas has not been previously dehydrated, the mixture is saturated in water at the nominal conditions of temperature and pressure. The typical composition of a raw natural gas mixture can be found in Table 1.1.

Table 1.1: Typical molar composition ranges (percent) of each component in raw natural gas (Häring, 2008).

Component	**Molar range [%]**
Methane	50 − 95
Ethane	2 − 20
Propane	1 − 12
Butane	0 − 4
Higher alkanes	0 − 1
H_2S	0 − 6
CO_2	0 − 99
N_2	0 − 70
O_2	0 − 0.02
Helium	0 − 1
Other inert gases	traces

Independently on the composition of the mixture extracted from the ground, the final product sent to the distribution pipeline network is almost pure methane and must meet some specifications. Frequently, the quality standards involve energy content, dew point temperature level, amount of 'critical' elements or compounds (such as H_2S or CO_2), humidity (H_2O content) and particulates content. Therefore, the natural gas produced from wells has to be processed and treated before it can be sent to the end users. Usually, in offshore operation some treatments, such as a rough dehydration or the removal of H_2S and CO_2, are performed on the platforms as soon as the gas is extracted, while the main purification is performed in onshore processing facilities (called terminals). In the case of associated natural gas there are two typical transport approaches: transporting the two-phase mixture as is, or performing a gas-liquid separation on the extraction site and transporting the two phases through separate pipelines.

1.1.2 Transport

Because of its low density, it is not easy to store and transport natural gas. However, due to increasing demands in many countries, transport of natural gas over long distances has become very important. Nowadays, natural gas can be transported from the extraction area to the processing facility in two ways: (i) using pipeline networks or (ii) compressing and cooling the gas to extremely low temperatures obtaining Liquefied Natural Gas (LNG). A third way to transport natural gas consists in its immobilisation by conversion to solid hydrates, but it is not used in commercial applications because not economically feasible.

Natural gas transport through pipelines is one of the most widely used (70% of total transported natural gas) because of its relatively low cost both in terms of investment and operating costs. In particular, land pipelines are cheap and easy to build, operate and control, while offshore pipelines are feasible but much more expensive. An offshore pipeline network links many platforms (each of which usually collects gas from many extraction wells) to one or more onshore terminals. The link between pipes is usually achieved through subsea tee junctions. Each production well must monitor the chemical and physical conditions of the gas, which have to meet some standards, usually determined by contract. The main problem of subsea pipeline networks is the impossibility to monitor and control their behaviour directly through measurement. This implies the need to rely on pipeline network simulations, which are in fact the main subject of this project.

Liquefied Natural Gas, which accounts for the remaining 30% of natural gas transport market, is more expensive than pipeline transport. In particular, the investment cost for LNG facilities is really high, mainly for liquefaction, then for shipping and regasification.

In conclusion, pipelines are a very convenient method of transport, but they are not as flexible as shipping (e.g. in the event a pipeline has to be shut down, the whole facility needs to be shut down). The choice of the method of transport needs to be done according to economical, geographical and practical considerations, and it needs to account also for difficult geopolitical aspects. However, in general, the higher the distance to cover the higher the cost for a pipeline, up to a point in which transportation via LNG route is economically favourable. This can be seen from Figure 1.1. From this picture it is also possible to notice the higher price of offshore pipelines with respect to onshore pipelines, and the fact that transporting a compressed gas is usually better (it increases the operating costs but decreases the capital costs).

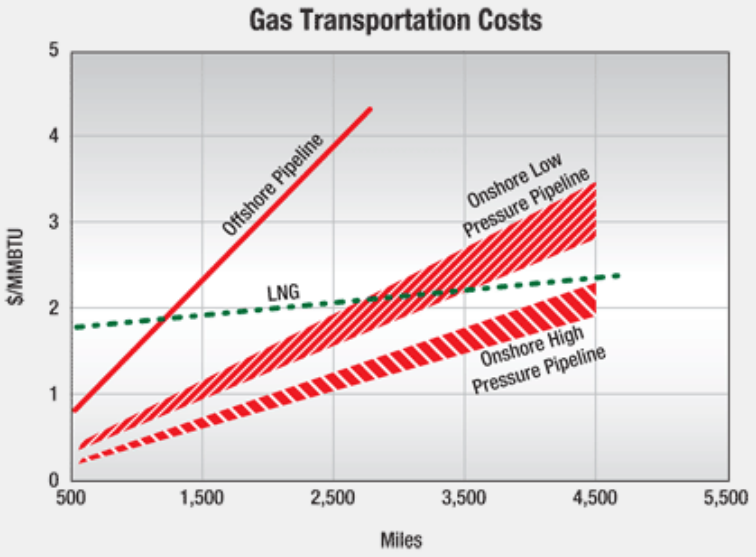

Figure 1.1: Gas transportation costs as function of the distance to cover (Wood et al., 2007).

1.1.3 Forecasts

The role of natural gas in the world has increased quite a lot in the recent years and is likely to continue to expand, as a result of its availability, utility and relatively low cost. Furthermore, natural gas burns cleaner and more efficiently than coal and oil, and the level of potentially harmful by-products that are released into the atmosphere is lower, making it environmentally more attractive. For this particular reason natural gas is now used also in non-typical applications, such as the production of electrical energy. Eventually, there are very large deposits of natural gas in the world (far more than oil), many of which are still not exploited. Figure 1.2 shows the recent growth in natural gas production and consumption per geographical region.

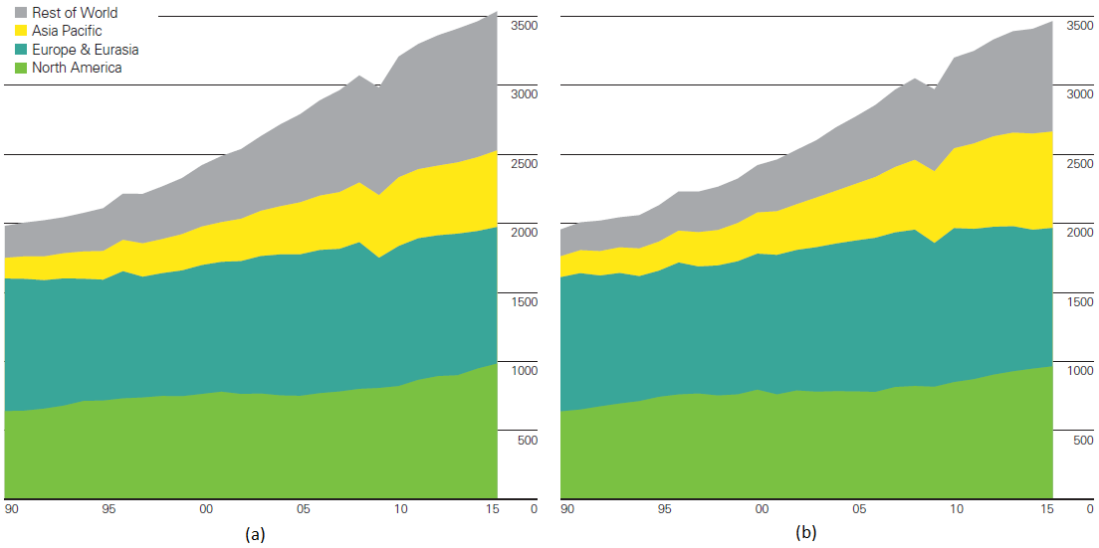

Figure 1.2: (a) Natural gas production recent growth per geographical region in Bcm; (b) Natural gas consumption recent growth per geographical region in Bcm (BP, 2016).

Accordingly with what recent history suggests, forecasts confirm that both natural gas production and consumption will increase. This can be noticed from Figures 1.3 and 1.4. Global natural gas production will increase by almost 50% in the next 20 years (from around 3500 to 5000 Bcm). It is also possible to see how the share of unconventional natural gas on the total will increase from around 20 to 35%. However, conventional natural gas market will increase as well, but with a smaller percentage with respect to the unconventional one. From Figure 1.3 one can also notice that the trends are reversed for Europe. This is due to the fact that European gas reservoirs are emptying out and the energy demand is not expected to increase after 2020.

Recent technological discoveries and improvements in the LNG field make it increasingly attractive against pipeline networks, but the pipeline market will increase as well, as one can notice from Figure 1.5. In conclusion, it is worth investing in the natural gas market and in its transport through pipeline networks.

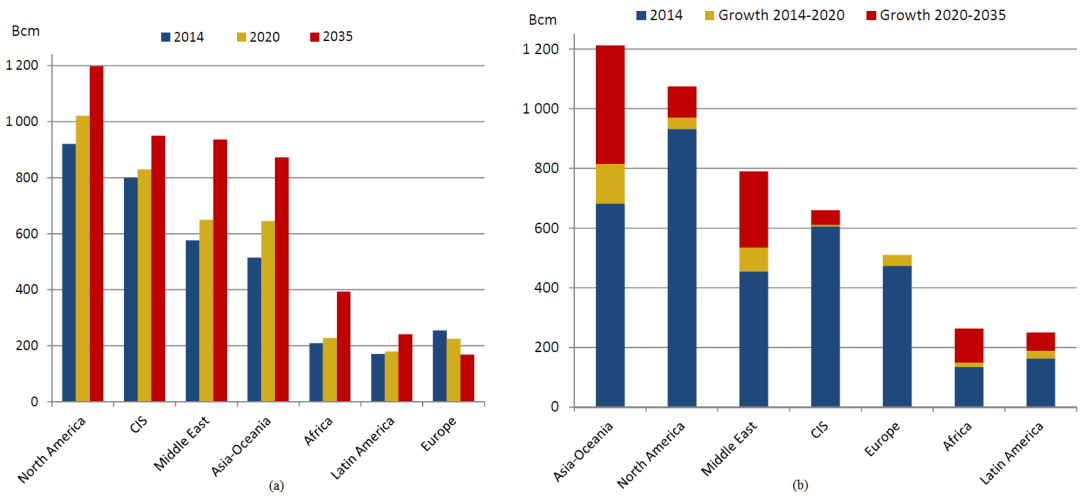

Figure 1.3: (a) NG production growth forecast per geographical region; (b) NG consumption growth forecast per geographical region (CEDIGAZ, 2016).

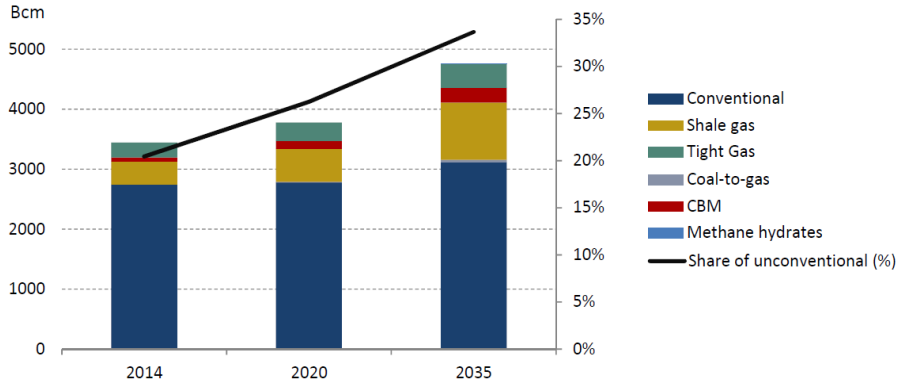

Figure 1.4: Global natural gas production forecasts per different NG kinds (CEDIGAZ, 2016).

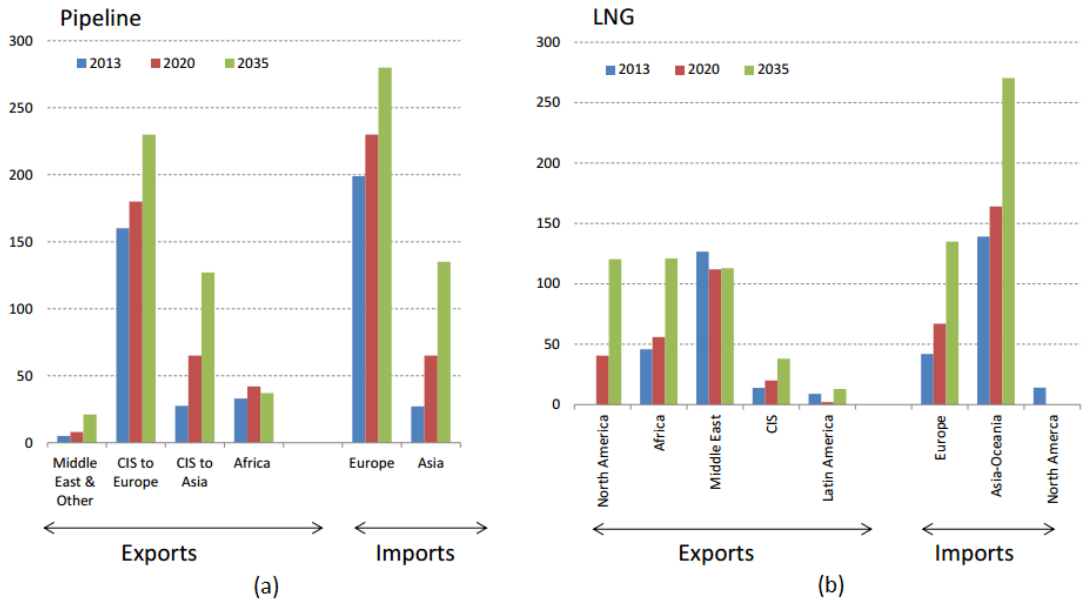

Figure 1.5: Prospects for net inter-regional trade of NG via (a) pipeline networks and (b) LNG (CEDIGAZ, 2015).

1.2 Flow assurance and pipeline modelling

In this section pipeline modelling is discussed, with an introduction to the different approaches, the features needed by *Process Systems Enterprise* for their flow assurance application (setting also the guidelines this project has followed), and some theoretical details of the model that has been chosen.

1.2.1 Different approaches

As already mentioned, pipelines and pipeline networks are difficult to monitor and control through measurements. In particular, this task becomes physically and economically impossible in the case of offshore operation. For this reason the so-called *flow assurance*, which consists in the maintenance of the desired fluid flow from inlet to outlet of a pipe system, has become fundamental, especially in the hydrocarbon industry. In fact, one needs to rely on simulations to effectively know and predict what is happening and could happen inside one or more pipelines.

Flow assurance is a newly-coined non-standardised term, and is still open to different interpretations due to the many aspects of a hydrocarbon transport chain (e.g. the possibility to define the system boundaries in different ways). The trend is to integrate in the simulations as many details as possible, such as wells, slug catchers, separators, processing facilities or whatever else the system contains. Furthermore, flow assurance is open to many levels of complexity depending on what the user needs to simulate and on the level of accuracy one requires (keeping in mind that the higher the complexity the higher the computational heaviness). The complexity in simulating pipeline flow can be summarised in the various options displayed in Figure 1.6, where the simplest alternatives are on the top of the boxes.

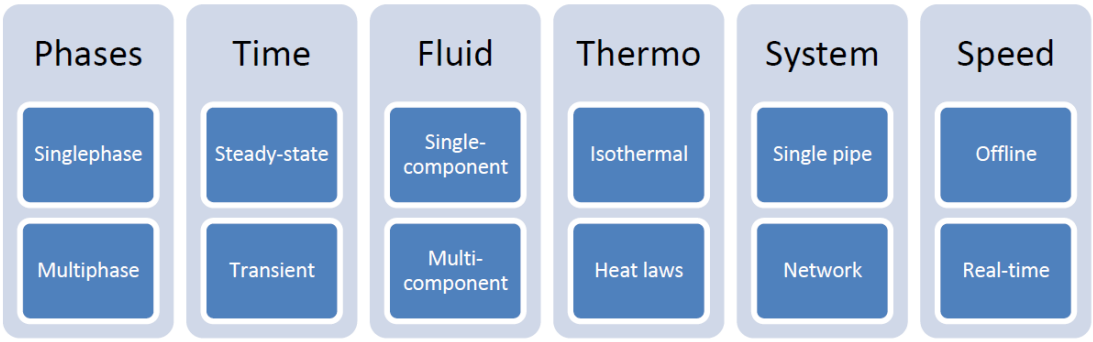

Figure 1.6: Parameters affecting complexity in simulating pipeline flow (Adapted from Bratland, 2013).

The most used way to classify pipeline modelling and simulation is by specifying how many separate fluids need to be considered simultaneously (single-phase, two-phase or three-phase), and by whether it is able to describe time-dependent phenomena (transient or dynamic simulations) or not (purely steady-state simulations). Then, simulations can be divided into single- or multi-component: the former, often labelled as the *black-oil* approach, is based on simple interpolation of PVT properties as a function of pressure, and is widely used in low-accuracy

reservoir simulations; the latter, named *compositional* approach, is based on a thermodynamically-consistent model such as an Equation of State (EoS), and is the usual one for pipeline simulations (unless one of the components is predominant). The model can then account for heat exchange in the pipelines (considering heat laws) or not (assuming isothermal pipelines), and the choice is case-dependent. The intrinsic structure of the system to be simulated determines the distinction between single pipe and network simulations (in which mixing-related variables need to be considered). Eventually, the speed of the simulations (i.e. the computational time required to reach convergence) leads to the definition of real-time (or online) simulations, whose results are obtained in a time interval which is much smaller than the 'characteristic time' of the system.

1.2.2 The company's choices

The focus of this project is on the transport of natural gas from offshore extraction platforms to onshore processing facilities. Natural gas is assumed to come from a non-associated source or, if it comes from an associated source, it is assumed that a gas/liquid separation is performed on the platform. For this reason the system to be modelled is a network of subsea natural gas pipelines, which therefore needs to account for the pipelines themselves as well as the junctions between different branches.

The main threat for a single-phase natural gas network is the possible condensation of the gas. Depending on the quantity of liquid condensed and on the flow regime, the liquid drops can either give problems of corrosion on the long term, or they can coalesce and, under the influence of gravity, settle on the bottom of the pipeline, creating the so-called liquid *slugs*. Slugs are extremely dangerous because they overload the gas/liquid handling capacity of the processing facility at the pipeline outlet, which is usually designed to collect gaseous mixtures with a small liquid fraction, or vice versa. Another critical problem linked to the phase behaviour of natural gas is the possible formation of solid hydrates, ice-like solids that form when water and natural gas combine at high pressure and low temperature. The formation of non-gaseous phases not only could lead to safety problems, but also modifies the properties of the gas and the system (e.g. density, viscosity, friction factor of the pipe walls). For this reason, if one does not simulate the multi-phase flow as is (which would need many complex features such as a flow regime calculator), the single-phase model needs to account for the possible formation of a liquid fraction in the mixture. This is usually obtained by averaging the properties of the phases but, indeed, disregarding all the effects due to their coexistence and interactions in the pipeline.

It has been decided to neglect the formation of hydrates and to assume that even the formation of a really small fraction of liquid in the pipeline needs to be avoided (which however could practically not be a problem for the pipeline). For this reason, and due to the main assumption of single-phase natural gas as inlet to the network, it has been decided to simulate single-phase pipelines.

Along with the choice between single- and multi-phase modelling, the choice between steady-state and transient modelling is critical for a flow assurance application. Even if developing and solving a steady-state model is much easier than a dynamic one, a steady-state model can only describe how the properties of the

fluid are distributed along the pipeline once the flow is fully developed and stable. However, a natural gas transport system is an intrinsically unstable system, in which each input specification is constantly fluctuating in time as the operation goes on. Furthermore, a pipeline network consists in many natural gas mixtures which are brought together at some point, so the mixing of the different gases accentuates these fluctuations. Therefore, it is fundamental for an efficient pipeline simulation to account for time in the equations, making the model transient (or dynamic), as a steady-state is never reached during normal operation. Steady-state models are typically used for design purposes, and this approach is not always correct, sometimes giving way to dangerous underestimations (e.g. flare systems). Due to the effort in modelling dynamic systems, most of the commercial pipeline simulation software can only simulate steady-state flow. In conclusion, it has been decided to use a dynamic model for the desired application.

Due to the continuous fluctuations of the gas entering the network, the mixing of different gases and the complexity of the networks to be simulated, it is fundamental for the model to take into account the compositions of the different natural gas mixtures, so the model needs to be multi-component, based on an adequate EoS. The comparison between EoSs is reported in Chapter 3.

Eventually, the main objective of this project is to develop an efficient monitoring and predictive flow assurance application, and to make it fast enough to be online (whose results can be checked almost in real-time by the operators). For this reason, throughout the whole project, the computational time of the simulations has been considered as a fundamental variable, along with the accuracy of the simulations, and many sensitivity analyses have been performed to reduce it.

1.2.3 Single-phase dynamic pipeline model

The basic principles for describing a dynamic single-phase gas flow inside a pipeline are mass, momentum and energy conservation.

Mass conservation

The mass conservation principle applied to a fluid control volume leads to the so-called *continuity equation* in its conservation form, which is

$$\frac{\partial \rho}{\partial t} + \frac{\partial (\rho v)}{\partial x} = 0 \ , \tag{1.1}$$

where ρ is the density of the gas, t is the independent variable time, v is the velocity of the gas and x is the axial direction of the pipeline.

Momentum conservation

By applying Newton's second law to a fluid control volume one can obtain, after various rearrangements and substitutions, the momentum balance written as

$$\frac{\partial (\rho v)}{\partial t} + \frac{\partial (\rho v^2)}{\partial x} = -\frac{\partial p}{\partial x} + \frac{f \rho}{2d} v|v| - \rho g sin\theta \ , \tag{1.2}$$

where p is the pressure, f is the Darcy-Weisbach friction factor, d is the internal diameter of the pipeline, g is the gravitational acceleration and θ is the angle that

the pipeline forms with the horizontal, therefore accounting for possible height variations.

Energy conservation

The energy conservation principle, according to which the rate of change of energy inside a fluid element is due to the net heat flux into the element and the rate of work done on the element, leads to the energy balance, which can be written as

$$\frac{\partial}{\partial t}\left(\rho\left(u+\frac{v^2}{2}+gz\right)\right)=-\frac{\partial}{\partial x}\left(\rho v\left(h+\frac{v^2}{2}+gz\right)\right)+q+w\ , \tag{1.3}$$

where u is the specific internal energy (so the energy of all the gas molecules inside the element), z is the element elevation from a reference level, h is the specific enthalpy, defined as

$$h=u+\frac{p}{\rho}\ , \tag{1.4}$$

q is the net heat flux into the element and w accounts for other possible sources of power added to the flow per unit pipe volume (such as shaft work by pumps).

The friction factor

The Darcy-Weisbach friction factor is defined as

$$f=\frac{\tau}{\rho\dfrac{v|v|}{2d}}\ , \tag{1.5}$$

where τ is the local shear stress, which consists in the friction term in the momentum balance (Equation 1.3). It can be calculated through graphs or correlations. The model needs to be solved automatically by the simulator, so the use of graphs is not possible. The most widely used correlation for calculating the Darcy-Weisbach friction factor under turbulent conditions (always found in natural gas pipeline networks) is the Colebrook-White equation (Colebrook, 1939)

$$\frac{1}{\sqrt{f}}=-2\log\left(\frac{2.51}{Re\sqrt{f}}+\frac{\epsilon}{3.7d}\right)\ , \tag{1.6}$$

where ϵ is the pipe effective roughness height and Re is the Reynolds number, defined as

$$Re=\frac{\rho v d}{\mu}\ , \tag{1.7}$$

with μ the fluid viscosity.
Many simplified correlations have been developed to by-pass Colebrook-White equation non-linearity. One of the most widely used is the Haaland equation (Haaland, 1983)

$$f=\left(-1.8\log\left(\frac{6.9}{Re}+\left(\frac{\epsilon}{3.7d}\right)^{1.11}\right)\right)^{-2}\ . \tag{1.8}$$

This equation has a slight inaccuracy with respect to Colebrook-White equation (around 1.5%) in a wide range of Reynolds numbers and wall roughness values.

Net heat flux correlations

The net heat flux term q accounts for heat transfer between the fluid and the pipe surroundings. Usually it is calculated neglecting radiation (because of the small temperatures), hence considering only conduction through the wall and forced convection, both on the inner and the outer pipe surface.
Because of the difficulties in modelling the axial and radial conduction phenomena through the wall, a common approach is to use correlations based on engineering considerations and experimental data.
The heat transfer rate Q is calculated as

$$Q = UA\ \Delta T\ , \tag{1.9}$$

where U is the heat transfer coefficient $[W/(m^2K)]$, A is the surface area and ΔT is the temperature difference between the two sides of the surface. Pipes can consist of many layers on top of each other, so the conduction term must account for this. It is usual practice in this case to refer to the outer diameter of the pipeline and consider conduction as a *series* process. In the case of multi-layer cylindrical geometry the heat transfer rate for a pipe section of length Δx is

$$Q = U_o \pi d_o\ \Delta x\ (T_o - T_f)\ , \tag{1.10}$$

where U_o is the overall heat transfer coefficient based on the outer diameter d_o, T_o is the outer (surrounding) temperature and T_f is the inner fluid temperature. Heat transfer by conduction is a series process, so $U_o d_o$ can be calculated as

$$U_o d_o = \Big(\frac{1}{U_1 d_1} + \frac{1}{U_2 d_2} + ... + \frac{1}{U_n d_n}\Big)^{-1}\ , \tag{1.11}$$

where U_j and d_j are the values of U and d for the n layers.
The net heat flux can be calculated as

$$q = \frac{Q}{\pi \dfrac{d_i^2}{4}\ \Delta x}\ , \tag{1.12}$$

where d_i is the inner diameter. Therefore, inserting Equation 1.10 in Equation 1.12, one can obtain

$$q = \frac{4 U_o d_o}{d_i^2}\ (T_o - T_f)\ . \tag{1.13}$$

The various layers $U_j d_j$ can be calculated as

$$U_j d_j = \frac{2 k_j}{\ln \dfrac{d_{j,i}}{d_{j,o}}}\ , \tag{1.14}$$

where k_j is the thermal conductivity of layer j $[W/(mK)]$, $d_{j,i}$ is the layer inner diameter and $d_{j,o}$ is the layer outer diameter.
Usually, the heat transfer coefficients for forced convection are considered as two additional layers in Equation 1.11. The internal heat transfer coefficient (which

can be therefore considered as the 'new' U_1) can be calculated with the Dittus-Bölter correlation (Dittus & Bölter, 1930)

$$Nu = 0.023 Re^{0.8} Pr^{0.4} \ , \tag{1.15}$$

where Nu is the Nusselt number, Re is the Reynolds number and Pr is the Prandtl number, respectively defined as

$$Nu = \frac{Ud}{\lambda_f} \ , \tag{1.16}$$

$$Re = \frac{\rho_f v_f d}{\mu_f} \ , \tag{1.17}$$

$$Pr = \frac{c_{p,f}\mu_f}{\lambda_f} \ . \tag{1.18}$$

The f subscript indicates the fluid properties. To calculate U_1 the diameter to be considered in Equation 1.16 is the inner diameter d_i .
Probably, the best correlation available at present for estimating the internal heat transfer coefficient (through the calculation of the Nusselt number) is the Gnielinski correlation (Gnielinski, 1976)

$$Nu = \frac{\frac{f}{8}\,(Re - 1000)\ Pr}{1.07 + 12.7\Big(\frac{f}{8}\Big)^{0.5}\,(Pr^{2/3} - 1)} \ , \tag{1.19}$$

where f is the Darcy-Weisbach friction factor.
The external heat transfer coefficient (which can be considered as U_{n+2}) is typically calculated with the Hilpert correlation (Hilpert, 1933)

$$Nu = C Re^m Pr^{1/3} \ , \tag{1.20}$$

where C and m are coefficients which depend on the value of Re. In this case, to calculate U_{n+2} the diameter to be considered in Equation 1.16 is the outer diameter d_o .
In the case of subsea pipelines as the ones dealt in this project, the best correlation has been proposed by Churchill & Bernstein (1977)

$$Nu = 0.3 + \frac{0.62 Re^{0.5} Pr^{1/3}}{\left(1 + \left(\frac{0.4}{Pr}\right)^{2/3}\right)^{0.25}} \left(1 + \left(\frac{Re}{282000}\right)^{5/8}\right)^{0.8} \ . \tag{1.21}$$

In this case the water thermal conductivity, kinematic viscosity $\nu = \mu/\rho$ and Prandtl number are evaluated with the data taken from Wagner & Kretzschmar (2007)

$$\lambda_{water} = -2.5 \cdot 10^{-5} T^2 + 0.0166 T - 2.1136 \ , \tag{1.22}$$

$$\log \nu_{water} = 25.22 (\log T)^2 - 131.76 \log T + 165.58 \ , \tag{1.23}$$

$$\log Pr_{water} = 28.343 (\log T)^2 - 148.12 \log T + 193.76 \ . \tag{1.24}$$

Chapter 2

Software and tools

In this chapter the main characteristics and features of the software used in the project, gPROMS® ProcessBuilder, are presented. In particular, the *Pipeline single-phase gML* model is analysed in details.

2.1 gPROMS® ProcessBuilder

As already discussed in the first chapter, the motivations of this project brought to the development of a single-phase dynamic model for the desired flow assurance application. *Process Systems Enterprise*'s advanced process modelling software gPROMS® ProcessBuilder provides, among its many functions, high-fidelity dynamic models for all the required units involved in a pipeline network through the gPROMS® Model Libraries (gMLs). This process simulator allows the user to easily build the flowsheet through a 'drag and drop' GUI (Graphical User Interface), but at the same time it preserves the capability of implementing custom models and modifying existing ones thanks to the gPROMS® ModelBuilder structure.

It has been decided to use the thermodynamic package Multiflash™, developed by *Infochem Computer Services Ltd*, for modelling physical properties and phase equilibria. This software, which supports all common thermodynamic and transport properties, can be used as a stand-alone or in conjunction with other software. In ProcessBuilder, a *mfl* file containing all thermodynamic information (the list of components and the thermodynamic models to be used in the simulation) is generated from Multiflash™ and called as foreign object in the required models through the dialog boxes.

2.1.1 Equation-oriented approach

One of the most significant advantage of the gPROMS® platform is its equation-oriented (EO) approach for process flowsheeting. This approach is opposed to the sequential modular (SM) approach, the traditionally most used in the commercial steady-state simulators due to its robustness and ease of implementation. Software based on the SM approach solve each unit operation individually and sequentially according to the flow direction. Each module includes a set of equations (material, energy and momentum balance), which is solved and whose output stream is the input for the following module (the solution is achieved in a 'circular' way).

On the other hand, EO software are able to solve the whole problem simultaneously, merging all unit operation models and connectivity relations into a non-linear equations system. This system (which can result in hundreds of thousands of equations depending on the complexity of the flowsheet) needs to be accurately initialised, and it is solved through optimisation techniques, such as those based on Newton's method (Pantelides et al., 2015). These systems are more difficult to construct and troubleshoot with respect to the SM software, but they lead to many advantages, such as in the case of multiple recycles or optimisation tasks, for which SM software may get stuck in calculation (due to the need of several iterations through the 'loop'). Furthermore, custom modelling is easier because the addition of new unit operations or the modification of the existing ones only requires the definition of the set of equations in the coding, and the solution is achieved at flowsheet level.

2.1.2 Dynamic simulations and pressure-driven mode

Network simulations need to be run dynamically, so including time as a variable of the model. ProcessBuilder allows to easily build and solve dynamic models. There are two ways to create a dynamic simulation. The first one is to include the dynamic specifications in the so-called *Schedule* tab, in which time-dependent variables are specified. Through a 'drag and drop' tool it is possible to easily build the desired sequence of operations, such as keeping specifications constant for a certain time (*Continue*), change some specifications (*Assign*), and so on. The other way consists in time-dependent models to be included in the flowsheet (such as the *Ramp gML* or the *Source Linear Interpolated gML* model) in which values changing with time are assigned directly to one specific variable at a flowsheet level from dialog boxes. By doing this, ProcessBuilder automatically creates a *Task*, which is simply added to the dynamic *Schedule*. The two ways are therefore identical, differing only on the tool to be used to define the variables (external tab or flowsheet).

The key variable in a dynamic simulation is time. Therefore, before running a simulation, one must assign the total simulation time, that is the time in seconds in which the software calculates all the variables of interest, and after which the simulation stops. It is as well important the reporting interval, that is the interval in seconds between the results collections made by the software throughout the simulation. It needs to be specified that the reporting interval does not modify the way the solver works, but it is linked only to the level of details one can obtain from a simulation, i.e. the number of time steps in which the solutions are saved.

Appropriately defining the simulation time and the reporting interval is fundamental to achieve a meaningful solution and to obtain an appropriate level of details. However, it is important to notice that the higher the simulation time and the smaller the reporting interval, the longer the simulation takes, and for designing an online flow assurance application the computational time is a key parameter.

Eventually, it has to be specified that in order to run dynamic simulations the *pressure-driven* mode must be selected for each model in the flowsheet. In this simulation mode the direction and intensity of the flow is determined by the pressure difference between the inlet and the outlet of each model.

2.1.3 gML models

The main unit operation in pipeline network systems is the pipeline itself, which has been decided to be single-phase. ProcessBuilder includes two pipeline models in the model library: the *Pipe gML* model and the *Pipeline single-phase gML* model. The former is a lumped model, which then considers the whole pipeline as a single perfectly-mixed volume. The natural gas pipelines are usually extremely long and it is fundamental to consider the axial variations of the gas properties (pressure drop is the most important), making the lumped model not suitable for the desired application. The latter is an axially-distributed model, which is then exactly what needed to develop an efficient flow assurance application. This model will be analysed in details in the following section.

Other unit operations and modules to be considered in a pipeline network are the junctions, usually tee-junctions, through which different branches of the network merge together their fluids. ProcessBuilder's *Junction gML* is modelled as a perfect mixer, and it allows to achieve the desired level of details. In fact, the model of the network is decided to be single-phase, and usually the network itself is much bigger than the junctions, i.e. the junctions represent a negligible volume with respect to the whole network. For these reasons the junction model does not need to include computational fluid dynamics analyses, which would be useless in the desired application. The *Junction gML* model mixes a given number of inlet material streams and splits the resulting flow into a number of outlet streams. To split the flow, the flowrate of each outlet stream can be specified or a split fraction can be given, which determines how much of the combined flow from the inlets goes to each outlet. In the case of a pipeline network the junctions are tee-junctions, therefore the inlets are usually two and the outlet is one. In dynamic simulations, a volume can be specified for the junction, but this aspect is disregarded as the junctions are a negligible part of the whole network. Furthermore, when in pressure-driven mode, the model will also equate all the inlet and outlet pressures in connecting pipelines, to keep continuity of the pressure profile in the whole network.

Eventually, the network model would be incomplete without considering the inlet and the outlet of the system. ProcessBuilder's models are *Source gML* for the inlets, and *Sink gML* for the outlets (usually just one, representing the inlet to the processing facility). In pressure-driven mode, either the stream pressure or the stream flowrate needs to be specified in the *Source gML* model, while the stream pressure needs to be specified in the *Sink gML* model. Consistently with what is usually known in real plants and, in particular, in the case study analysed in Chapter 5, it has been decided to specify the flowrate at the inlets.

It has been decided not to include any other downstream unit operation in the flowsheet in order to focus purely on the gas transport through the network. However, ProcessBuilder has the capability of integrating and simulating many other modules in the flowsheet if needed, which is in fact the trend in the flow assurance software market.

2.2 The *Pipeline single-phase gML* model

ProcessBuilder *Pipeline single-phase gML* model is a single-phase axially distributed pipe model. It includes the equations theoretically described in Chapter 1 (mass, momentum and energy balance, as well as the related correlations). In particular, the heat transport term has been analysed in details due to the multilayer configuration of the pipelines used in subsea applications. Eventually, some numerical details about the model are mentioned, as well as some of the most important features.

2.2.1 Conservation equations

The mass balance (Equation 1.1) is applied to each single component of the mixture, and it does not include the diffusive term (according to which each species moves due to a concentration gradient). However, this effect has been considered as a minor contribution if compared to the convection, due to the high turbulence of the gas, and thus is negligible in the model.

The momentum balance (Equation 1.2) can be modelled in different ways. One of the basic choices regards the friction factor correlation. The chosen correlation is the Colebrook-White one, because due to ProcessBuilder equation oriented approach the non-linearity of the equation is not a limit, and in this way the Haaland equation slight inaccuracy is avoided. It needs to be mentioned that the *Pipeline single-phase gML* model uses the Fanning friction factor instead of the Darcy-Weisbach one, so the equations and correlations are slightly different from the ones listed in Chapter 1 (corrected by a factor of 4). An important feature of *Pipeline single-phase gML* is the possibility to include/exclude singularly the dynamic and convective terms from the model in a really simple way through the dialog box (thanks to the deep modularity of all ProcessBuilder's models). These two terms are respectively $\partial(\rho v)/\partial t$ and $\partial(\rho v^2)/\partial x$ in Equation 1.2. The choice whether to include these terms or not is fundamental because it affects the accuracy of the results and the computational time of the simulations.

The energy balance (Equation 1.3) does not include the kinetic term $v^2/2$, potential term gz and shaft work w. The kinetic term has an impact on the equation because for gases the velocity is strictly related to the density, which can vary along the pipe due to fluctuations in composition (molecular weight of the mixture), pressure and temperature. However, velocity in gas pipelines is usually not high. A quick calculation shows that, assuming a common pipeline works at 100 bar and 5 °C, the velocity of the gas never exceeds 1 m/s. Therefore, the kinetic term $v^2/2$ is at maximum 0.5 m^2/s^2 [= 0.5 J/kg]. This value is extremely low if compared to the value of the specific enthalpy of the gas, which is usually around 50 kJ/kg. Eventually, neglecting the kinetic term in the energy balance is a good approximation for pipeline network applications. Furthermore, the potential term can be neglected because the subsea networks usually do not have big elevation changes on their path, and the shaft work term is negligible because they do not include pumping stations or any other source of power.

2.2.2 Heat transfer modelling

In *Pipeline single-phase gML* the net heat flux q is modelled considering the inner surface of the pipeline as a reference so, according to what already said about the energy balance, this reduces to

$$\frac{\partial(\rho u)}{\partial t} + \frac{\partial(\rho v h)}{\partial x} = -\frac{q_{f,w} A_i}{L A_{cross}} = -\frac{4 q_{f,w}}{d_i} \ , \tag{2.1}$$

where $q_{f,w}$ is the heat flux from the fluid to the wall, A_i is the inner surface, L is the length and A_{cross} is the cross section of the pipeline. *Pipeline single-phase gML* models the conduction through the pipe wall using the dynamic heat balance:

$$\frac{\partial u_w}{\partial t} - \frac{\partial}{\partial x}\left(k_w \frac{\partial T_w}{\partial x}\right) = -\frac{q_{f,w} A_i + q_{w,a} A_o}{V_w} = -4\frac{q_{f,w} d_i + q_{w,a} d_o}{d_o^2 - d_i^2} \ , \tag{2.2}$$

where u_w is the internal energy of the wall, calculated as

$$u_{wall} = \rho_w c_{p,w} T_w \ , \tag{2.3}$$

and ρ_w, $c_{p,w}$ and k_w are respectively the density, specific heat capacity and thermal conductivity of the wall, T_w is the radial average temperature of the wall, $q_{w,a}$ is the heat flux from the wall to the surrounding ambient (water), A_o is the outer surface of the pipeline and V_w is the volume of the wall. The two net heat fluxes are calculated as

$$q_{f,w} = U_{f,w}(T_f - T_w) \ , \tag{2.4}$$

$$q_{w,a} = U_{w,a}(T_w - T_a) \ , \tag{2.5}$$

where T_f is the temperature of the fluid flowing inside the pipeline and T_a is the temperature of the water surrounding the pipeline.

Usually, in subsea pipeline networks the temperatures are almost constant (seabed temperature is subject to slow seasonal variations and the temperature at the wells can be assumed as constant), and the pipes are extremely long, so the effect of axial conduction is imperceptible. For these reasons, the left hand side of Equation 2.2 is typically negligible. This means that the heat which is entering the wall from the inner surface leaves the outer surface at the same rate.

Unfortunately, the radial heat conduction in the pipe (which would be related to the radial variable r) is not modelled in the *Pipeline single-phase gML* model. Therefore, infinitely fast radial heat conduction is inevitably assumed.

Furthermore, common subsea pipelines consist of three layers whose thickness is proportional to the diameter of the pipeline itself. The core of the pipe is made of steel. A thick external concrete coating protects the pipe from corrosion by the sea water and gives weight to the pipe, ensuring that it tightly lies on the seabed. A thin internal synthetic resin film reduces friction with the flowing gas (thus reducing the pressure drop and increasing the pipeline capacity) and protects the pipe from corrosion by the natural gas. For this reason, Equation 1.13 would be the most appropriate, combined with Equation 1.11. However, *Pipeline single-phase gML* does not support multi-layer modelling, so the wall had to be considered as a singular entity, somewhat merging the effects of the three layers, as depicted in Figure 2.1. The key phenomena are conduction through the wall

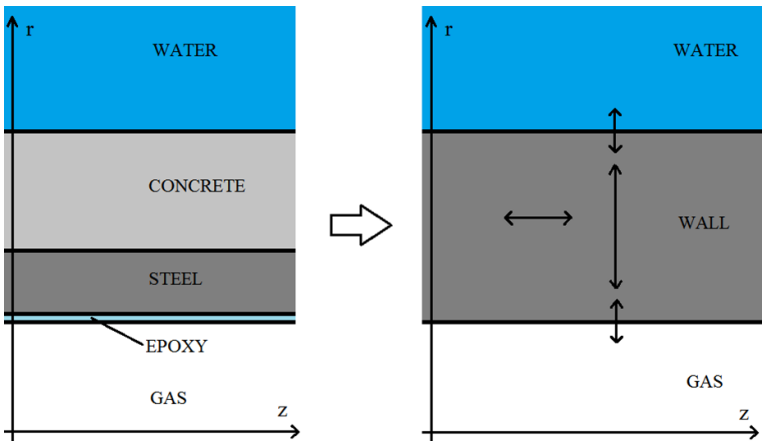

Figure 2.1: Modelling of the heat transport phenomena in a model not supporting multilayer walls. Heat is conduced radially and axially in the pipe wall and by forced convection at the inner and outer surfaces.

(both axial and radial) and convection on the inside and outside of the pipe.

Due to the high total thickness of the pipe walls, the infinitely fast heat conduction assumption can be considered as unrealistic. Therefore, it has been thought to customise the model in order to include the radial dynamic heat balance. However, it has been decided not to customise it because the temperature profile in the wall is not needed (and it would even be just an approximation of the actual one due to the absence of a multi-layer model).

An engineering approach has then been considered, in order to account for the conduction through the wall. The resistance that the three layers oppose to radial heat transfer can be seen as a phenomenon in series, in which the effect of each single resistance is summed up, in a way somewhat similar to the approach used in Chapter 1 for finding the overall heat transfer coefficient. In fact, radial heat conduction through the wall can be modelled using the total thermal resistance of the pipe, defined as

$$R_{wall} = R_{cyl,1} + R_{cyl,2} + R_{cyl,3} = \frac{\ln {}^{r_2}/_{r_1}}{2\pi L k_1} + \frac{\ln {}^{r_3}/_{r_2}}{2\pi L k_2} + \frac{\ln {}^{r_4}/_{r_3}}{2\pi L k_3} \ , \tag{2.6}$$

where r_i are the radiuses of the different layers and k_i are the different materials thermal conductivity, as depicted in Figure 2.2.

Simple test calculations showed that the resistance of the lining and the steel pipe (respectively $R_{cyl,1}$ and $R_{cyl,2}$) can be neglected. In fact, the fusion bonded epoxy is thermally resistant (typical k is 0.251 $W/m{\cdot}K$), but its thickness is only some micrometers. On the contrary, the steel core is thicker, but its thermal resistance is really low (typical k is 50 $W/m{\cdot}K$). The concrete coating, being usually thicker (up to two or three times more) than the steel core and more thermally resistant (typical k is 1 $W/m{\cdot}K$) accounts for more than the 98% of the total thermal resistance.

Therefore, the best approach from a modelling point of view is to neglect the effect of the epoxy and steel layers, and to modify the external heat transfer coefficient (which accounts for the forced convection between the external surface and the surrounding water), as depicted in Figure 2.3. It would not make any difference to modify the internal heat transfer coefficient instead of the external.

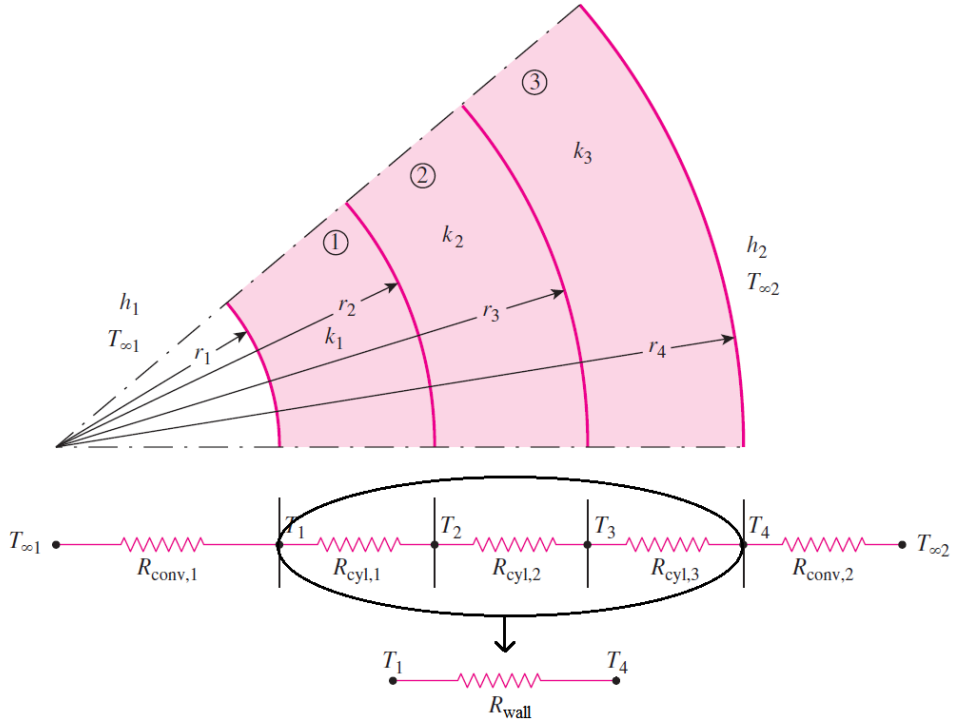

Figure 2.2: Modelling of the conduction through the multilayer wall by finding an overall wall thermal resistance (Adapted from Cengel, 2006).

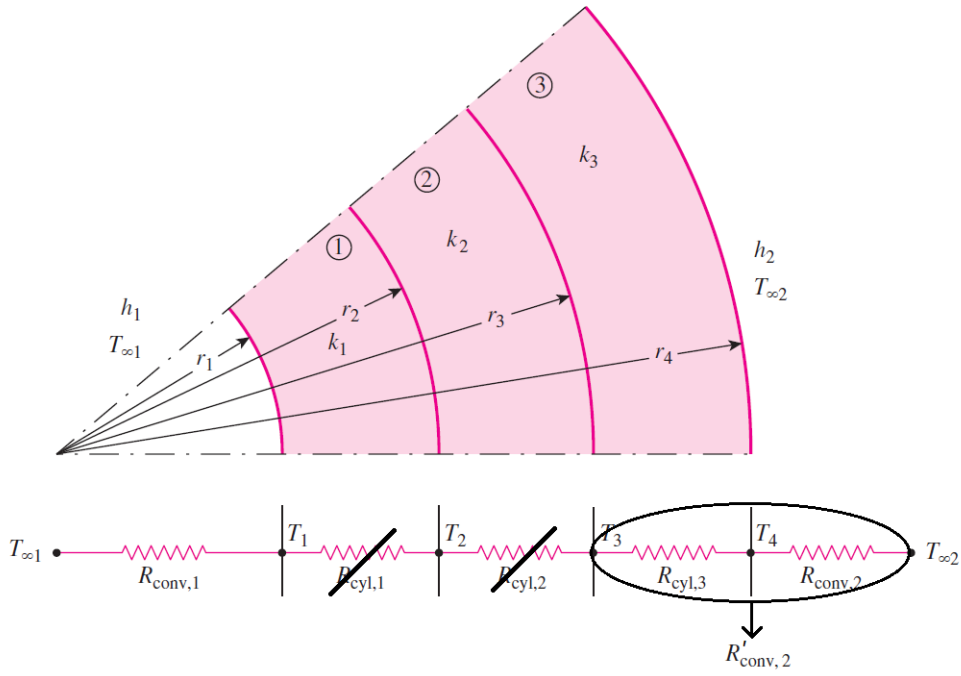

Figure 2.3: Modelling of the conduction through the multilayer wall by neglecting the epoxy and steel resistance and modifying the external thermal resistance (Adapted from Cengel, 2006).

In this way, the total thermal resistance has been calculated as

$$R_{tot} = R_{conv,1} + R'_{conv,2} \ , \tag{2.7}$$

where $R_{conv,1}$ is calculated by *Pipeline single-phase gML*, while $R_{conv,2}$ (which is calculated by the model too) has been customised into $R'_{conv,2}$, defined as

$$R'_{conv,2} = R_{cyl,3} + R_{conv,2} = \frac{\ln {}^{r_4}/_{r_3}}{2\pi L k_3} + \frac{1}{U_{w,a} A_o} \ . \tag{2.8}$$

Then, the corrected external heat transfer coefficient $U'_{w,a}$ is calculated as

$$U'_{w,a} = \frac{1}{R'_{conv,2} A_o} \ , \tag{2.9}$$

and used in the heat transfer equations previously explained (2.1 to 2.5).

Simple test simulations showed that the concrete layer insulation is low, so the heat transfer bottlenecks are internal and external forced convection. In fact, the layer is usually needed just to give weight to the pipeline and stabilise it, with no insulation intents. The axial profiles of the temperature with the customised model are perfectly overlapping the ones with the original model. In conclusion, infinitely fast heat conduction through the walls can be considered as a good assumption, leading to a negligible inaccuracy.

2.2.3 Discretisation and other features

The *Pipeline single-phase gML* model is a distributed one, so it needs to account for the properties variations along the pipeline length. For this reason, an axial discretisation must be included in the pipeline model, because solving the model in each single point of the pipeline is practically not feasible. In particular, the number of discretisation points, to be specified in each pipeline dialog box, consists in the number of points (equally spaced along the pipeline) in which the calculations are performed. Therefore, this number is not the number of volumes the pipeline is divided into, because it includes also the pipeline inlet and outlet.

It has to be specified that *Pipeline single-phase gML* uses a forward discretisation approach, meaning that the finite difference method for approximating derivatives in the numerical solution of differential equations is used in the forward form, in which the difference is calculated as

$$\Delta_h f(x) = f(x+h) - f(x) \ , \tag{2.10}$$

where f is the function, x is the variable and h is the increment.

Due to the fact that the pipeline is discretised, it is practically impossible to start a simulation from a dynamic condition. In fact, this feature is included in the *Pipeline single-phase gML* model but does not allow the user to specify each dynamic variable of interest in all the discretisation points, but only in the inlet of the pipeline. For these reasons the simulations have to start from a steady-state condition, in which the main assumption is that the initial conditions at the inlet are stable and propagate in the network, hence reaching the steady-state.

Eventually, it needs to be specified that the *Pipeline single-phase gML* model includes a multi-phase flow flag, which signals the formation of liquid in a gaseous flow, and vice versa. In particular, this feature performs a flash calculation in each discretisation point and time step of the simulation (through the Multiflash™ platform), and if even just one of these calculations leads to a vapour fraction which is different from 0 or 1, the software flags the multi-phase flow. This is achieved from and output point of view by colouring in red the pipeline (or pipelines) in which multi-phase flow is happening.

Chapter 3

Natural gas thermodynamics

The aim of this project is to predict, using a process simulator, the condensation of natural gas inside pipeline networks. Therefore, in this chapter natural gas thermodynamics will be discussed, introducing briefly the characteristic equilibrium between vapour and liquid, some key definitions and the main condensation phenomenon, called retrograde condensation. Then, some thermodynamic models that describe natural gas properties are discussed, and the thermodynamic validation against literature data is reported. The thermodynamic models have then been tested in gPROMS® ProcessBuilder to understand which is the most appropriate one for dynamic simulations.

3.1 Phase behaviour and definitions

Natural gas is a mixture of different light hydrocarbons and some contaminants, and the physical properties depend strongly on this variety of constituents. Understanding the equilibrium between vapour and liquid and the characteristic phenomena linked to it, as well as describing accurately this equilibrium with a thermodynamic model, is key in predicting the possible liquefaction, which represents a threat to the gas processing facility.

3.1.1 Phase diagram

The equilibrium between vapour and liquid for natural gas mixtures is depicted in phase diagrams, also known as phase envelopes, mostly plotted with temperature on the x-axis and pressure on the y-axis (therefore called P-T phase envelopes). The P-T phase envelope of a natural gas mixture can be seen in Figure 3.1. As a rule of thumb, the heavier is the mixture the bigger is the phase envelope, but there are exceptions and the shape is strictly dependent on each component molar fraction. For example, if a mixture is particularly rich in CO_2 its phase envelope tends to be narrower and pushed towards higher temperatures and pressures.

The key components of a phase envelope are the lines of equilibrium, where multiple phases can coexist at equilibrium. They are also known as phase boundaries because phase transitions occur along them. In particular, the bubble point curve is the set of points which separates the pure liquid region from the multi-

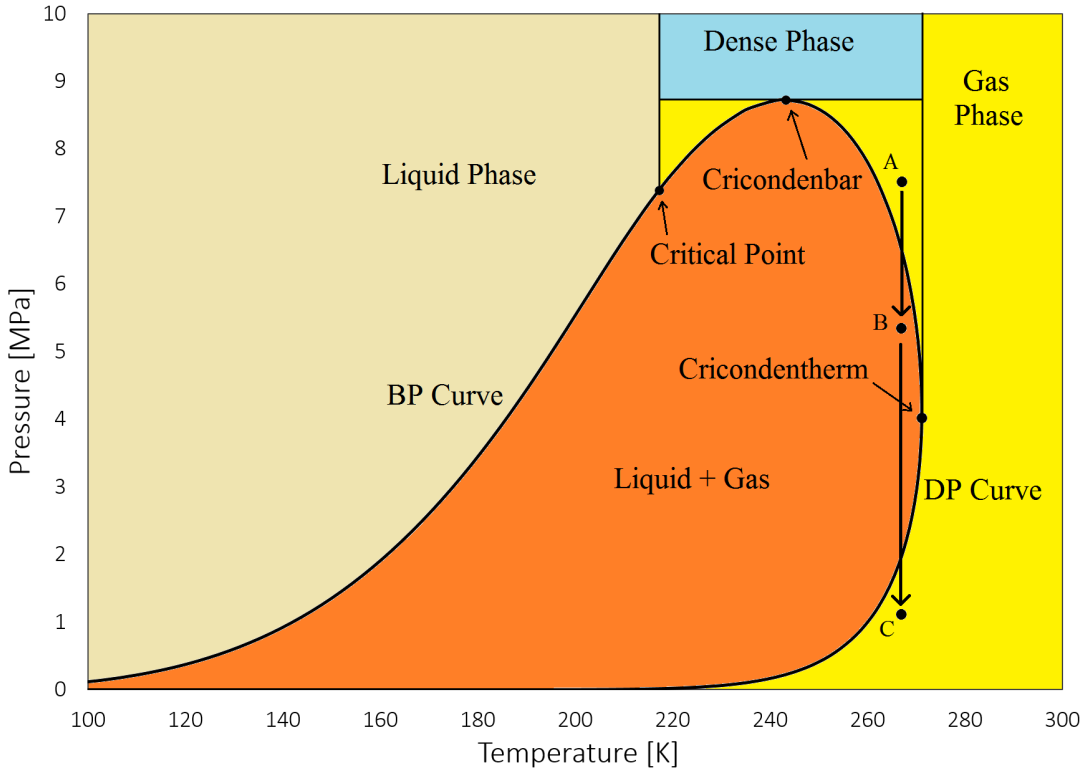

Figure 3.1: Typical phase envelope of a natural gas mixture with main definitions. The arrows and points explain the retrograde condensation phenomenon. Source: Multiflash™ calculation with custom natural gas mixture.

phase region, while the dew point curve is the set of points which separates the pure gas region from the multi-phase region. Another important component of a phase envelope is the critical point, where the bubble point curve and the dew point curve meet, and the properties of the gas and the liquid are identical. An equally important component in a phase envelope is the triple point, where the lines of equilibrium insect and vapour, liquid and solid phases coexist. However, natural gas is a light mixture which freezes at extremely low temperatures (under −180°C), so usually in its phase envelope the solid phase is not considered. Furthermore, natural gas P-T phase envelope needs two 'exclusive' definitions due to its characteristic and unique shape. The *cricondentherm* is the highest temperature at which liquid and vapour can coexist, (at higher temperatures there is only gas) while the *cricondenbar* is the highest pressure at which liquid and vapour can coexist. At pressures higher than the cricondenbar the state of the fluid depends only on the temperature: above the cricondentherm it is considered as a gas, below the critical point as a liquid, and in between it is in a particular state called *dense phase*. Natural gas in the dense phase has a high density (similar to that of a liquid), but a low viscosity (similar to that of a gas), making this state the most favourable for transporting compounds through pipelines.

One has to specify that there is much uncertainty about the definition of natural gas phases, and that different papers give different interpretation to the same phase envelope. This uncertainty is increased by the fact that all the so-called PVT software (such as the Multiflash™ platform used in this project), which calculate the phase behaviour of fluids, do not have the definition of dense phase,

but only that of the main phases: gas, liquid and solid. The PVT software interpretation of the natural gas phase envelope can be seen from Figure 3.2. Above the cricondenbar temperature (the highest temperature at which it is possible to find two phases) PVT software consider the fluid as a gas, while below the cricondenbar temperature it is considered as a liquid. This interpretation could lead to incongruencies and errors when simulating a pipeline in order to predict liquid formation, because the software can consider as a liquid a fluid which is actually in the dense phase. However, the physical properties of the natural gas vary with continuity when temperature and pressure change also during the phase transitions, so uncertainty is just a matter of labels and names, while what really matters are the fluid properties (such as the density). For example, from the dense phase, decreasing the temperature the molecules aggregate and the fluid reaches the liquid phase without step changes in the density.

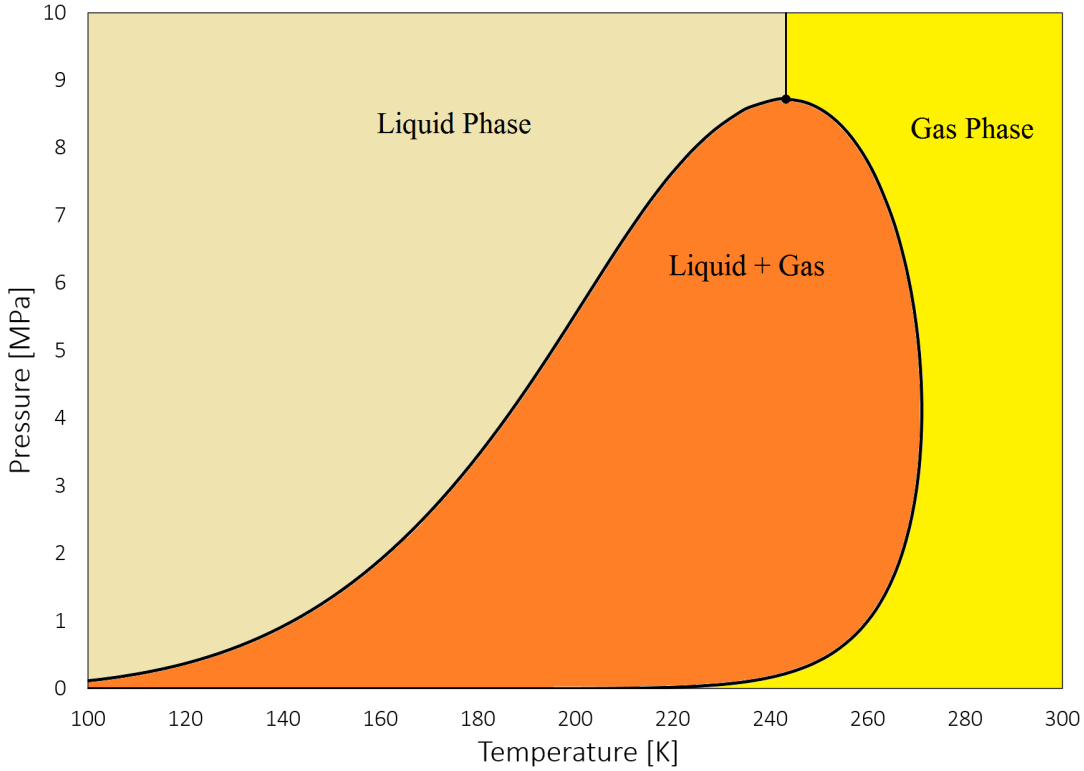

Figure 3.2: PVT software interpretation of a natural gas phase envelope. Source: Multiflash™ calculation with custom natural gas mixture.

3.1.2 Retrograde condensation

A key phenomenon in natural gas phase behaviour is retrograde condensation, which leads to multi-phase flow inside of pipelines. Retrograde condensation path is described by the vertical arrows and points in Figure 3.1. This phenomenon consists in the partial condensation of a natural gas mixture originally in gas phase or dense phase (path from point A to B in Figure 3.1), following a decrease in pressure, which is usually due to the pressure drop inside a pipeline network (but can also be due to an abnormal situation such as a leakage or an equipment failure). Then, if the pressure keeps decreasing, there is total vaporisation (path

from point B to C in Figure 3.1). This phenomenon is called *retrograde* because it is opposed to normal fluid behaviour, for which an increase in pressure leads to condensation, and it appears only among hydrocarbon mixtures. Ideally, one would wish the natural gas to be always over the cricondentherm, so it cannot be retrograde condensed by the pressure drop in the network.

3.2 Thermodynamic models

In order to account for the fluctuations in the composition of the gas mixture, the thermodynamic model used to describe the natural gas behaviour has to be compositional. Compositional models are based on a thermodynamically consistent model such as a cubic equation of state, and take into account the composition fluctuations that take place in pipeline networks. They are usually much more detailed than the black-oil models, which are based on simple interpolation of PVT properties as a function of pressure and are therefore independent on composition. The Equations of State (from now on referred as EoSs) considered in the thermodynamic validation are the Soave-Redlich-Kwong EoS, the Peng-Robinson EoS, and the GERG-2008 EoS.

3.2.1 Soave-Redlich-Kwong Equation of State

The Soave-Redlich-Kwong Equation of State is a cubic EoS developed by Giorgio Soave in 1972 at ENI by modifying the Redlick-Kwong EoS (which dates back to 1949). Cubic EoSs are called such because they can be rewritten as a cubic function of the molar volume V_m. Soave's modification replaces the $\sqrt{T}$ found in the denominator of the attractive term in the original equation with a more complicated temperature-dependent expression ($\alpha = f(T)$). It is currently one of the most widely used EoSs for describing VLE in the refinery and gas-processing industry, along with Peng-Robinson EoS. Soave-Redlich-Kwong EoS is described by

$$p = \frac{RT}{V_\mathrm{m} - b} + \frac{a}{V_\mathrm{m}(V_\mathrm{m} + b)} \ , \tag{3.1}$$

where, in case of mixtures, a and b are parameters calculated from functions of each pure component's critical temperature $T_{c,i}$, critical pressure $p_{c,i}$ and acentric factor ω_i :

$$a_i = a_{c,i}\,\alpha_i \ , \tag{3.2}$$

$$a_{c,i} = 0.45724\frac{R^2 T_{c,i}^2}{p_{c,i}} \ , \tag{3.3}$$

$$\alpha_i = \left(1 + \kappa_i\left(1 - \sqrt{T/T_{c,i}}\right)\right)^2 \ , \tag{3.4}$$

$$\kappa_i = 0.48 + 1.574\omega_i - 0.17\omega_i^2 \ . \tag{3.5}$$

The standard van der Waals mixing rules for EoSs are applied:

$$a = \sum_{ij} y_i y_j \sqrt{a_i a_j}(1 - k_{ij}) \ , \tag{3.6}$$

$$b = \sum_{i} y_i b_i \ , \tag{3.7}$$

$$b_i = 0.0778 \frac{R T_{c,i}}{p_{c,i}} \ . \tag{3.8}$$

k_{ij} , usually known as binary interaction parameters (BIPs), are adjustable factors used to alter the predictions from a model in order to improve its efficiency and reproduce as closely as possible the experimental data. BIPs are *binary* because they apply between pair of components. They are usually calculated by fitting experimental VLE and LLE experimental data to the equations of the model, and are therefore considered as *adjustable*. Most frequently, the fitting procedure is based on binary equilibria data, but it could also be based on information involving more than two components. The smaller is the value of the BIP, the closer is the binary system to ideality. If the thermodynamic model is more complicated (e.g. when non-standard mixing rules are used) more than one BIP might be required for each couple of components. The BIPs for Equation of State methods are usually dimensionless.

3.2.2 Peng-Robinson Equation of State

The Peng-Robinson cubic Equation of State was developed by Ding-Yu Peng and Donald B. Robinson in 1976 at The University of Alberta by further modifying the Redlich-Kwong EoS (in particular, its attractive term). The temperature dependence of the α term is kept, as suggested by Soave's modification. Peng-Robinson EoS is described by

$$p = \frac{RT}{V_\mathrm{m} - b} + \frac{a}{V_\mathrm{m}^2 + 2bV_\mathrm{m} - b^2} \ , \tag{3.9}$$

where, in a similar way to Soave-Redlich-Kwong EoS,

$$a_i = a_{c,i}\, \alpha_i \ , \tag{3.10}$$

$$a_{c,i} = 0.45724 \frac{R^2 T_{c,i}^2}{p_{c,i}} \ , \tag{3.11}$$

$$\alpha_i = \left(1 + \kappa_i \left(1 - \sqrt{T/T_{c,i}}\right)\right)^2 \ , \tag{3.12}$$

$$\kappa_i = 0.37464 + 1.54226\omega_i - 0.26992\omega_i^2 \ . \tag{3.13}$$

The standard van der Waals mixing rules for EoSs are applied, as for Soave-Redlich-Kwong EoS. The equations are identical to 3.6 and 3.7, and there is a slight change in the coefficient to calculate the b_i parameter:

$$b_i = 0.08664 \frac{R T_{c,i}}{p_{c,i}} \ . \tag{3.14}$$

The Peng–Robinson EoS typically gives similar VLE equilibria properties as Soave-Redlich-Kwong EoS, but often gives better estimations of the liquid phase density, especially if it is nonpolar.

3.2.3 GERG-2008 Equation of State

The GERG-2008 EoS is an industry standard (ISO 20765-2/3) model, recommended for natural gases, which has a strong empirical nature. It has been developed at the Ruhr-Universität Bochum (University of Bochum), and is described in a publication by Kunz and Wagner (2012). The equation is based on 21 natural gas components: methane, ethane, propane, n-butane, isobutane, n-pentane, isopentane, n-hexane, n-heptane, n-octane, n-nonane, n-decane, nitrogen, hydrogen, oxygen, carbon monoxide, carbon dioxide, water, hydrogen sulfide, helium, and argon. GERG-2008 EoS covers the homogeneous gas phase, liquid phase, supercritical region (dense phase), and vapour-liquid equilibrium states for mixtures of the components mentioned above (each component can cover the entire composition range). The extended validity range reaches from 60 to 700 K and up to 70 MPa. Moreover, the equation can be reasonably extrapolated beyond the extended range.

The GERG-2008 EoS is based on a multi-fluid mixture model, which is explicit in the Helmholtz free energy a as a function of the density ρ, the temperature T and the composition $\bar{x}$ (mole fractions) of the mixture. The EoS is usually reported using the dimensionless Helmholtz free energy $\alpha = a/RT$, which can be split into a term α^0, representing the properties of ideal-gas mixtures, and a term α^r, accounting for the residual mixture behaviour:

$$\alpha(\delta, \tau, \bar{x}) = \alpha^0(\rho, T, \bar{x}) + \alpha^r(\delta, \tau, \bar{x}) \ , \tag{3.15}$$

where δ is the reduced density of the mixture and τ is the inverse reduced temperature of the mixture according to

$$\delta = \frac{\rho}{\rho_r(\bar{x})} \quad \text{and} \quad \tau = \frac{T_r(\bar{x})}{T} \ , \tag{3.16}$$

with ρ_r and T_r being the reducing functions for density and temperature, which only depend on the composition of the mixture and turn into the critical properties ρ_c and T_c, respectively, for the pure components.

The dimensionless Helmholtz free energy for the ideal-gas mixture α^0 is given by

$$\alpha^0(\rho, T, \bar{x}) = \sum_i x_i \Big(\alpha^0_{0,i}(\rho, T) + \ln x_i \Big) \ , \tag{3.17}$$

where $\alpha^0_{0,i}$ is the dimensionless Helmholtz free energy in the ideal-gas state of component i.

The residual part of the dimensionless Helmholtz free energy of the mixture α^r is calculated as

$$\alpha^r(\rho, \tau, \bar{x}) = \sum_i x_i \alpha^r_{0,i}(\delta, \tau) + \Delta\alpha^r(\delta, \tau, \bar{x}) \ , \tag{3.18}$$

where $\alpha^r_{0,i}$ is the residual part of the reduced Helmholtz free energy of component i, and $\Delta\alpha^r$ is the so-called departure function. Therefore, the first term of equation 3.18 takes into account the contribution of the pure substances, while the second

term additionally depends on the composition of the mixture. The departure function is calculated as

$$\Delta\alpha^r(\delta,\tau,\bar{x}) = \sum_{i=1}^{N-1}\sum_{j=i+1}^{N} x_i x_j F_{ij}\alpha_{ij}^r(\delta,\tau) \ , \tag{3.19}$$

where α_{ij}^r is the part of $\Delta\alpha_{ij}^r(\delta,\tau,\bar{x})$ (the reduction function of the components i and j) which does not depend on the composition of the mixture. F_{ij} parameter is fitted to improve the results in the calculation of the properties of some specific binary mixture.

Unless specified otherwise, each summation term is extended to the total number of components in the mixture N (which in the case of GERG-2008 EoS can be at most 21). For a detailed description of each single equation and term of the model, and for the calculation of the physical properties, see the original publication by Kunz and Wagner (2012).

3.3 Choice of the thermodynamic model

The choice of the thermodynamic model to be used in dynamic simulations is critical in terms of accuracy and computational times. For this reason a thermodynamic validation has been done against two experimental mixtures, to assess which model gives the highest accuracy, and the models have then been tested in dynamic simulations to understand their computational heaviness.

3.3.1 Thermodynamic validation

The thermodynamic validation has been done using two different experimental mixtures from Avila et al. (2002). The compositions of the mixtures are reported in Table 3.1. The results of the validation are shown in Figure 3.3 (Gas 1) and 3.4 (Gas 2).

The most accurate model is, as expected, the GERG-2008 EoS, which fits the experimental data almost perfectly, except for the highest pressures. The Peng-Robinson EoS is less accurate in the prediction of the lines of equilibrium, so it should not be used unless the use of GERG-2008 EoS is not feasible. In between stands the Soave-Redlich-Kwong EoS, with an accuracy slightly higher than the Peng-Robinson EoS. However, for neither of the models the Binary Interaction Parameters have been regressed. The BIPs have been kept as the ones regressed and stored in the Multiflash™ database, as their regression for the desired range of specifications has been considered as not part of the project (and the accuracy of the default Multiflash™ BIPs has been considered as plausible). It is therefore not correct to classify the GERG-2008 EoS as the best one, because the Peng-Robinson EoS and Soave-Redlich-Kwong EoS results might be more accurate if the BIPs are re-regressed. For sure, from a theoretical point of view, the higher number of parameters and the empirical nature of the GERG-2008 EoS make it the most trustful one when dealing with natural gas mixtures.

One can notice that the predicted phase envelope of Gas 2 is less accurate than the one for Gas 1, and in both of the cases accuracy is lower at high pressures. Inaccuracy is more marked in the Gas 2 validation because the mixture is more

Table 3.1: Code names and compositions (molar fraction) for natural gas experimental mixtures. Both mixtures from Avila et. al. (2002).

Component	Gas 1	Gas 2
N_2	0.05651	0.069
CO_2	0.00284	0.0051
C1	0.833482	0.88188
C2	0.07526	0.0272
C3	0.02009	0.0085
i-C4	0.00305	0.0017
n-C4	0.0052	0.0032
i-C5	0.0012	0.00085
n-C5	0.00144	0.00094
n-C6	0.00068	0.00119
n-C7	0.000138	0.00026
n-C8	0.00011	0.00018

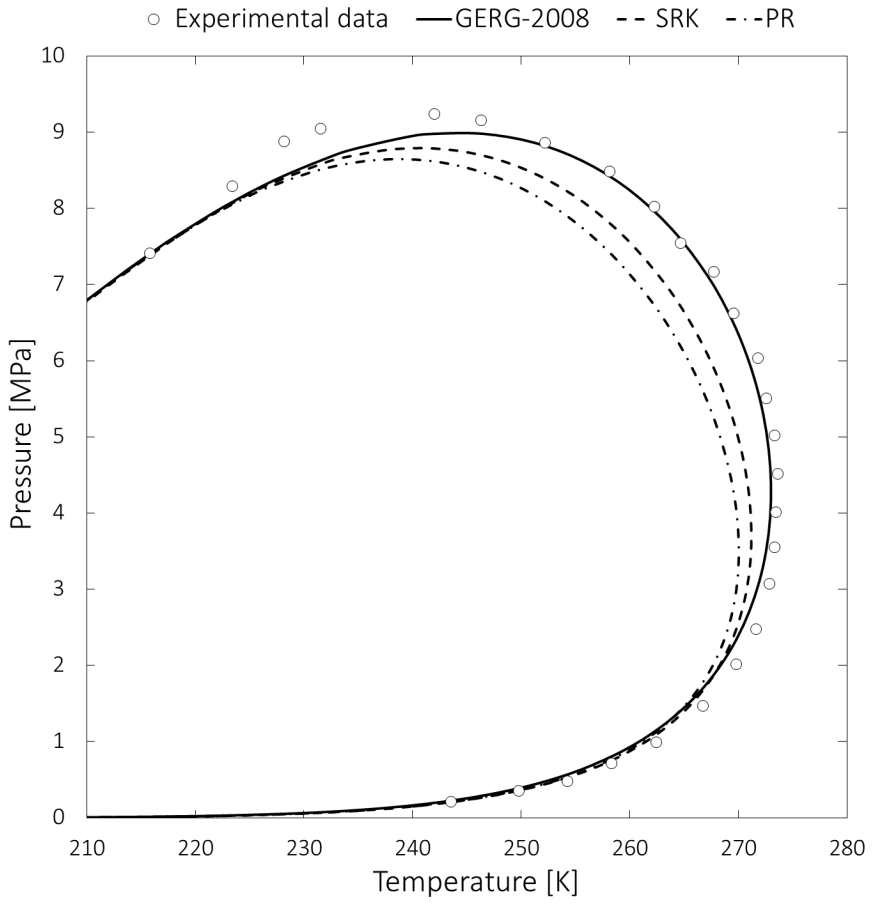

Figure 3.3: Experimental points and predicted phase envelopes for the mixture Gas 1. Source: Multiflash™.

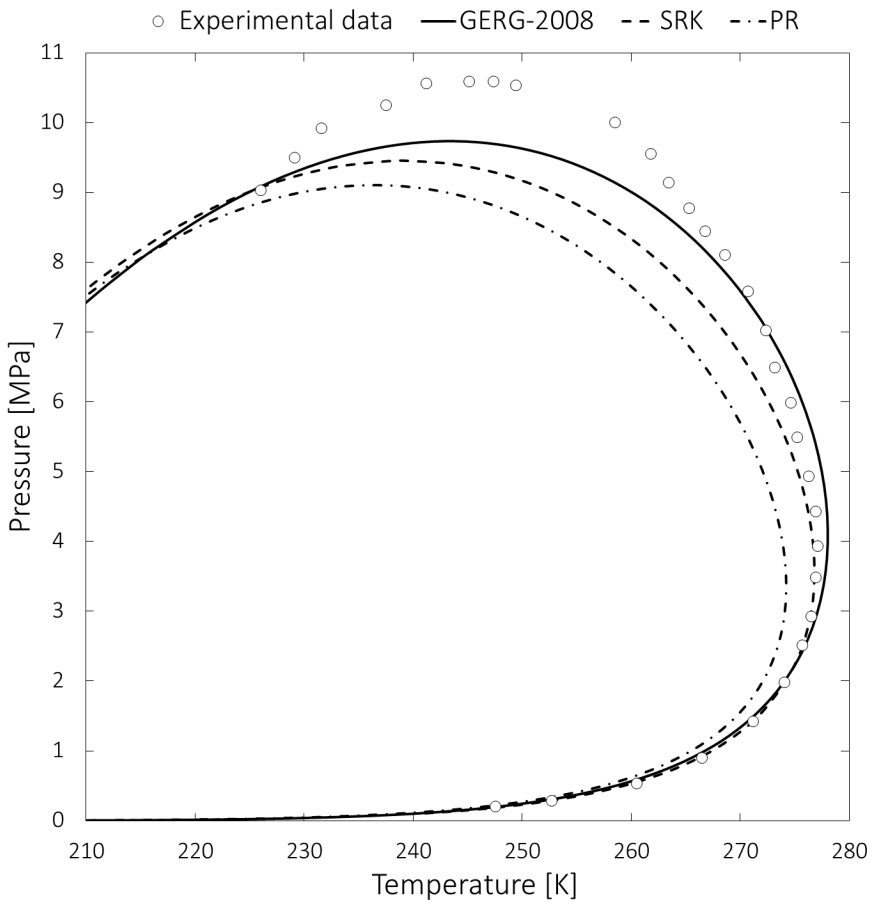

Figure 3.4: Experimental points and predicted phase envelopes for the mixture Gas 2. Source: Multiflash™.

condensable than Gas 1, and therefore has an higher cricondenbar (around 11 MPa). The fact that Gas 2 is more condensable than Gas 1 can be difficult to be seen from Table 3.1. In fact, Gas 2 is richer in light components (5% more in methane at the expense of ethane), therefore is lighter than Gas 1 (average molecular weight of respectively 18.06 g/mol and 18.98 g/mol), but it is also richer in heavy components (almost double the molar fractions in hexane, heptane and octane). Test simulations and theoretical studies, e.g. Voulgaris (1995), showed that the phase envelope of a natural gas, hence its cricondenbar and the retrograde condensation phenomenon, is strongly affected by the heavy fractions of the mixture. Therefore, in order to assess if a mixture can be labelled as light or heavy in terms of condensability, one needs to look not only to the preponderant light components (and to the molecular weight of the mixture), but also to the smaller fractions of heavy components.

In conclusion, if the aim of a simulation is to predict the condensation of natural gas, using Peng-Robinson EoS or Soave-Redlich-Kwong EoS can be risky because of their inaccuracy. In fact, the phase envelope is always under-estimated, and this leads to non-conservative results in terms of condensation (there might be unpredicted condensation if the pressure or the temperature in the network decrease). However, none of the EoSs is perfectly accurate, therefore there might be unpredicted condensation in the network also using the most accurate GERG-2008 EoS.

3.3.2 Thermodynamic model in dynamic simulations

As already mentioned earlier on, the main feature of an online flow assurance software is the small computational time. Therefore, some tests have been run to understand the difference in computational time of the three thermodynamic models when used in gPROMS® ProcessBuilder dynamic simulations.

The flowsheet, named 'Test Pipeline' and shown in Figure 3.5, includes a *Source gML*, a *Sink gML*, and a single *Pipeline single-phase gML* model whose specifications are collected in Table 3.2. The specifications have been selected to be similar to those of pipelines which could be found in existing networks. The solver used in this set of simulations has been DASOLV, a slow 'old-generation' solver, which is still the default one in gPROMS® ProcessBuilder. This justifies the huge difference in computational time between these simulations and the ones in the following chapters, in which the fast 'new-generation' DAEBDF solver has been used.

Figure 3.5: 'Test Pipeline' flowsheet. Source: gPROMS® ProcessBuilder.

Table 3.2: Specifications of the 'Test Pipeline' flowsheet.

Specification	[−]
Lenght	50 km
Internal Diameter	0.4 m
Wall thickness	0.04 m
Surface roughness	5E−5 m
Sink pressure	110 bar
Simulation mode	Pressure-driven
Heat Transfer Coefficients	Calculated
Dynamic Momentum Balance	On
Convective Transport of Momentum Term	On
Initial conditions	Steady-state
Simulated time	100 000 sec
Reporting interval	100 sec

The case study considers a step change in the composition of the mixture, and it has therefore been named *Heavier* (widely analysed in the following chapter, its details are collected in Table 4.1). The number of discretisation points of the pipeline has been changed in simulations using both the thermodynamic models, and the different computational times are collected in Table 3.3.

This analysis showed that, due to its high complexity, GERG-2008 EoS is extremely more computationally burdensome than the Peng-Robinson and Soave-Redlich-Kwong EoSs. Furthermore, one can see from Table 3.3 that the computational times of the Peng-Robinson and Soave-Redlich-Kwong EoSs have the same

Table 3.3: Computational times of the 'Test Pipeline' simulations with different number of discretisation points and thermodynamic models (Soave-Redlich-Kwong, Peng-Robinson and GERG-2008 EoSs). The simulations involve a composition step change.

Discretisation points	**Computational time [s]**		
	SRK	PR	GERG-2008
10	40	61	2 256
20	59	69	4 351
30	184	154	8 403
40	1 113	543	196 133

order of magnitude. In particular, the Soave-Redlich-Kwong EoS has a slightly smaller computational time if the number of discretisation point is low, while its computational time is almost twice as the Peng-Robinson EoS one when the flowsheet is more detailed (higher number of discretisation points).

It is important to mention that the results of the simulations with the different EoSs are almost identical, meaning that the physical properties calculated with different models are similar. Tests showed that this stands unless a high fraction of liquid is formed in the pipeline (which is usually not the case). The main difference between the models is therefore just the prediction of the lines of equilibrium, so of the condensation in the pipeline.

In conclusion, it has been decided to use the simple Peng-Robinson EoS for the first tests and sensitivity analysis. In fact, until the network flowsheet is built, having a precise calculation of the fluid properties and predicting the condensation is not critical. However, these analyses are extremely useful to know if the results of the dynamic simulations are physical and to understand the best ways to reduce the computational time (which can prove as a difficult task from network simulations). The objective is to eventually switch to GERG-2008 EoS in network simulations in order to predict the condensation in the network, if the computational times are within the constraints. Therefore, from now on, unless specified otherwise, all the simulations are run with the Peng-Robinson EoS.

Chapter 4

Single pipeline simulations and sensitivity analyses

In this chapter the first simple simulations run in the gPROMS® ProcessBuilder environment are reported. These simulations are based on the 'Test Pipeline' flowsheet (shown in Figure 3.5), already used in Chapter 3 for the choice of the thermodynamic model. The aim of these simple simulations is to understand the behaviour of the natural gas flowing into a pipeline, which can be difficult from more complex simulations (such as network simulations). Furthermore, various sensitivity analyses have been performed on this simple model in order to obtain meaningful information on how to reduce the computational time of network simulations without performing them in the whole flowsheet itself. All simulations have been run in pressure-driven mode, in which the specifications are the flowrate at the source and the pressure at the sink, because those are the specifications in the actual network case study. While performing these simple simulations it has been noticed that the new DAEBDF solver is more stable and computationally faster than the default DASOLV, therefore the former has been used in all the following simulations.

4.1 Dynamic response

The response of the pipeline to dynamic inputs has been studied by individually step-changing two of the most important specifications which affect the behaviour of a network: the flowrate coming from each source, and the composition of the mixture that each source delivers. The details of the pipeline are the same as in the choice of the thermodynamic model, and are collected in Table 3.2. Then, the consistency of the results of the simulations has been proven by comparison with the results of gFLARE® (*Process Systems Enterprise*'s Oil & Gas technology whose model library includes a distributed pipeline model) and of a custom model built with lumped (non-distributed) pipelines.

After a step change occurs, the simulation is left running for 100 000 seconds, in order to reach a new steady-state. In fact, the length of the pipeline is 50 km and, with the chosen specifications, the residence time is approximately 60 000 seconds. However, physical phenomena and numerical effects (which will be discussed later in this chapter) make the steady-state to be reached only after around

80 000 − 100 000 seconds, and this justifies the choice of the simulation time. Due to the simplicity of the simulations, the reporting interval can be chosen as relatively small (100 seconds). The initial conditions are, as always, steady-state, and the number of discretisation points of the pipeline is 20.

4.1.1 Composition step change

In this analysis the composition of the mixture at the source has been step-changed keeping the flowrate constant. In the first case study the step change made the mixture heavier (thus it has been named *Heavier*), while in the second case study the step change made the mixture lighter (thus it has been named *Lighter*). In order to reduce the computational time of the simulations, the mixtures have been selected as simpler than the actual ones which can be found in existing networks. In fact, just four components have been simulated, and the various compositions (specified as molar fractions) have been customised as round numbers. The flowate was fixed at 3 000 kmol/h and the compositions can be found in Table 4.1.

Table 4.1: Mixtures A, B and C used in the *Heavier* case study (step change from composition A to B) and in the *Lighter* case study (step change from composition A to C).

Component	**Molar fraction** [−]		
	A	B	C
CO_2	0.05	0.05	0.03
CH_4	0.85	0.8	0.9
C_2H_6	0.05	0.1	0.05
C_3H_8	0.05	0.05	0.02

The results show that the response time of the pipe to the change is really small. In fact, after changing the composition, the pressure at the source (and consequently in the whole pipe) changes almost instantaneously to keep the pressure at the sink (which is a specification) constant. This can be seen from Figure 4.1. Consistently with the pressure, also the density and the flowrate in the pipe change. When the heavier (or lighter) fluid reaches the sink the molar flowrate changes (Figure 4.3), and finally, when the new steady state is reached, it settles to the original value (which is a specification). One can see from Figure 4.4 that the mass flowrate settles instead to a new value because the average molecular weight of the mixture is changed. It can also be observed that the flowrate settles to the new value at a time which is the residence time in the pipeline (60 000 seconds). The same can be noticed with the molar fractions (Figure 4.5). The pressure settles to a value which is slightly different from the original one because the density of the mixture is changed (Figure 4.1).

The profiles in the *Heavier* and *Lighter* case studies are almost symmetrical, so reported in the figures are many profiles of the *Heavier* case study (from Figure 4.1 to 4.2), while just one for the *Lighter* case study (Figure 4.6) in order to compare the case studies and notice the symmetry. The chosen point of the pipe in which the profiles are plotted is the sink, because it has been considered as

the most meaningful one. In fact, in network simulations the focus is mainly on the terminal. However, the pressure at the sink is a non-changing specification, so pressure and density profiles are reported far from the sink and closer to the source, precisely at axial position 0.1 ($1/10^{\text{th}}$ of pipeline). Figure 4.7 shows the axial profile of the methane molar fraction in the pipe after 30 000 seconds in the *Heavier* case study. Close to the source (which coincide to axial position 0) the molar fraction is the one correspondent to the new mixture (mixture B in Table 4.1), while close to the sink (which coincide to axial position 1) the perturbation has not arrived yet, so the molar fraction is the one correspondent to the mixture before the step change (mixture A in Table 4.1).

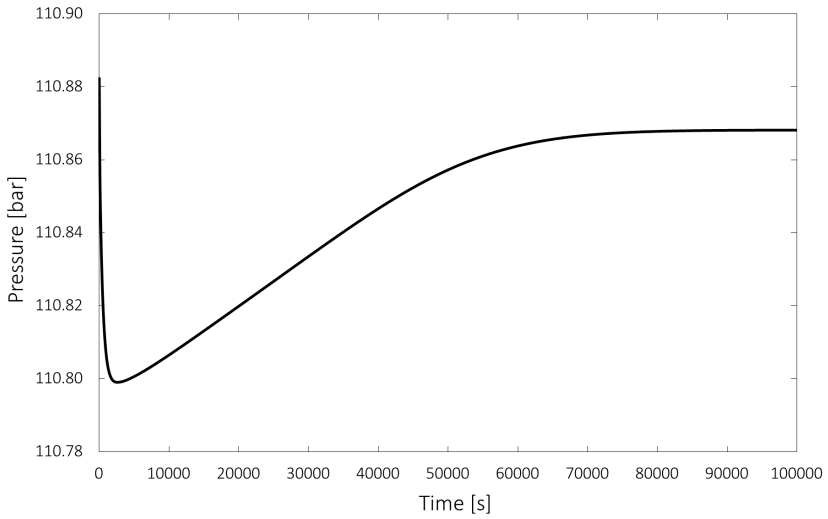

Figure 4.1: Profile over time of the pressure at axial position 0.1 in the *Heavier* case study, 'Test Pipeline' flowsheet. Source: gPROMS® ProcessBuilder.

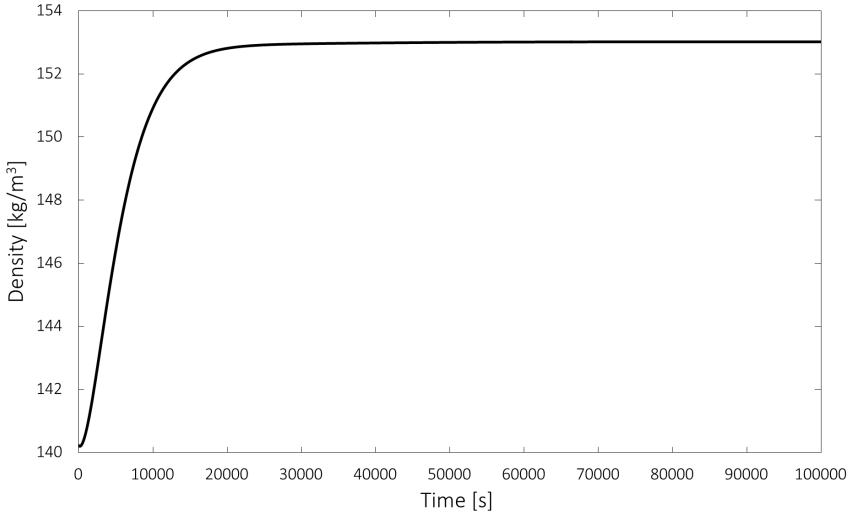

Figure 4.2: Profile over time of the density at axial position 0.1 in the *Heavier* case study, 'Test Pipeline' flowsheet. Source: gPROMS® ProcessBuilder.

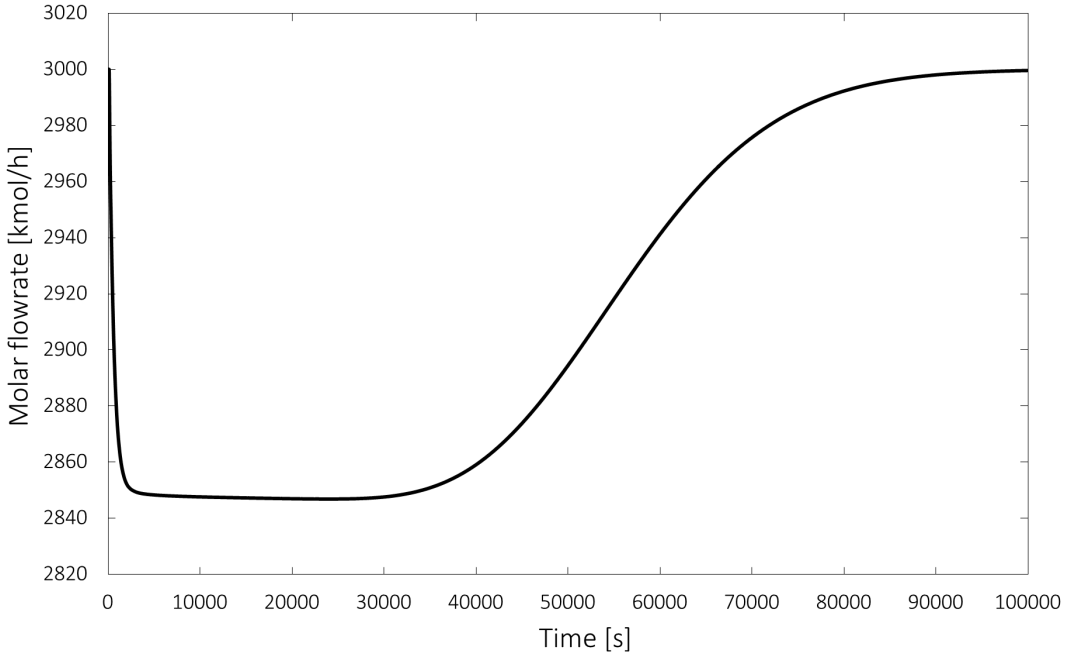

Figure 4.3: Profile over time of the molar flowrate at the sink in the *Heavier* case study, 'Test Pipeline' flowsheet. Source: gPROMS® ProcessBuilder.

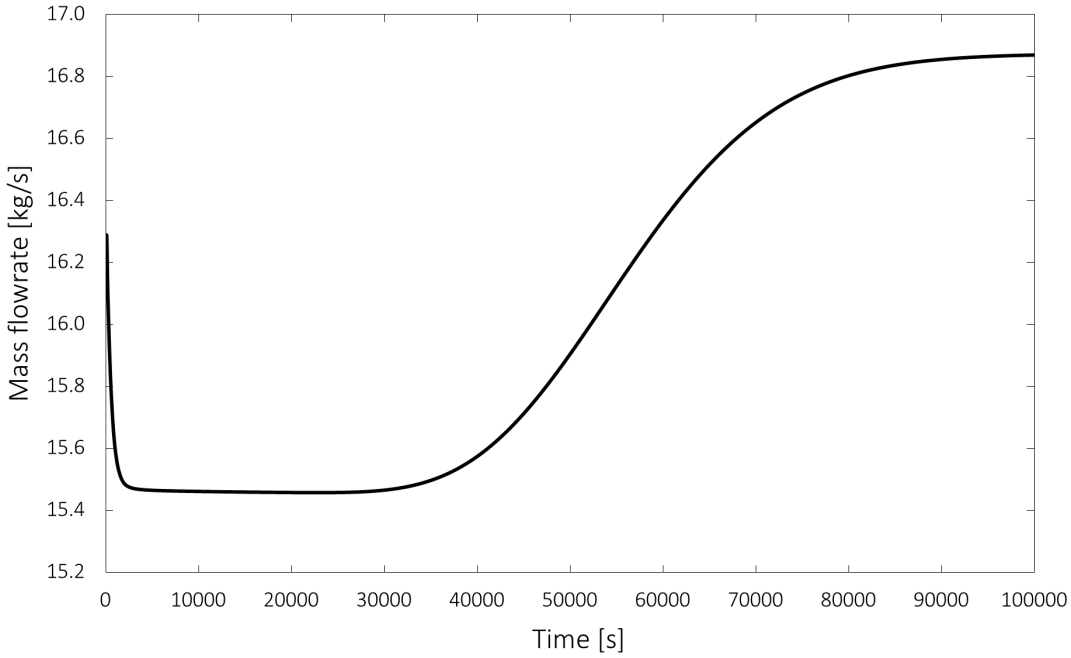

Figure 4.4: Profile over time of the mass flowrate at the sink in the *Heavier* case study, 'Test Pipeline' flowsheet. Source: gPROMS® ProcessBuilder.

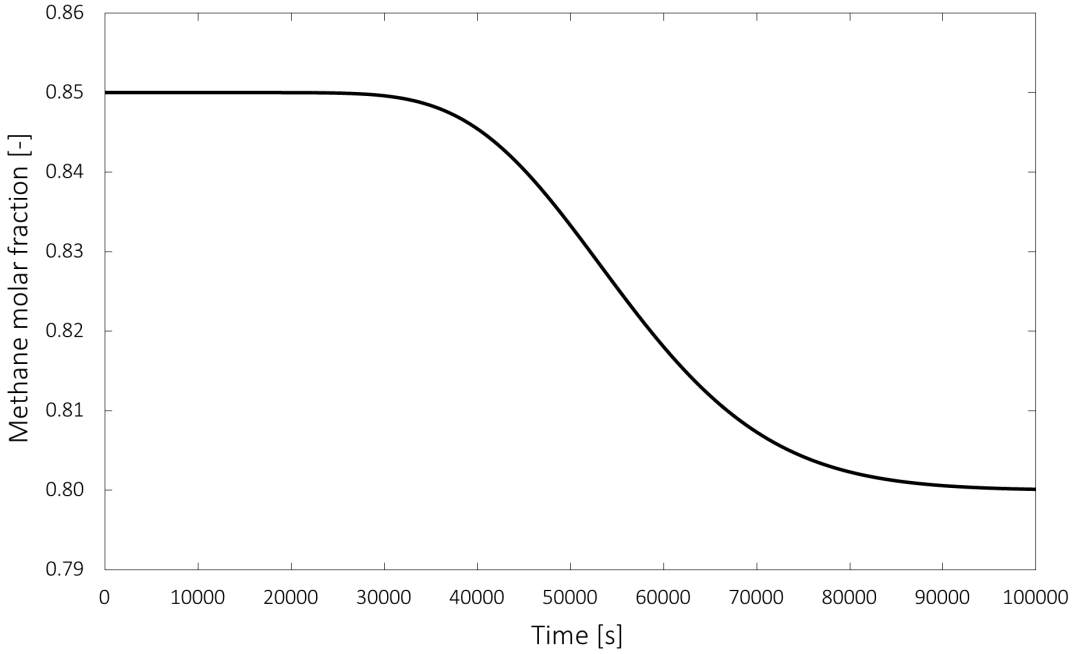

Figure 4.5: Profile over time of the methane molar fraction at the sink in the *Heavier* case study, 'Test Pipeline' flowsheet. Source: gPROMS® ProcessBuilder.

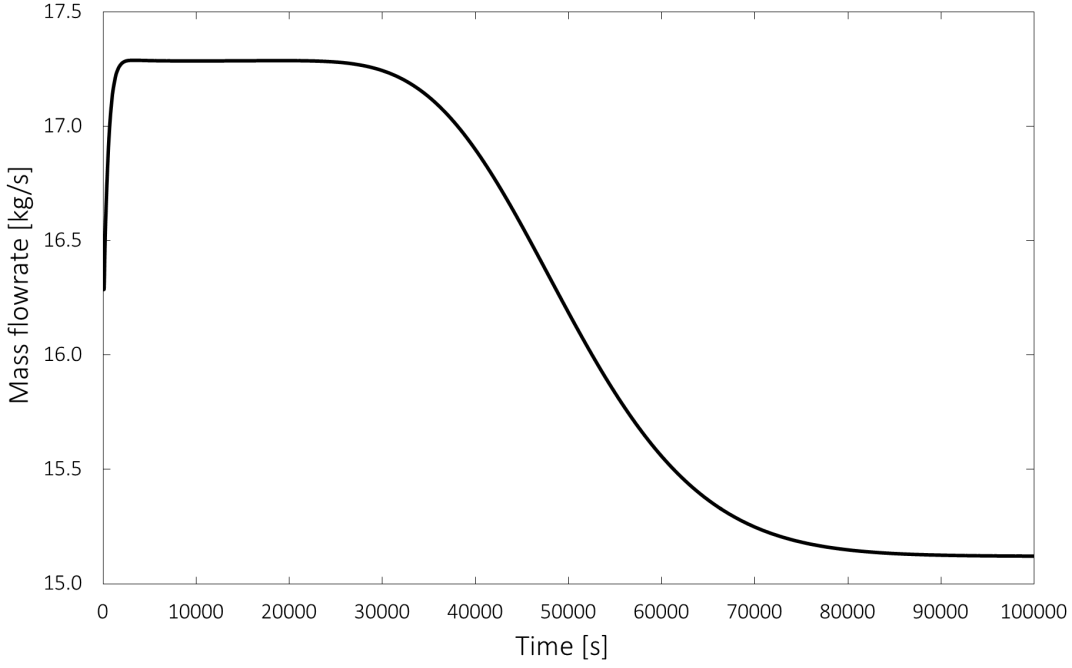

Figure 4.6: Profile over time of the mass flowrate at the sink in the *Lighter* case study, 'Test Pipeline' flowsheet. Source: gPROMS® ProcessBuilder.

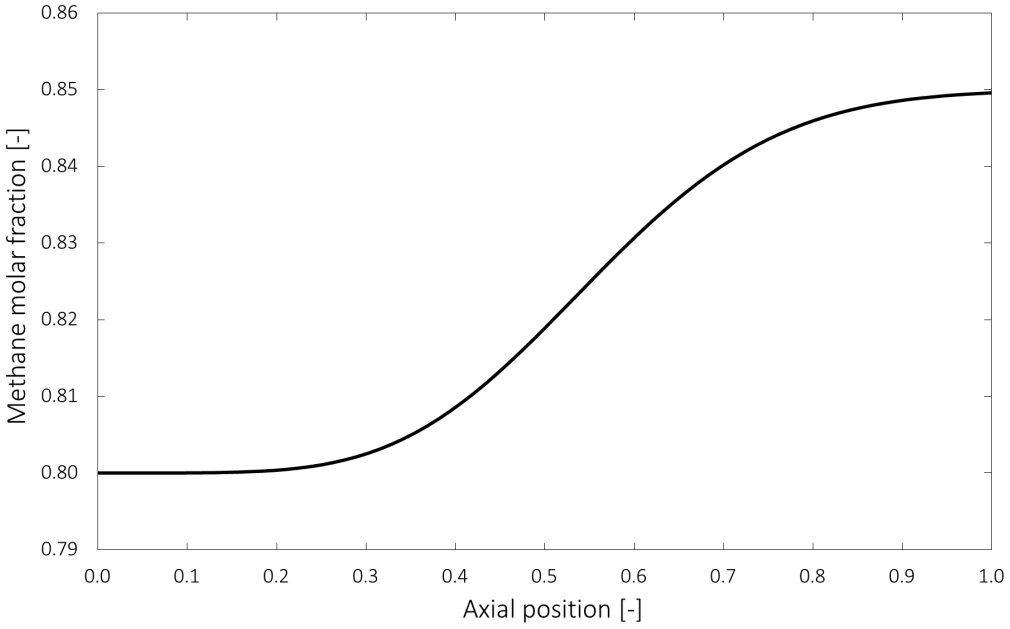

Figure 4.7: Axial profile of the methane molar fraction after 30 000 seconds in the *Heavier* case study, 'Test Pipeline' flowsheet. Source: gPROMS® ProcessBuilder.

4.1.2 Flowrate step change

In this analysis the flowrate at the source has been step-changed keeping the composition of the mixture constant (equal to composition A in Table 4.1). In both the case studies the starting flowrate is 3 000 kmol/h. In the first case study the step change is positive (increase of the flowrate to 3 500 kmol/h, thus named *More* case study), while in the second case study the step change has the same magnitude but is negative (decrease of the flowrate to 2 500 kmol/h, thus named *Less* case study).

As already seen with composition step changes, also with flowrate step changes the response time is really small. This is, again, due to the sudden change in the pressure, needed to flow more (or less) material in the pipe. However, in this case study there is no variation in the composition of the mixture, therefore the changes in the properties are monotonic. The flowrate 'travels' along the pipeline much faster than the species themselves, and consequently the response time is much smaller than the residence time. After just 3 000 seconds the new steady-state is reached in the pipeline, and it has been demonstrated that this time would have been even smaller if the fluid was incompressible (e.g. a liquid). The profiles are shown (in Figures 4.8 to 4.11) up to 10 000 seconds, because afterwards properties plateau to the final values. The results are shown for the *More* case study, while for the *Less* case study just one profile is reported to notice the symmetry with the *More* case study.

After modifying the flowrate at the source, the pressure changes accordingly in order to keep the pressure at the sink (which is a specification of the model in pressure-driven mode) constant. The density of the fluid is slightly modified by the pressure change, while the molar fractions are constant during the whole duration of the simulation. For this reason all the profiles are monotonic. As for

Heavier and *Lighter*, also for the *More* and *Less* case studies the pressure profile is plotted at axial position 0.1, while the flowrates are plotted at the sink.

From a closer look at the profiles of the molar and mass flowrate (Figures 4.9 to 4.11), one can spot a little delay in the first seconds of simulation (in which the property remains constant). This is a physically reasonable phenomenon, caused by the momentum which is propagating in the pipeline, in particular to its dynamic term. This topic will be analysed in detail in the following section.

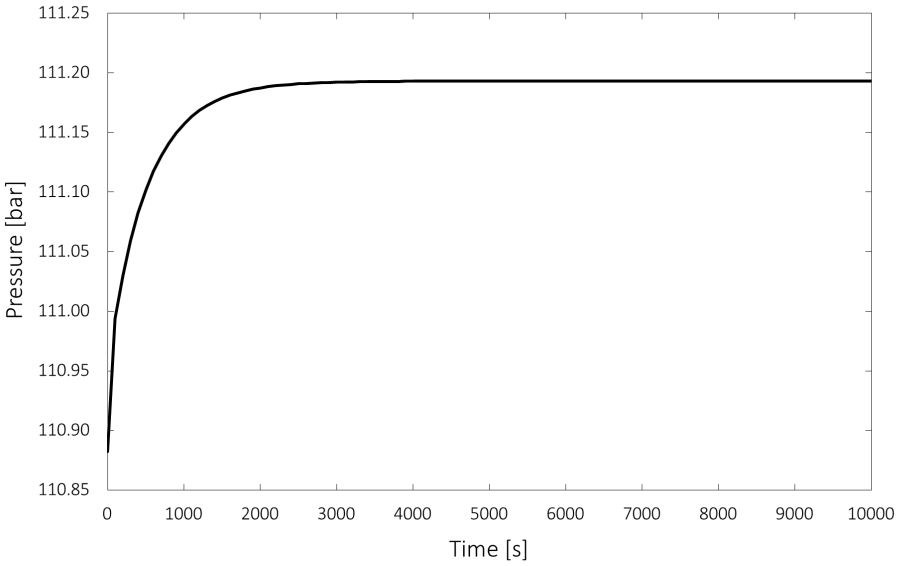

Figure 4.8: Profile of the pressure at axial position 0.1 over the first 10 000 seconds of simulation in the *More* case study, 'Test Pipeline' flowsheet. Source: gPROMS® ProcessBuilder.

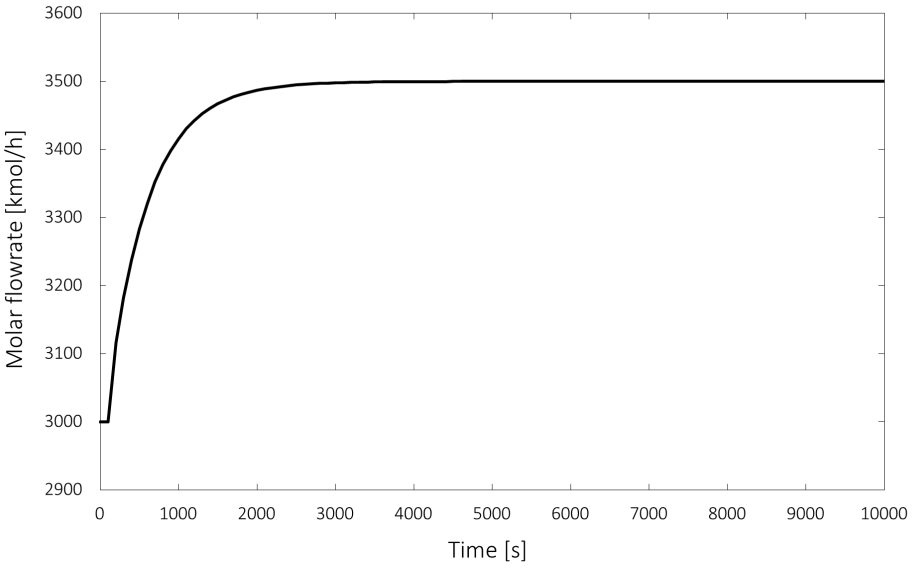

Figure 4.9: Profile of the molar flowrate at the sink over the first 10 000 seconds of simulation in the *More* case study, 'Test Pipeline' flowsheet. Source: gPROMS® ProcessBuilder.

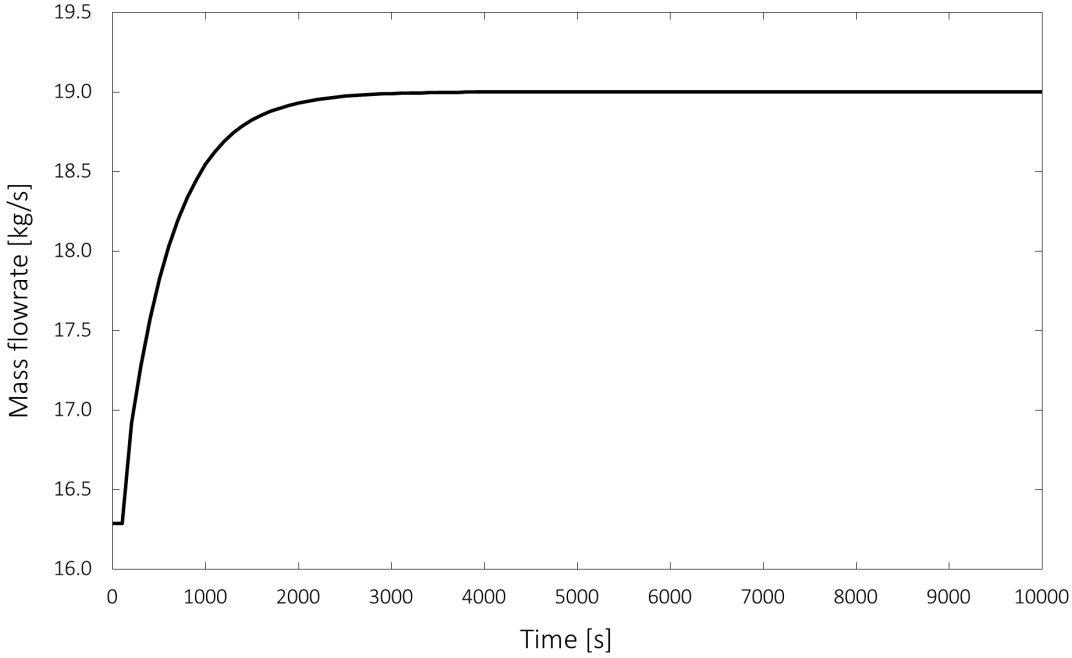

Figure 4.10: Profile of the mass flowrate at the sink over the first 10 000 seconds of simulation in the *More* case study, 'Test Pipeline' flowsheet. Source: gPROMS® ProcessBuilder.

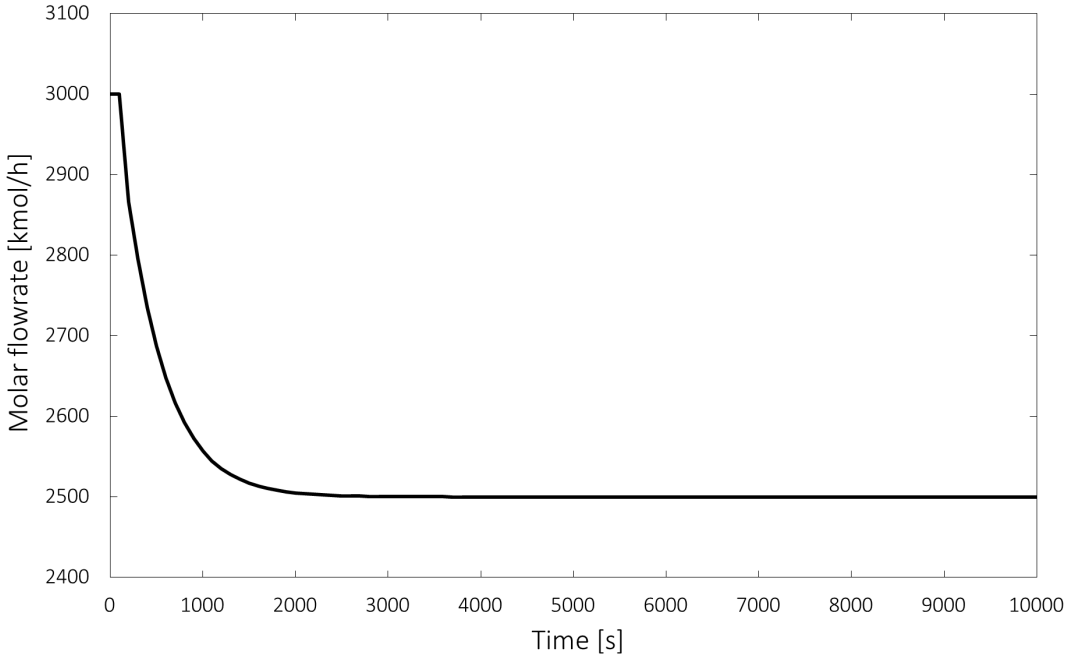

Figure 4.11: Profile of the molar flowrate at the sink over the first 10 000 seconds of simulation in the *Less* case study, 'Test Pipeline' flowsheet. Source: gPROMS® ProcessBuilder.

4.1.3 Consistency of the dynamic response

The consistency of the *Pipeline single-phase gML* results has been proven by comparison with the results of the gFLARE® distributed pipeline model and of a custom model built with lumped pipelines in gPROMS® ProcessBuilder.

gFLARE® is a product of *Process Systems Enterprise* which is mainly used by the Oil & Gas sector to model process equipment and piping in blowdown, pressure relief and flare systems. Its model library includes a distributed pipeline model similar to the ProcessBuilder one, but different from a numeric point of view. In fact, while *Pipeline single-phase gML* uses a forward discretisation scheme, gFLARE® model uses a finite volume approach.

The custom model is built in gPROMS® ProcessBuilder using the *Pipe gML* model. This model is lumped, meaning that the variation of the properties along the pipeline are not modelled, but each property is constant. Instead, the pressure drop in the pipe is considered, so by alternating the *Pipe gML* model with a *Junction gML* model, in which a volume (hence a dynamic hold-up) is defined, the distributed *Pipeline single-phase gML* is reproduced. 'Test Pipeline' had 20 discretisation points, so the custom flowsheet has been built alternating 19 *Pipe gML* model with 20 *Junction gML* model whose total volume is equal to the 'Test Pipeline' one. The two flowsheets used for the analysis are shown in Figure 4.12.

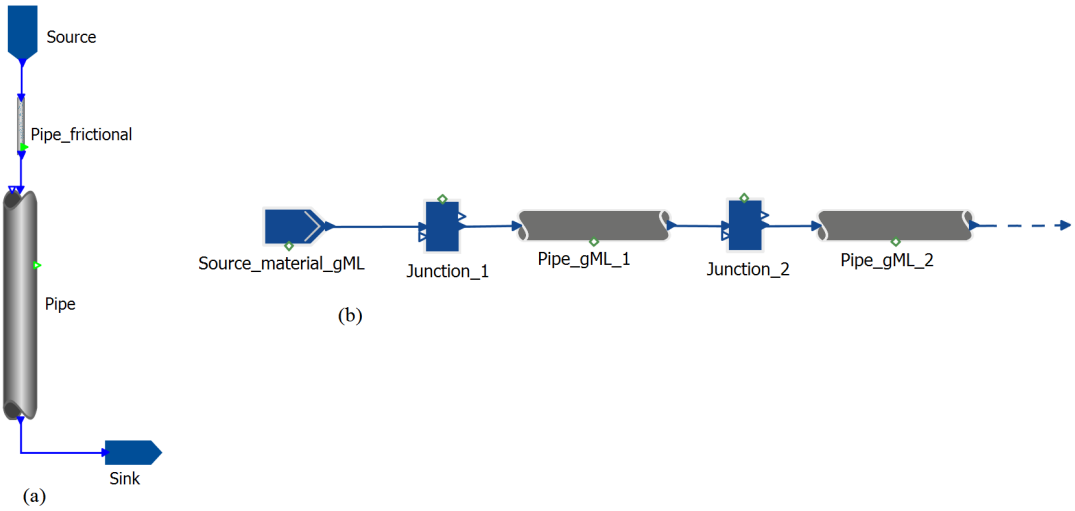

Figure 4.12: a) gFLARE®'s pipeline flowsheet; b) Custom flowsheet built with the alternation of 19 *Pipe gML* and *Junction gML* models in gPROMS® ProcessBuilder.

The case study involved a positive step change of the mass flowrate at the source, from 17 kg/s to 18 kg/s (really similar to the specifications of the *More* case study), and the results of the simulations with the three different models are almost identical. In particular, the profiles of the mass fraction at half pipe in the first 5 000 seconds of simulation are shown in Figure 4.13. The slight differences might be due to the numerical approaches and ways of discretisation of the models.

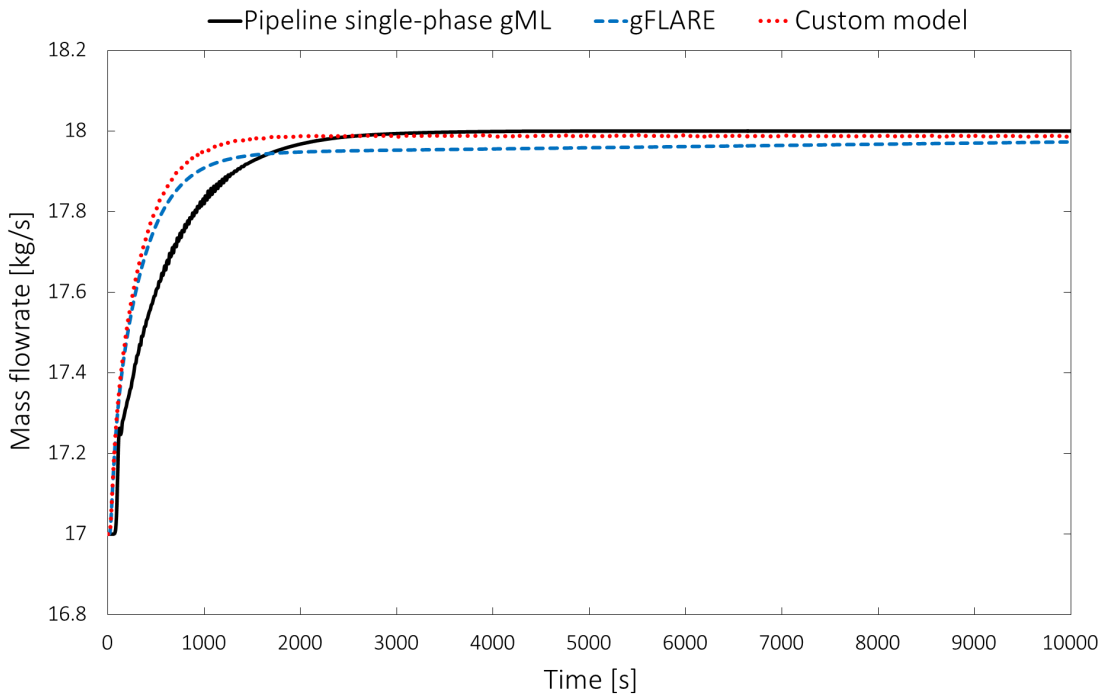

Figure 4.13: Profiles of the mass flowrate at half pipe over the first 10 000 seconds of simulation using the gPROMS® *Pipeline single-phase gML* model, the gFLARE® model and the custom model. Sources: gPROMS® ProcessBuilder and gFLARE®.

4.2 Sensitivity analyses

After proving the consistency of the simple simulations results, in order to make the network simulations feasible for online flow assurance applications the computational time must be reduced. This can be difficult and time-consuming if done on complicated flowsheets, so some sensitivity analyses have been performed on the 'Test Pipeline' flowsheet. The most meaningful analyses took into account the heat exchange, the momentum balance, the discretisation of the pipeline and the reporting interval of the simulation.

4.2.1 Heat exchange

In the *Pipeline single-phase gML* model the heat exchange can be either calculated for each discretisation point with various models (as already discussed in Chapter 1), fixed for the entire pipeline, or simply neglected (hence assuming adiabatic pipeline). The tests have been run on the 'Test Pipeline' flowsheet with 20 discretisation points and the *More* case study. In the case with calculated heat transfer coefficients, the chosen correlation is the Dittus-Bölter correlation (Equation 1.15). In the case with fixed heat transfer coefficient, the value has been calculated as an average of all the heat transfer coefficients (for each single discretisation point) from a steady-state simulation. The computational times of the simulations with different heat exchange specifications are collected in Table 4.2.

Table 4.2: Computational times of the *More* case study with calculated heat transfer coefficient, fixed heat transfer coefficient and no heat exchanged (adiabatic pipeline).

Case study	**Computational time** [s]
Calculated HTC	66
Fixed HTC	33
Adiabatic	44

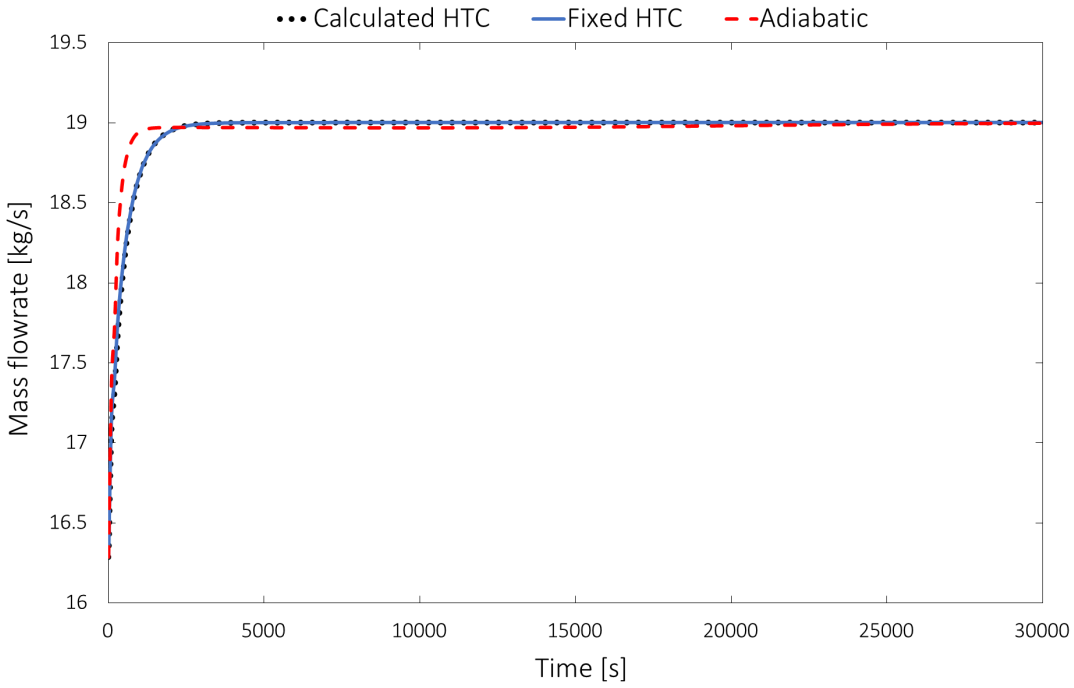

Figure 4.14: Profile of the mass flowrate at the sink over the first 30 000 seconds of simulation in the *More* case study, 'Test Pipeline' flowsheet, with calculated heat transfer coefficients, fixed heat transfer coefficient and no heat exchanged (adiabatic pipeline). Calculated HTC and Fixed HTC curves are perfectly overlapping. Source: gPROMS® ProcessBuilder.

As one can see from Figure 4.14, the results of dynamic simulations (*More* case study) with calculated and fixed heat transfer coefficients are the same, while the results with adiabatic pipeline are different and, basically, incorrect. In fact, the temperature of the source is higher than the sea temperature, but heat exchange with the sea is fast (with respect to the residence time) and after just 1 km from the source the sea temperature is reached inside the pipe. In addition, the Joule-Thomson effect is slow enough to be always neglected by the heat supplied by the sea (thus the temperature remains constant), as one can see from the axial temperature profile in Figure 4.15. Therefore, fixing the heat transfer coefficients might be the best approach to reduce the computational time without losing accuracy. However, the heat transfer coefficients depend strongly on the internal flowrate, which is constantly changing. For this reason the best and fastest approach is to periodically update an averaged heat transfer coefficient in each pipeline of the network. Alternatively, one could modify the model to calculate in each time step one single heat transfer coefficient for each pipeline, instead of calculating it for

each discretisation point. In this project temperature has been considered as not really relevant, therefore the heat transfer coefficients have been fixed but not periodically updated.

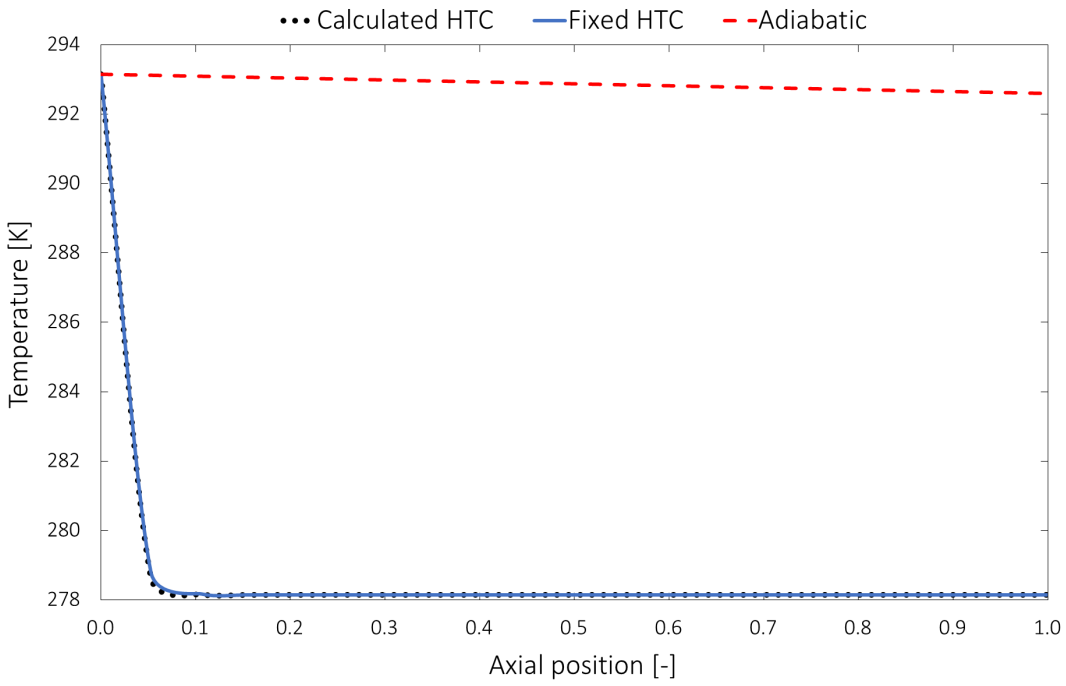

Figure 4.15: Axial profile of the temperature in the *More* case study, 'Test Pipeline' flowsheet, with calculated heat transfer coefficients, fixed heat transfer coefficient and no heat exchanged (adiabatic pipeline). The profiles are plotted at the end of the simualation, after 100 000 seconds, but they do not depend on time. Calculated HTC and Fixed HTC curves are perfectly overlapping. Source: gPROMS® ProcessBuilder.

From Figure 4.15 one might think that a good approach to emulate an isothermal behaviour might be modelling adiabatic pipeline with temperature at the source equal to the sea temperature, therefore disregarding the first temperature drop and avoiding the problems related to the calculation of the heat transfer coefficients (such as the calculation and update of fixed heat transfer coefficient or the high computational time for calculating them). This procedure would basically shift the adiabatic profile in Figure 4.15 along the y-axis to the sea temperature, but it would produce wrong results. In fact, the Joule-Thomson effect makes the temperature decrease along the pipeline due to the pressure drop. This effect is slightly visible from the axial temperature profile in Figure 4.15 (decrease is less than 1 °C), but it becomes really relevant for long pipelines such as those in a network, leading to a temperature well below 0 °C at the terminal. Furthermore, as one can see from Table 4.2, modelling adiabatic pipeline leads to higher computational times with respect to fixing the heat transfer coefficient.

In conclusion, if the temperature is considered as not relevant, the best option to strongly reduce the computational time is to implement an isothermal flowsheet, modifying each model in order to exclude from the equations the heat balance and all the connected correlations, disregarding all properties linked to the energy (e.g. enthalpy, temperature, energy flux). However, this would have required a long time (it is not a straightforward procedure), and it has not been considered as part of the project.

4.2.2 Dynamic and convective terms of the momentum balance

The *Pipeline single-phase gML* model allows the user to exclude either one or both the dynamic term and the convective term from the momentum balance (Dynamic Momentum Balance and Convective Transport of Momentum Term in the model dialog box). These two terms are respectively $\partial(\rho v)/\partial t$ and $\partial(\rho v^2)/\partial z$ in Equation 1.2. The *Heavier* case study on the 'Test Pipeline' flowsheet (whose specifications can be found in Table 3.2) has been run including and excluding either one of the two terms. The computational times of the simulations have been collected in Table 4.3.

Table 4.3: Computational times of the *Heavier* case study, including and excluding the dynamic and convective terms individually.

Dynamic term	Convective term	Computational time [s]
On	On	58
On	Off	39
Off	On	14
Off	Off	14

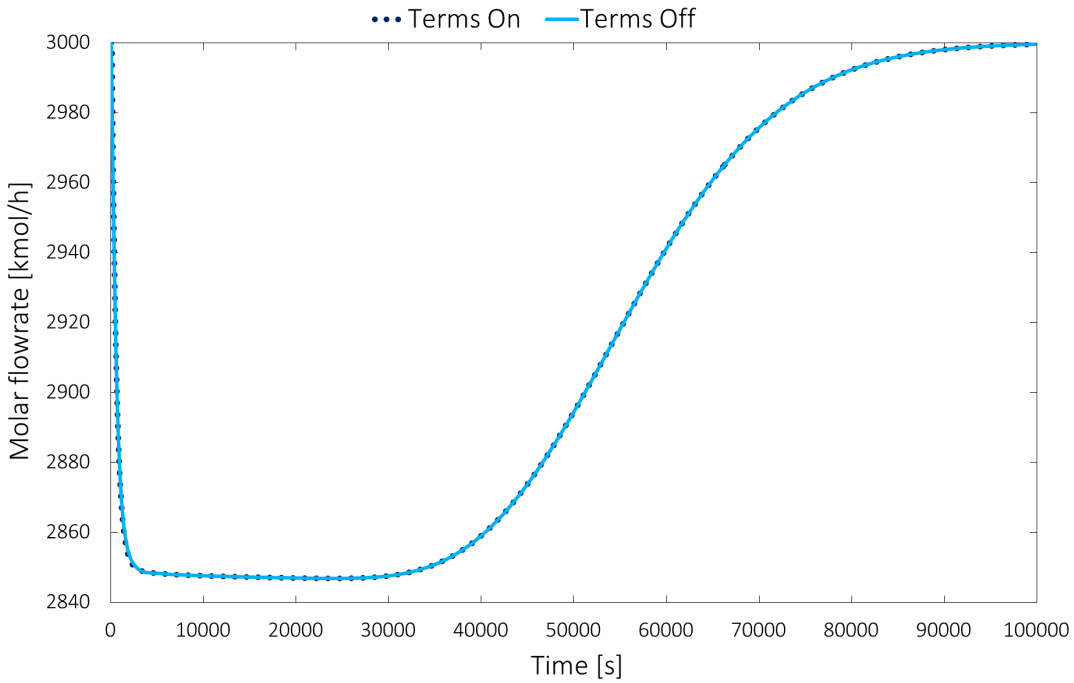

Figure 4.16: Profiles of the molar flowrate at the sink over the entire simulation time in the *Heavier* case study, 'Test Pipeline' flowsheet, with dynamic and convective term both included (Terms On) or excluded (Terms Off) from the momentum balance. Source: gPROMS® ProcessBuilder.

The computational time is highly affected by the dynamic term, while the convective term has a smaller impact on the complexity of the model and therefore on the effort of the solver to reach convergence. However, as one can see from Figure 4.16, neither one of these two terms has an impact on long period simulations. The dynamic term becomes significant in impulsive phenomena, especially when the velocity of the fluid is high (Mach number approaching or even exceeding the value of 1). This situation is typical in depressurisations and blowdowns. The convective term becomes significant only when there is a sudden and sharp variation in the velocity among a discretisation section (or volume). This situation is usually found when there is condensation inside a pipeline (the liquid, being much more dense, has a lower velocity).

To assess the importance that the convective and dynamic terms might have, the *Heavier* case study has been run with a simulated time of just 200 seconds and 1 second reporting interval. With this short period simulation some differences in the results including and excluding the terms of the momentum balance can be seen. The profiles of the molar flowrate at the sink and in the first part of the pipeline, in Figure 4.17, show that the dynamic term causes an oscillation (in particular in the first discretisation points) and an overall delay in the response (more visible at the sink). It has also been verified that, as expected, the convective term has no visible effect on the profiles. In fact, the profiles are perfectly overlapping both with and without the dynamic term regardless of the convective term.

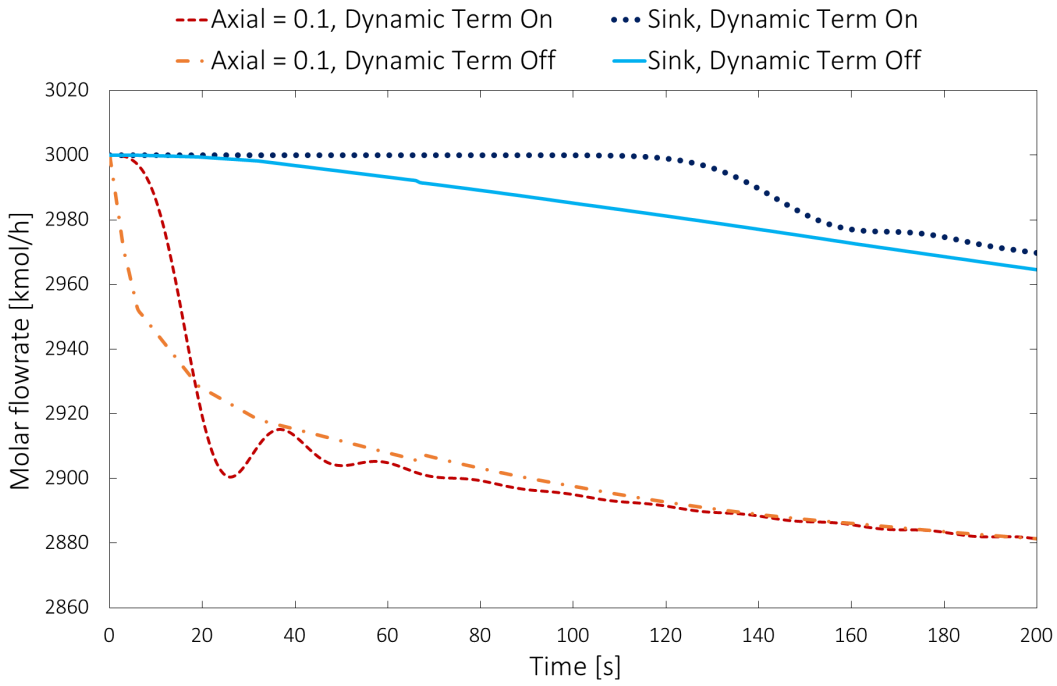

Figure 4.17: Profile of the molar flowrate at the sink and at axial position 0.1 ($1/10^{\text{th}}$ of pipeline) over the first 200 seconds of simulation in the *Heavier* case study, 'Test Pipeline' flowsheet, with dynamic term included (Dynamic Term On) or excluded (Dynamic Term Off) from the momentum balance. The profiles are independent on the convective term. Source: gPROMS® ProcessBuilder.

4.2.3 Discretisation points

Pipeline single-phase gML dialog box allows the user to select the number of discretisation points, which are the points in which each physical property is calculated. Obviously, using more discretisation points leads to an higher computational time because more calculations need to be done by the model. However, increasing the number of discretisation points leads also to an increase in the accuracy of the model, because numerical dispersion of the properties is reduced. Numerical dispersion is a purely numerical phenomenon which is intrinsic to the discretisation of a pipeline (or, in general, of a process unit). If the number of discretisation points (or volumes, depending on the numerical method to solve the differential equations) is higher, the dimension of each section in which the pipeline is divided is smaller and therefore the properties along the pipeline are calculated with an higher precision.

The sensitivity analysis has been performed on the 'Test Pipeline' flowsheet using the *Heavier* case study. The profiles of the molar flowrate are shown in Figure 4.18, and the computational times are collected in Table 4.4.

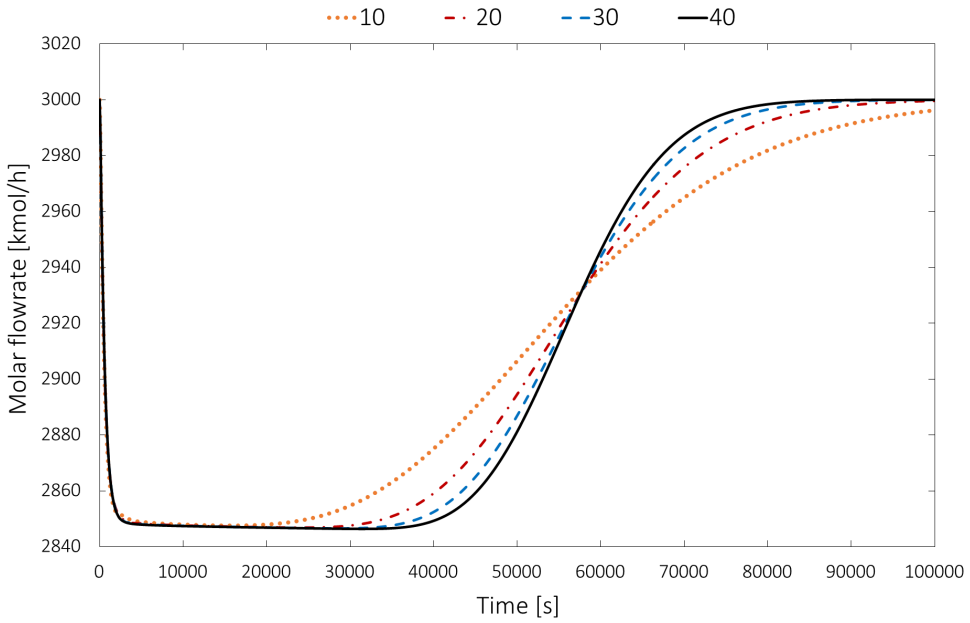

Figure 4.18: Profiles over time of the molar flowrate at the sink in the *Heavier* case study, 'Test Pipeline' flowsheet, with different numbers of discretisation points. Source: gPROMS® ProcessBuilder.

Table 4.4: Computational times of the *Heavier* case study with different numbers of discretisation points.

Discretisation points	Computational time [s]
10	10
20	14
30	23
40	28

One can see that with the smallest number of discretisation points the profile is extremely smoothed, and there is an inaccuracy of almost 20 000 seconds on the time in which the molar fraction starts to change. On the other hand, however, excessively increasing the number of discretisation points does not lead to strong improvements in the accuracy, but instead leads just to an increase in the computational time. It has also been noticed that the molar flowrate at the terminal is not affected by the number of discretisation points of the pipeline, as the profiles are perfectly overlapping (and therefore have not been reported). In conclusion, a sensitivity analysis on the number of discretisation points must be performed on the network flowsheet in order to find the best trade-off between accuracy and computational time.

4.2.4 Reporting interval

The reporting interval is the time interval between each collection of results in a dynamic simulation. The collection of results (each physical property) is computationally expensive, and an excessively small reporting interval might prove useless and result in high computational time. On the other hand, an high reporting interval might cause the loss of important information and therefore reduce the accuracy of a simulation.

It is important to underline that the results of the simulation are exactly the same independently on the reporting interval, and the only thing which changes with the reporting interval is the frequency with which these results are stored and, consequently, made available as output. The analysis of the computational times and the accuracy of the results has been done using the *Heavier* case study. The profiles of the molar flowrate at the terminal are shown in Figure 4.19, and the computational times are collected in Table 4.5.

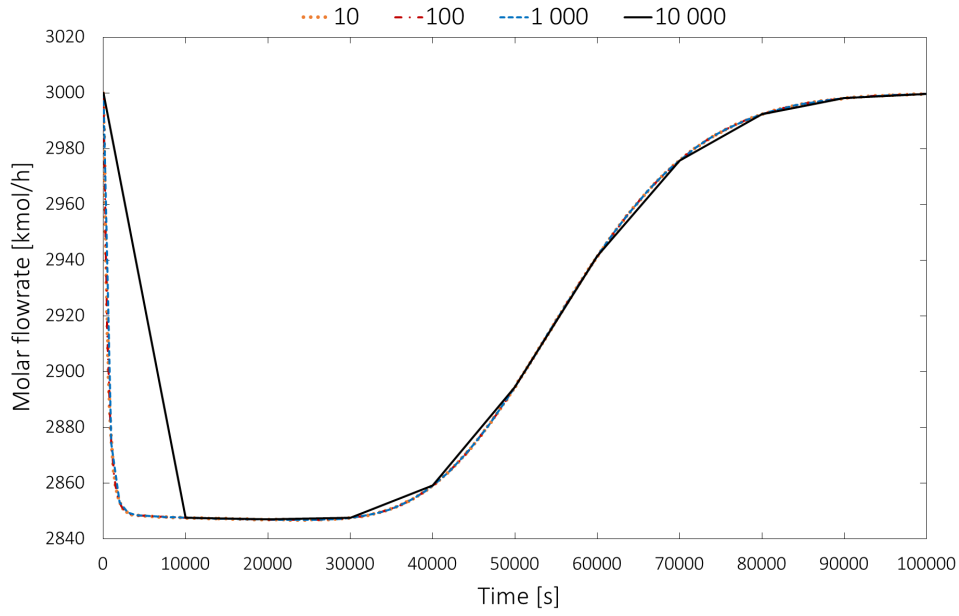

Figure 4.19: Profiles over time of the molar flowrate at the sink in the *Heavier* case study, 'Test Pipeline' flowsheet, with different values of the reporting interval. Source: gPROMS® ProcessBuilder.

Table 4.5: Computational times of the *Heavier* case study with different reporting intervals.

Reporting interval [s]	**Computational time** [s]
10	37
100	14
1 000	12
10 000	13

One can see from Figure 4.19 that the profile with 10 000 seconds reporting interval is storing too few results, leading to a loss of important data (causing overall inaccuracy) and, unexpectedly, a higher computational time (probably due to an heavier initialisation procedure). On the other hand, one can also see that the profiles with 10, 100 and 1 000 seconds reporting intervals are almost identical, therefore using the most accurate reporting interval is useless because it causes a sharp increase in the computational time. In conclusion, a good rule of thumb for long period simulations in which the interest is not in short time phenomena, is to use between 100 and 1 000 seconds of reporting interval each 100 000 seconds of simulation.

Chapter 5

Whole network simulation

After testing and validating the pipeline model, the existing network flowsheet has been built taking into account the results of the various sensitivity analyses reported in Chapter 4.

The first section of this chapter reports the information about the network and the results of simple test simulations, run specifying a single step change in each variable through the *Schedule* tab. These simulations were useful to assess if the mixing in the junctions was modelled accurately and to understand the response and residence time of the network. Then, a new set of sensitivity analyses confirmed what already found with the 'Test Pipeline' flowsheet in terms of heat exchange, momentum balance, discretisation and thermodynamic model.

In gPROMS® ProcessBuilder the simulations start from steady-state so, in order to have meaningful results, a long period of specifications must be simulated (this procedure is known as *packing* of the network). A problem linked to the discretisation approach of the *Pipeline single-phase gML* model arised and made step changes impossible to be simulated. Therefore, the flowsheet has been modified to simulate ramp changes, which made it less exposed to failure problems, but still not completely immune. These issues are explained in details in the second section. Then, the most significant achievements in terms of simulation rationale and computational time are explained.

The third section reports the validation of the network simulations results, done against actual data coming from the plant, which finally confirmed that the pipeline model can be used for flow assurance applications.

In the fourth section some test simulations involving condensation of the gas in the network are reported. These tests confirmed the importance of having a good thermodynamic model, but also of keeping the computational time small in order for the application to be considered as online.

All data reported in this chapter have been modified or scaled in order to respect the confidentiality with the owner and operator of the pipeline network, both in terms of topology and data.

5.1 The network flowsheet and test simulations

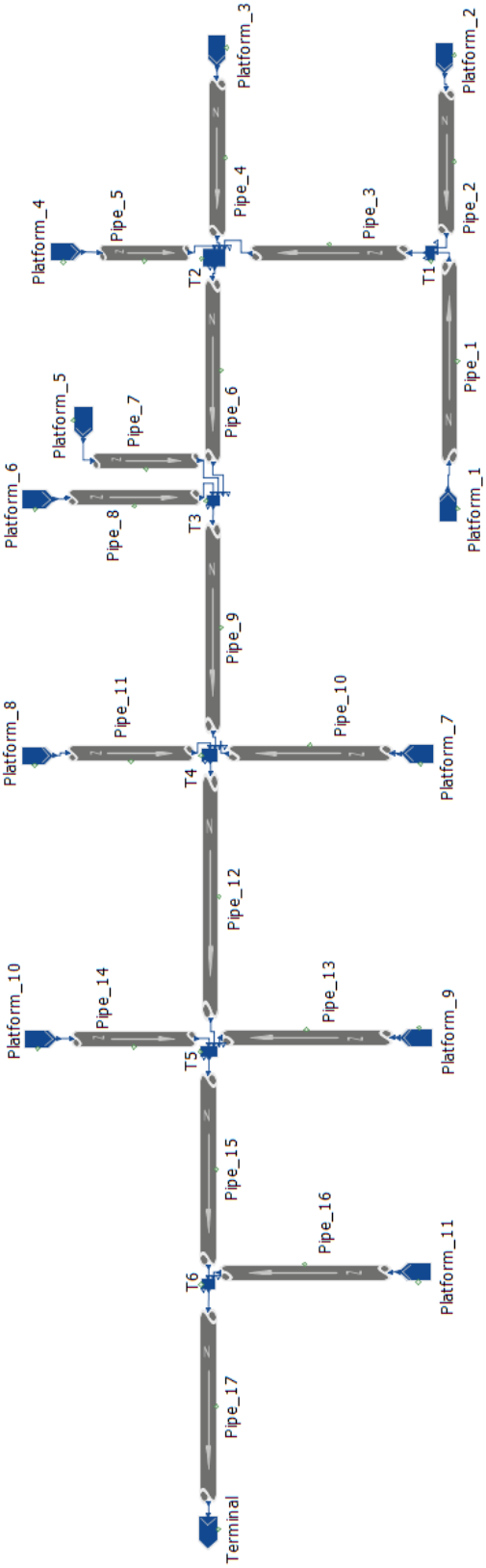

Figure 5.1: 'Network' flowsheet. Source: gPROMS® ProcessBuilder.

The first flowsheet of the existing network used as case study has been built in gPROMS® ProcessBuilder (a simplified version of it is shown in Figure 5.1), using *Pipeline single-phase gML*, *Junction gML*, *Source gML* and *Sink gML* models. The network, which needs to remain anonymous, includes 11 platforms and 17 pipelines. The flowsheet has been named 'Network' flowsheet. The topology data, as well as all the input data used in the simulations, have been taken from an Excel spreadsheet collecting actual data coming from measurement systems located in each platform and at the onshore processing facility (terminal). The available data are those required by the pressure-driven mode (which is needed to run dynamic simulations): the composition and the flowrate in each platform, and the pressure at the terminal, collected with a 30 minutes frequency. From now on this will be referred as the *set* of specifications.

Some dynamic simulations have been run to assess whether the response of the network to dynamic inputs was correct. The reported case study involves an actual step change in the set of specifications (hence it has been named *Step*). The general aim of pipeline network simulations is to monitor and predict the behaviour of a network over long periods of time. Therefore, the simulation time must be chosen accordingly, considering the total residence time of the pipeline. For the first test simulations of the network the simulation time has been selected as 800 000 seconds, which allows the system to reach the new steady-state, and the reporting interval has been fixed to 1 000 seconds according to the optimal ratio found in the sensitivity analysis in Chapter 4.

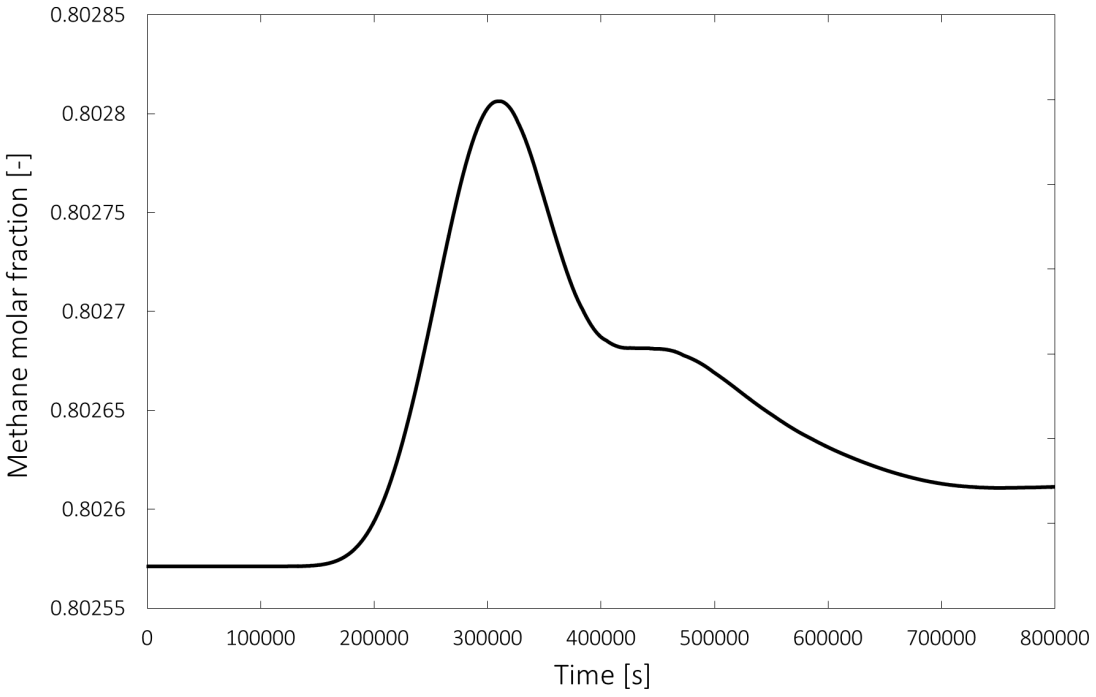

Figure 5.2: Profile over time of the methane molar fraction at the terminal in the *Step* case study, 'Network' flowsheet. Source: gPROMS® ProcessBuilder.

From Figure 5.2 one can see how the methane molar fraction at the terminal starts changing only after 200 000 seconds. This happens because the simulation starts from steady-state and the perturbation (the step change) reaches the terminal only after almost 3 days. In fact, each branch of the network has its own

residence time (the time for the gas coming from each single platform to reach the terminal is different). Then, the new steady-state is reached after almost 700 000 seconds. For this reason one can consider the *total* residence time of the network as the one from the further source to the terminal, so the highest among the residence times of each single branch.

In general, the results of the *Step* case study are difficult to analyse due to the high number of properties which change (a total of 177 variables) and the complexity of the network topology. For example, as one can see from Figure 5.2, after around 300 000 seconds of simulation there is a peak in the methane molar fraction at the terminal. From an analysis of the residence times of each branch of the network and the composition and flowrate which each source is delivering, one can notice that, during the simulated step change, the flowrate of a source whose gas is particularly rich in methane and which has a residence time of approximately 300 000 seconds increases. For this reason the methane molar fraction at the terminal increases when that fluid reaches the terminal. After this peak the methane molar fraction decreases because the gas coming from the further sources reaches the terminal and 'mitigates' the effect of the richer source with an increased flowrate of gas poor in methane. Even if simulating single step changes in a network is meaningless (as well as starting a simulation from the steady-state), this case study has been useful to understand the time needed for the system to reach a steady-state after the change, to have a first idea about the computational times needed by the simulation to reach convergence, and to perform the sensitivity analyses focused on decreasing the computational time.

5.1.1 Sensitivity analyses

On the above-mentioned *Step* case study some sensitivity analyses have been performed to assess the response of the computational time of network simulations to the different variables reported in Chapter 4. All sensitivity analyses confirmed what already found with the 'Test Pipeline' flowsheet.

Modelling the heat exchange by calculating with a correlation (the most appropriate one is the Dittus-Bölter equation) the heat transfer coefficient for each discretisation point is computationally burdensome. The profiles of the molar flowrate at the terminal in the three cases are reported in Figure 5.3. Identical results are achieved if the heat transfer coefficients are fixed (as equal to the values found from a steady-state calculation) or calculated for each discretisation point, while the results with adiabatic pipelines are different and, as already explained in Chapter 4, incorrect. In fact, heat exchange with the sea is fast and the temperature of the fluid is always equal to the sea temperature (apart from the first portion of pipeline close to the platform in which the fluid is warmer), neglecting also the Joule-Thomson effect. The computational times are collected in Table 5.1, from which one can see that by fixing the heat transfer coefficients the computational time is much smaller than the one with calculated heat transfer coefficients. For these reasons the choice to fix the heat transfer coefficients for each pipeline is reasonable.

One needs to remember that the heat transfer coefficient depends heavily on the flowrate, which is constantly changing during normal operation of the network. For this reason, each heat transfer coefficient should be updated periodically. In

this project this detail has been disregarded because, as already mentioned, the best effective way to decrease the computational time without losing much accuracy is to exclude the heat balance from the set of equations (hence assuming isothermal pipelines and neglecting every variable and phenomena linked to the temperature). However, this would require not only to modify the equations in the *Pipeline single-phase gML* model, but also the dialog boxes and the connectivity with the *Junction gML* model, which is a difficult and time-consuming task.

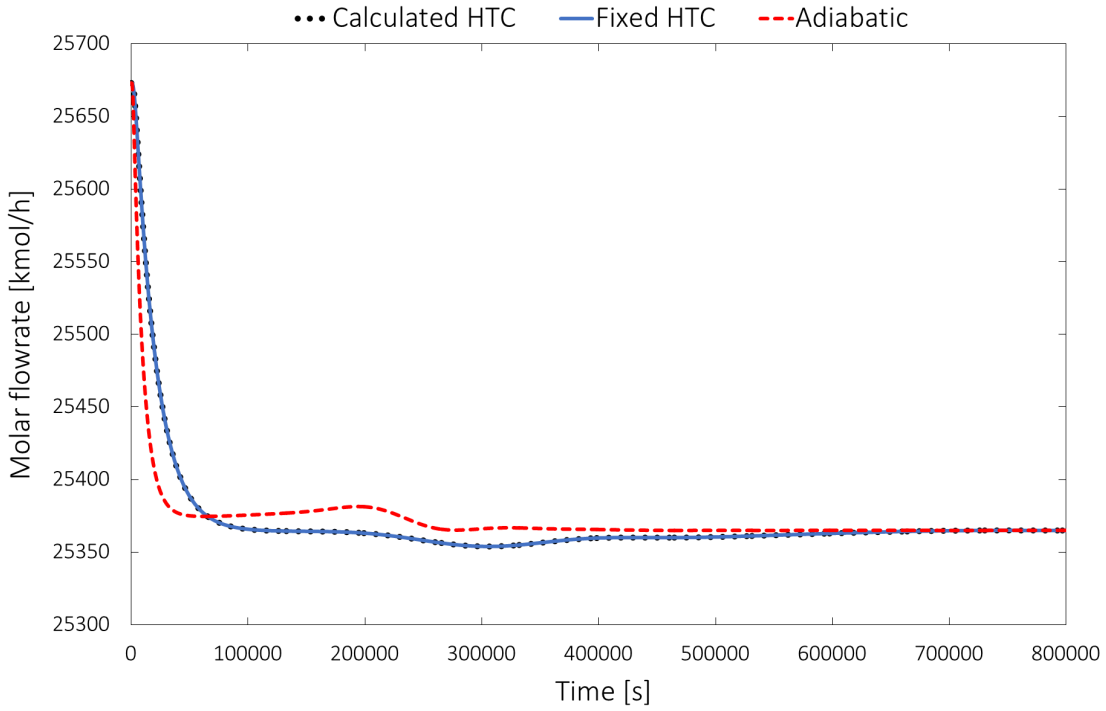

Figure 5.3: Profile over time of the molar flowrate at the terminal in the *Step* case study, 'Network' flowsheet, with calculated heat transfer coefficients, fixed heat transfer coefficients and no heat exchanged (adiabatic pipelines). Source: gPROMS® ProcessBuilder.

Table 5.1: Computational times of the *Step* case study with calculated heat transfer coefficient, fixed heat transfer coefficient and no heat exchanged (adiabatic pipelines).

Case study	**Computational time** [s]
Calculated HTC	367
Fixed HTC	253
Adiabatic	222

In network simulations, even more than in simple pipeline models, the phenomena involve long periods of time, and there is no reason to focus on small-scale details. For this reason, modelling the dynamic term of the momentum balance, which leads to a small-amplitude oscillation and a little delay in the first seconds of simulation, is meaningless because the computational time increases more than proportionally (due to the higher complexity of the flowsheet). The convective term of the momentum balance has not been included in the study because, as

already demonstrated in Chapter 4, it has no impact on the simulation results. The profiles are not reported because they are perfectly overlapping.

The number of discretisation points has a strong impact on network simulation due to the high number of pipelines in the flowsheet. For the 'Network' flowsheet three different discretisation schemes have been used, named A, B and C, whose details are collected in Table 5.2, along with the length of the pipelines. All these values have been scaled and rounded because the precise topology of the network is covered by the confidentiality. The number of discretisation point of each pipeline is directly proportional to its length: roughly one point each 5 kilometres in Scheme A, one point each 3 kilometres in Scheme B, and one point each kilometre in Scheme C.

Table 5.2: Number of discretisation points used in schemes A, B and C.

Pipeline no.	**Length [km]**	**Discretisation points**		
		Scheme A	Scheme B	Scheme C
17	350	75	125	350
1, 3, 13, 16	75	15	25	75
9, 12, 15	50	10	20	50
4, 11	25	5	8	25
6, 8, 10, 14	15	4	5	15
2, 5, 7	5	3	3	5

As one can see from Figure 5.4, the profile of the propane molar fraction at the terminal changes with different discretisation schemes. The computational times are different as well, in a way somehow proportional to the total number of discretisation points in the flowsheet, as one can see from Table 5.3.

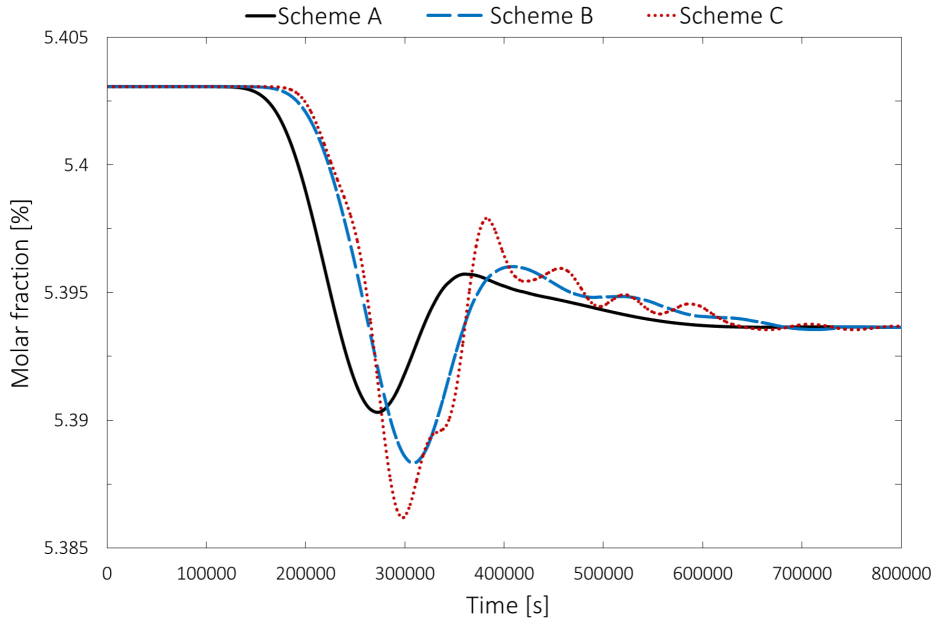

Figure 5.4: Profile over time of the propane molar fraction at the terminal in the *Step* case study, 'Network' flowsheet, with different discretisation schemes.

Table 5.3: Computational times of the *Step* case study with different discretisation schemes.

Discretisation scheme	Computational time [s]
A	253
B	360
C	1 012

As already noticed in Chapter 4, using a small number of discretisation points numerical dispersion phenomenon arises, smoothing the profiles and leading to less accurate results. Therefore, a sufficiently high number of discretisation points must be used. It has been proven that using more than one discretisation point per kilometre (discretisation schemes more precise than Scheme C) does not improve the accuracy effectively, while the computational time becomes extremely high. For this reason, using discretisation Scheme C is a good choice if the Peng-Robinson EoS is used.

5.2 Making the simulations meaningful

Starting a simulation from steady-state and simulating only one step change is physically meaningless. For an efficient flow assurance application, simulations must be meaningful, have a small computational time, and effectively predict what is about to happen in the pipeline (under some assumptions). The input and validation data in the following sections are actual data coming from the network, which have been scaled and set to start at a fictional date (1st January 2016, at 00:00) in order to respect the confidentiality.

5.2.1 Packing the network

In the *Pipeline single-phase gML* model the only feasible initial condition for a dynamic simulation is the steady-state. This is done automatically by the software, and it assumes that the initial input specifications 'propagated' in the network for a sufficient time, hence settling to a steady-state. Then, all the successive inputs on the so-called *Schedule* will follow and make the simulation dynamic (considering time as an independent variable). In network simulations the steady-state assumption is meaningless because a steady-state is never reached due to the continuous fluctuations in all the properties. Therefore, in order to achieve meaningful results, each branch of the network must be 'filled' with a fluid which is not affected by the steady-state initial conditions, and instead reflects what really happens in the network. This means that the simulations must include a sufficiently high number of specifications, in order for the fluid coming from each platform to reach the terminal. The number of specifications must cover at least a period equal to the total residence time of the network. This operation is technically referred as the *packing* of the pipeline network. If the specifications do not cover a period at least equal to the total residence time, the results would be affected by the fictitious assumption of steady-state initial condition. For example, if only 4 days of specifications are simulated, the conditions at the terminal

would not account for the platforms whose residence time is higher than 4 days, because the fluid reaching the terminal from those platforms would still be the one specified as steady-state initial condition.

Data coming from the plant need to be used to *pack* the network. The time interval between each data collection is 30 minutes, and due to the fact that there is no interest in the evolution of the system during the step change, the reporting interval of the simulation has been selected as 1 800 seconds (30 minutes) instead of 1 000 seconds (this choice slightly reduces the computational time).

When the pipeline network is packed the simulations are meaningful (they reflect what is really happening inside of the network). Therefore, if data coming from the terminal are available for a period covering more than the total residence time, the model could be validated and its accuracy could be evaluated. The validation of the model against plant data is reported in the following section. The rationale of the *packing* procedure and results validation is depicted in Step 1 of Figure 5.5.

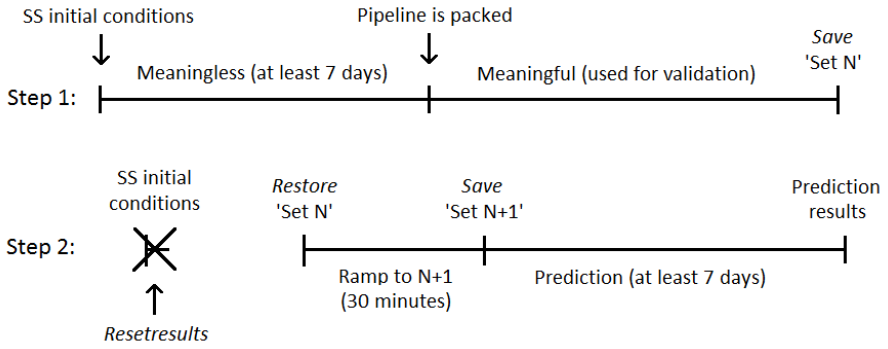

Figure 5.5: Rationale of the procedure to make the simulations meaningful and have an efficient online flow assurance application. Step 1 simulation consists on the *packing* procedure. It starts from steady-state initial conditions and covers a period at least equal to the total residence time, after which the pipeline is packed. Then, if needed, further specifications can be simulated in order to validate the results. Step 2 simulation is the one to be performed during online monitoring of the network. It starts from a steady-state calculation, which needs to be erased, after which the new specifications are simulated dynamically (as ramps). Then, the system settles to a new steady-state in order to predict the arrival conditions at the terminal.

Practically, to *pack* the network in ProcessBuilder a high number of step changes must be included in the dynamic *Schedule*. However, simulations including more than a couple of step changes fail because of a backflow problem. In fact, backflow is not supported by the *Pipeline single-phase gML* model due to its forward discretisation approach for solving differential equations. Failures caused by the backflow problem are impossible to predict or correct, and they are mainly due to the fact that step changes are sharp, therefore bringing instability to the system. For this reason, the problem has been bypassed modifying the flowsheet in order to model ramp changes instead of step changes. Ramp changes are smoother than step changes, so they add stability to the system. Furthermore, ramping each variable from the original value to the following one is closer to reality, in which each variable changes with continuity, not in a discrete way.

In ProcessBuilder it is not possible to model ramp changes from the *Schedule* tab, therefore the flowsheet has been modified by including a *Source linear interpolated gML* model and a *Set signal to bus gML* model for each variable which

needs to be ramped. Due to this additions, to the ramps themselves (which include more information than step changes), and to the high number of specifications to be simulated, the flowsheet has become heavier.

Source linear interpolated gML is a model through which it is possible to 'draw' a profile (which can be a sequence of equally-distanced ramps such as in this case study), with a chosen number of time intervals and values. Then, the model is connected to a *Set signal to bus gML* model that allows to select which variable to assign the desired profile. The *Set signal to bus gML* model is connected either to a *Source gML* model to ramp a molar fraction or the flowrate, or to a *Sink gML* model to ramp the pressure. An example of the *Source linear interpolated gML* and *Set signal to bus gML* models connectivity is shown in Figure 5.6. The modified network flowsheet, which can be considered as the definitive one, is shown in Figure 5.7.

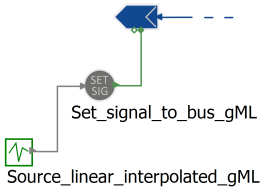

Figure 5.6: Schematic of the connection of the *Source linear interpolated gML* and *Set signal to bus gML* models to the *Sink gML* model to ramp the pressure at the terminal. Source: gPROMS® ProcessBuilder.

Unfortunately, the backflow problem was not completely bypassed by the new approach. In fact, a small (or zero) flowrate at the source still leaded to unpredictable failure. Many tests have been performed, and it has been found that, under the simulated conditions, a sufficiently high flowrate to avoid failures is 100 kmol/h. Therefore, a flowrate of 100 kmol/h must be used as input if the actual specification is lower than that value. This introduces inaccuracy in the model, as the simulation considers a fluid entering the system which is actually not reflecting the reality. In those cases, one could assign as input composition to the sources whose flowrate is less than 100 kmol/h the composition at the terminal (which can be considered as a 'standard' composition for the network) in order to reduce to the minimum the inaccuracy on the molar fraction, leaving however the same inaccuracy on the flowrate. The best solution to this problem could be that of disconnecting from the flowsheet the sources who are not delivering fluid (hence not considered in the model). In fact, during normal operation of a network, many sources could be disconnected for certain periods of time, then connected back again. Developing this feature is time-consuming and has not been considered as part of the project.

5.2.2 *Save* and *Restore* tasks

Due to the high complexity of the flowsheet and of the simulation to be run, the computational time is extremely high, and a way to decrease it is needed. The gPROMS® *Save* and *Restore* tasks have proven perfect to cut the computational time. The *Save* task allows to store the condition of a flowsheet during a simulation (or at the end of it) as a *Saved Variable Set* (a text file). In Figure

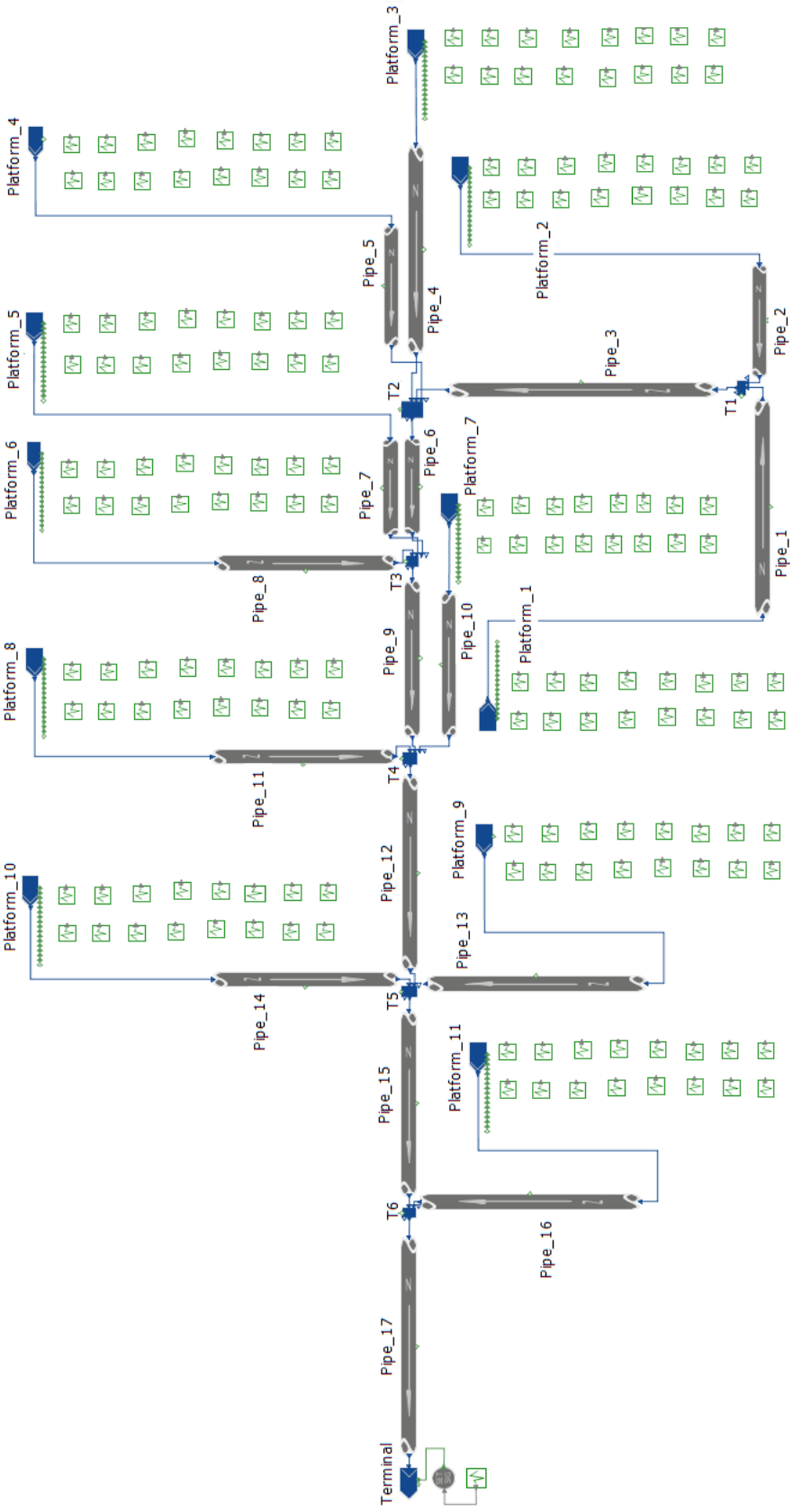

Figure 5.7: 'Network' flowsheet modified to model ramp changes instead of step changes. Each *Source gML* model has 16 *Source linear interpolated gML* models (the boxes) and 16 *Set signal to bus gML* models (which are hidden from the flowsheet, so the connecting lines are hidden as well). See Figure 5.6 for comparisons on each *Source gML* connectivity. Source: gPROMS® ProcessBuilder.

5.5 this set is called 'Set N'. The set can then be restored and used as initial condition for a following simulation using the *Restore* task. Both the *Save* and *Restore* tasks are called from the *Schedule* tab. This procedure allows to cut the number of specification to be simulated during normal operation. In fact, just one ramp (the one which brings the system from 'Set N' to the new 'Set N+1' set of specifications, coming after a 30 minutes interval) needs to be simulated during normal operation, and simulations keep their physical consistency. The new 'Set N+1' needs to be saved in order to be restored and used as initial condition of the following simulation, and so on. In conclusion, the *packing* does not need to be performed in each simulation, so the simulation can be divided into two parts, as described by Figure 5.5: Step 1 simulation is run once, in order to *pack* the network when the system is to be put online, while Step 2 simulation (including only the last ramp) is run each 30 minutes during normal operation.

The accuracy of the *Save* and *Restore* tasks has been tested both on the 'Test Pipeline' flowsheet and on the 'Network' flowsheet. The test consisted of running first a continuous simulation, and then comparing its results with the same simulation divided into two simulations. An error has been noticed in the divided simulations, at the time in which the *Saved Variable Set* is restored. In fact, before it is restored as initial condition of the simulation, ProcessBuilder performs the default steady-state calculation with the input specifications. This leads to a meaningless solution which can be erased by calling the *Resetresults* task (as reported in Figure 5.5).

5.2.3 Predicting the arrival conditions

Usually the aim of a flow assurance application is not only to monitor in real time what is happening inside a pipeline network, but also to predict what a set of specifications could lead to. In fact, if one wants to avoid hazardous situations on the network, ensuring stable operation, it is needed to have a certain amount of time to effectively act on the network (the residence times are on the order of days). Therefore, after a new set of specifications is simulated (ramp to 'Set N+1'), the system must be given enough time to settle to a new steady-state. This happens in a time equal to what has been called the *total* residence time of the network, which in the case study is about 7 days. The main assumption is that each variable is kept constant after the last ramp ('Set N+1'). However, this is not what really happens in the network, as it is extremely unlikely that the set of specifications does not change for a long period of time. Other approaches could be to look at a large period of historian data and use statistic data to simulate and predict what each variable could be (e.g. oscillating or linear profile). This approach would require a big number of data, and it has not been considered as relevant for the purposes of this project.

The correctness of the *Save* and *Restore* tasks has been assessed again on the complete Step 2 simulation (including the prediction procedure), and the results are reported in Figure 5.8. The profiles of the divided simulations are perfectly overlapping the profile of the continuous simulation.

The simulated time of the Step 2 simulation is 800 000 seconds (as in the first network simulation tests). However, from Figure 5.8 one can notice that the steady-state is reached already after 600 000 seconds, which is, indeed, the

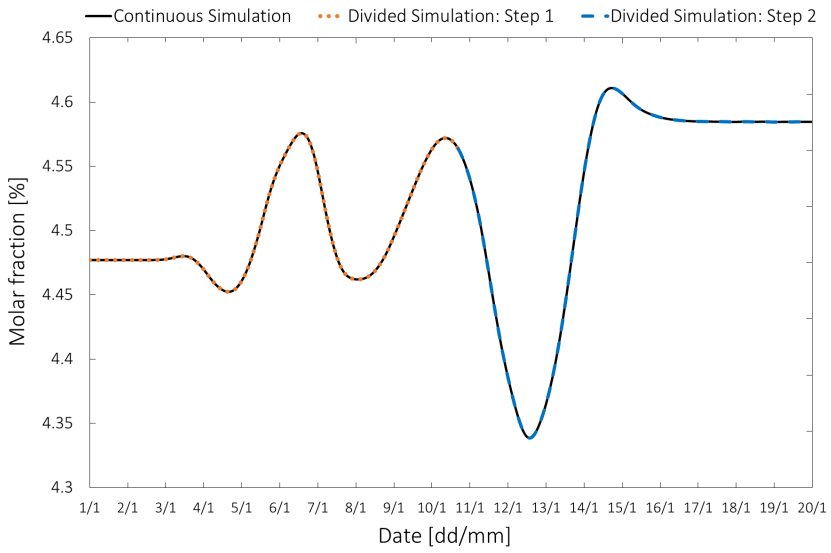

Figure 5.8: Profile of the propane molar fraction at the terminal in the divided simulation (Step 1 and Step 2), and in the continuous simulation.

total residence time of the network (Step 2 simulation starts on the 10^{th} of January and the steady-state can be considered as reached on the 17^{th} of January). The simulation time can therefore be reduced, but this has a small effect on the computational time. In fact, the solver 'works' faster when the steady-state is reached, because the system is indeed not changing. For example, using discretisation Scheme C, the computational time of the 800 000 seconds simulation is 1 024 seconds while the computational time of the 600 000 seconds simulation is 919 seconds.

5.3 Results validation

As explained in the previous section, once the pipeline is *packed* the simulations are meaningful, and successive results can be validated against plant data. The available output data useful for the validation are the molar fractions of propane, CO_2 and H_2S, and the flowrate at the terminal. The validation has been done using the three different discretisation schemes, also trying to eventually use the GERG-2008 EoS instead of the Peng-Robinson EoS. The results are collected in Figures 5.9 to 5.12, in the period of time in which the validation can effectively be done (after the pipeline is packed on the 8^{th} of January). All values have been scaled to respect the confidentiality.

As one can see from Figure 5.9, the propane molar fraction profile is well followed by the results of the simulations, in particular using the most accurate discretisation Scheme C. However, many peaks are not seen by the simulations. This can be due to the fact that the peaks are not real but generated by measurement noise and errors (such as the one happening at around 18:00 on the 8^{th}, in which the actual value falls to 4.7%), but also to the fact that the numerical dispersion effect smooths the profiles. In general, as expected, the higher the number of discretisation points, the more the results of a simulation are accurate, but also the higher the computational time is (as one can notice from Table 5.4).

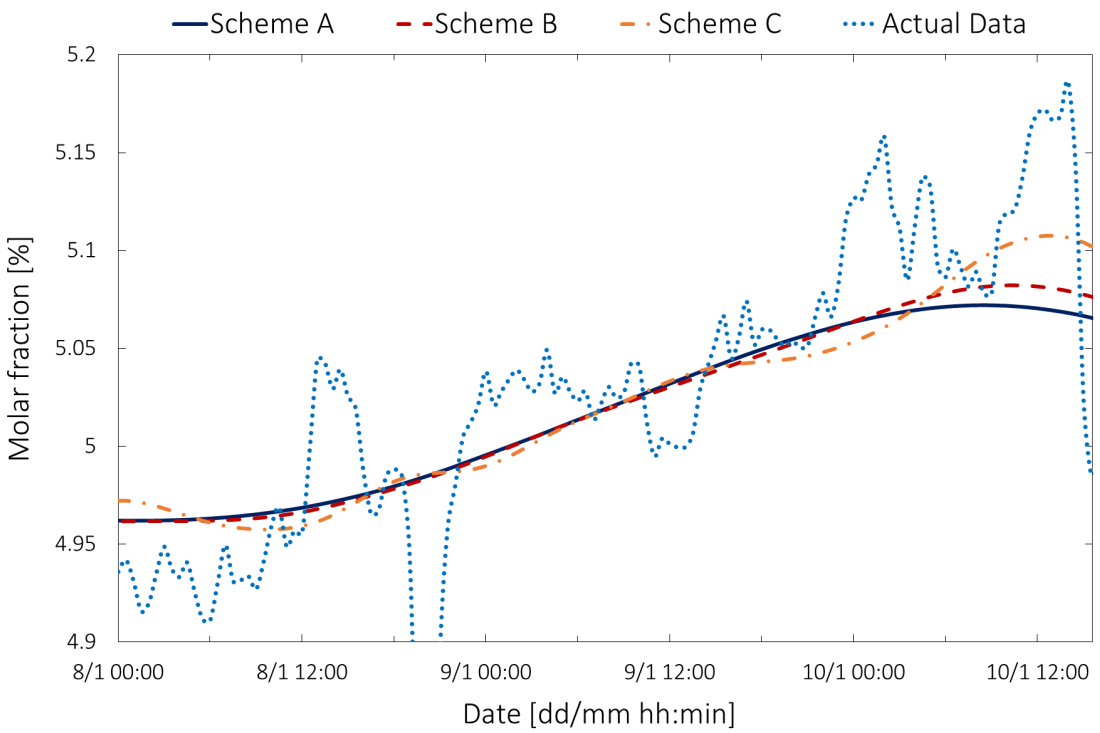

Figure 5.9: Profile over time of the propane molar fraction at the terminal with the different discretisation schemes, and actual data.

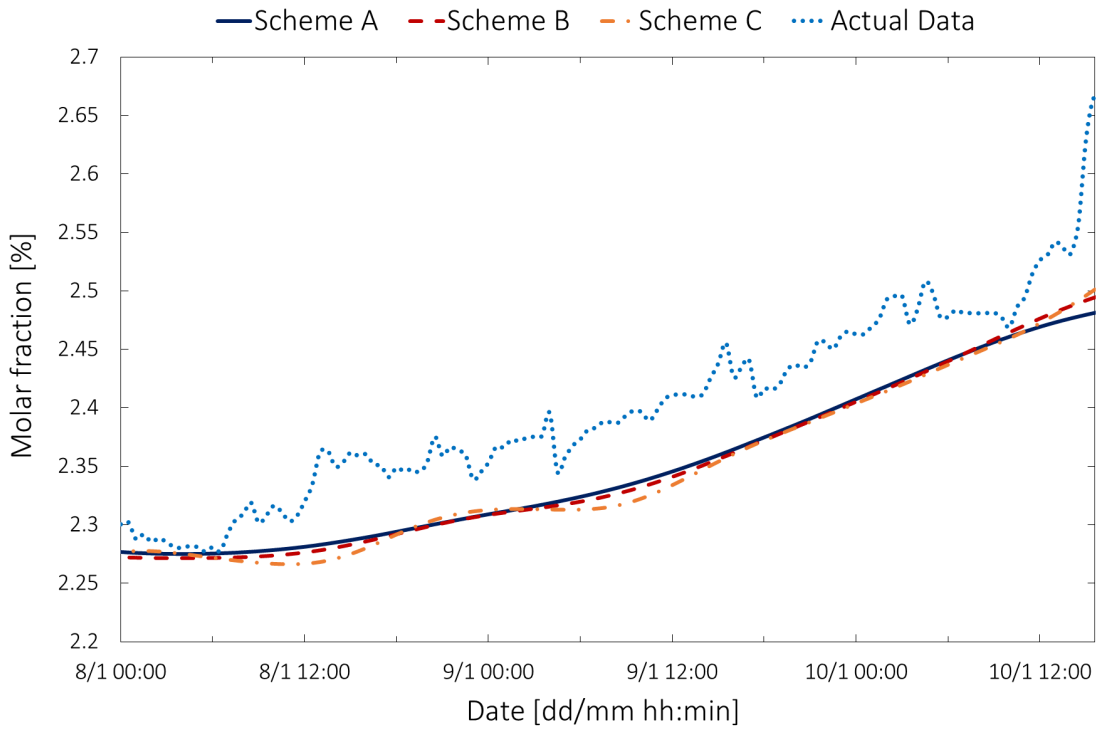

Figure 5.10: Profile over time of the CO_2 molar fraction at the terminal with the different discretisation schemes, and actual data.

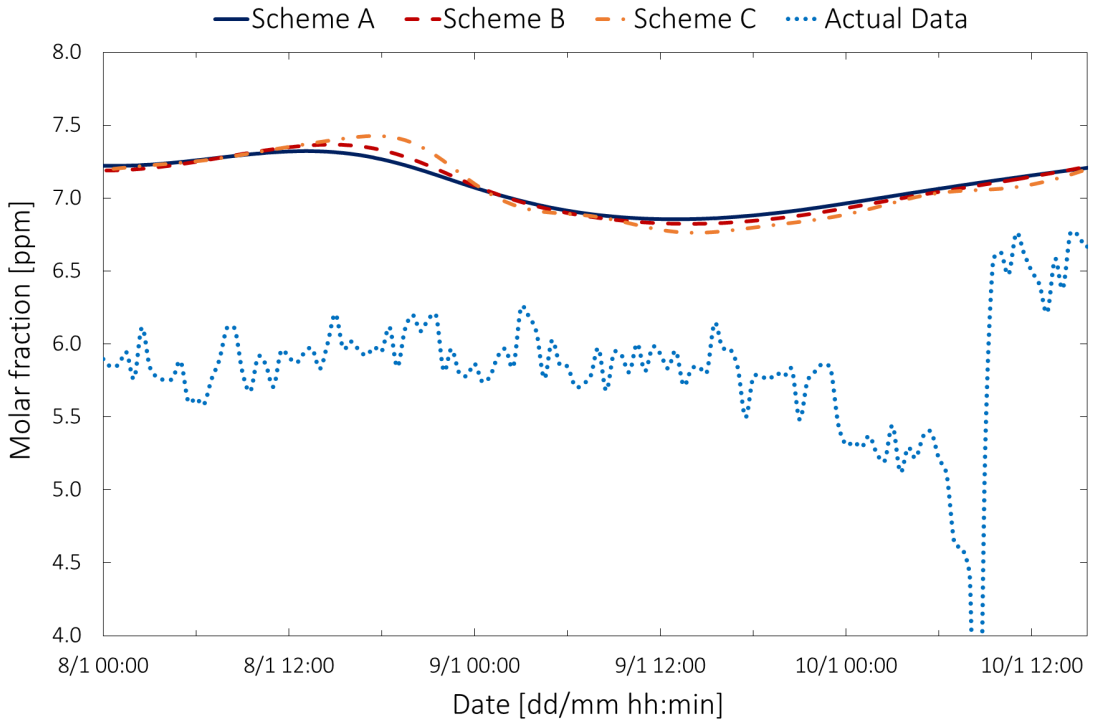

Figure 5.11: Profile over time of the H_2S molar fraction at the terminal with the different discretisation schemes, and actual data.

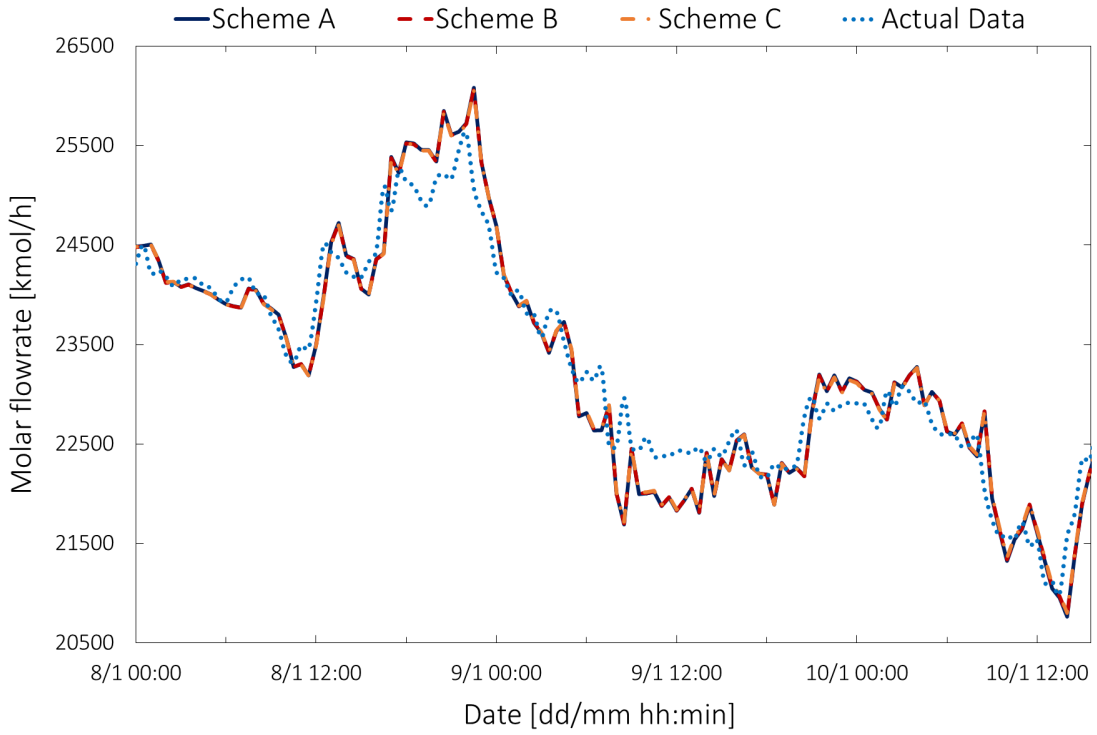

Figure 5.12: Profile over time of the molar flowrate at the terminal with the different discretisation schemes, and actual data. The calculated profiles (Scheme A, Scheme B and Scheme C) are perfectly overlapping.

Table 5.4: Computational times of Step 1 and Step 2 simulations using different discretisation schemes and thermodynamic models.

Discretisation Scheme	Equation of State	Computational time [s]	
		Step 1	Step 2
A	PR	6210	120
B	PR	9211	196
C	PR	28036	1024
A	GERG-2008	339403	4716

The errors and noise of the measurements, not only at the terminal but also at each single source, are not negligible and, being the input of the model, lead to inaccuracy of the results. From Figures 5.10 and 5.11 one can see how there is an error in the prediction of the molar fraction of CO_2 and H_2S at the terminal. While the CO_2 molar fraction is just slightly underestimated, but the profile is followed (the value increases with time), the H_2S molar fraction is strongly overestimated, and the profile is not followed. This is evidence that some data (either at the source or at the terminal) are wrong or missing, as the conservation of mass would not stand otherwise (what enters the pipeline network exits after a certain period of time). The error on the H_2S molar fraction is huge also because it is on the order of magnitude of the parts per million, so its measurement is more difficult than propane and CO_2 (whose molar fractions are expressed as percent). It needs to be specified that the underestimation of the CO_2 is not conservative in terms of condensation, while the slight overestimation of the H_2S does not have visible effects on the condensability of the mixture.

From Figure 5.12 one can notice that the profiles of the molar flowrate at the terminal calculated with the different discretisation schemes are exactly the same. This confirms the fact that the discretisation of the pipelines has a visible effect (in terms of numerical dispersion) only on the composition of the mixture (e.g. molar fractions). Because of that, the profile of the actual flowrate is followed accurately by the simulations. The errors could be due to measurement errors or, more likely, due to the pressure-driven mode needed to run the dynamic simulations. In fact, the set of specifications include the pressure at the terminal but no information about the pressure at the sources. For this reason the pressure profile is calculated using the flowrate and is not based on actual data. Having data about the pressure at the sources would improve the accuracy of the results because the parameters of the model could be tuned on plant data (e.g. the surface roughness, which has been taken from literature data).

The same simulations have then been run using the GERG-2008 EoS in order to assess if the improvements in terms of computational time made the model usable for an online flow assurance solution which can efficiently predict condensation. In Table 5.4 the computational times of the simulations are reported, for both Step 1 and Step 2 simulations, with the different discretisation schemes and thermodynamic models. Only Step 2 simulation has to be run under normal operation, and it would start from an already *packed* network, so the time spent

by the solver to reach convergence on Step 1 simulations is unimportant (it has been reported just to notice the huge improvements in terms of computational time produced by the *Save* and *Restore* tasks).

The profiles using the GERG-2008 EoS are overlapping the ones using the Peng-Robinson EoS (being equal the discretisation scheme), and therefore have not been reported. Further tests showed that, as long as there is no condensation in the network, or even if the fraction of liquid condensing is small, the difference in the calculation of the physical properties by the two EoSs is negligible, so the pressure profiles, as well as the flowrate and the composition, are almost identical. However, the main difference is in the computational time, which is much higher when using the GERG-2008 EoS as one can notice from Table 5.4. Another fundamental difference is in the prediction of condensation, and this issue is reported in the following section.

5.4 Predicting condensation in the network

The GERG-2008 EoS is computationally burdensome to be used in dynamic simulations, and the high computational times might not be compatible with the aim to operate an online flow assurance application. However, if one wants to efficiently predict the condensation of the natural gas in the network (which is the main threat for a pipeline network), the Peng-Robinson EoS might not be enough. Some simple steady-state simulations have been run to underline the importance of using an accurate thermodynamic model and to test the efficiency of the *Pipeline single-phase gML* multi-phase flag. The 'standard' flowrate has been modified for some certain sources, in particular to those delivering an easily condensable fluid which, as already mentioned in Chapter 3, is particularly rich in heavy fractions. The composition at each source has not been modified, in order to reflect what could actually happen on a real case (the flowrate is more likely subject to big changes than the composition). The pressure at the terminal has been selected as the lowest one amongst the input data, in order to facilitate condensation in the network, but still simulating what could happen during normal operation. Reported is one of the most meaningful case studies, which has been named *Condensation* case study.

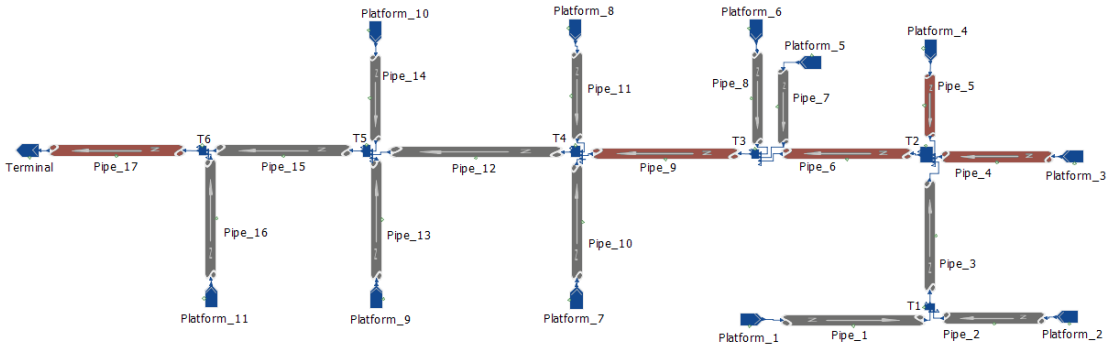

Figure 5.13: Execution output of the *Condensation* case study, 'Network' flowsheet, using the GERG-2008 EoS. The red *Pipeline single-phase gML* models (Pipe 4, Pipe 5, Pipe 6, Pipe 9 and Pipe 17) are the ones in which there is multi-phase flow. Source: gPROMS® ProcessBuilder.

Using the GERG-2008 EoS as thermodynamic model leads to the prediction of condensation in many branches of the pipeline, including the terminal. This can be seen from the flowsheet execution output because the pipelines in which the flow is multi-phase are coloured in red (as one can see from Figure 5.13). It is also possible to notice that the problem has its origin from Platform 3 and Platform 4. The condensation is then reduced by the mixing with lighter sources, and it is eventually neglected in Pipe 12. However, the mixture condenses again in Pipe 17 due to the strong pressure drop (the last pipeline of the network is the longest one). This is a clear example of how retrograde condensation works.

Then, the *Condensation* case study has been simulated using the Peng-Robinson EoS, and condensation is not predicted. However, the liquid fraction is small and the two EoSs lead to the same results in terms of physical properties (and, in particular, to the same composition at the terminal). In Figure 5.14 the phase envelope of the mixture at the terminal in the *Condensation* case study using the two different thermodynamic models is reported. The operating point in the P-T diagram is 'between' the two phase envelopes, so only the GERG-2008 EoS predicts and signals condensation through the flash calculation. This can be considered as a proof that the multi-phase flag works properly. The fact that the Peng-Robinson EoS 'fails' to predict condensation represents a real problem, and confirms that it cannot be used in accurate online flow assurance applications.

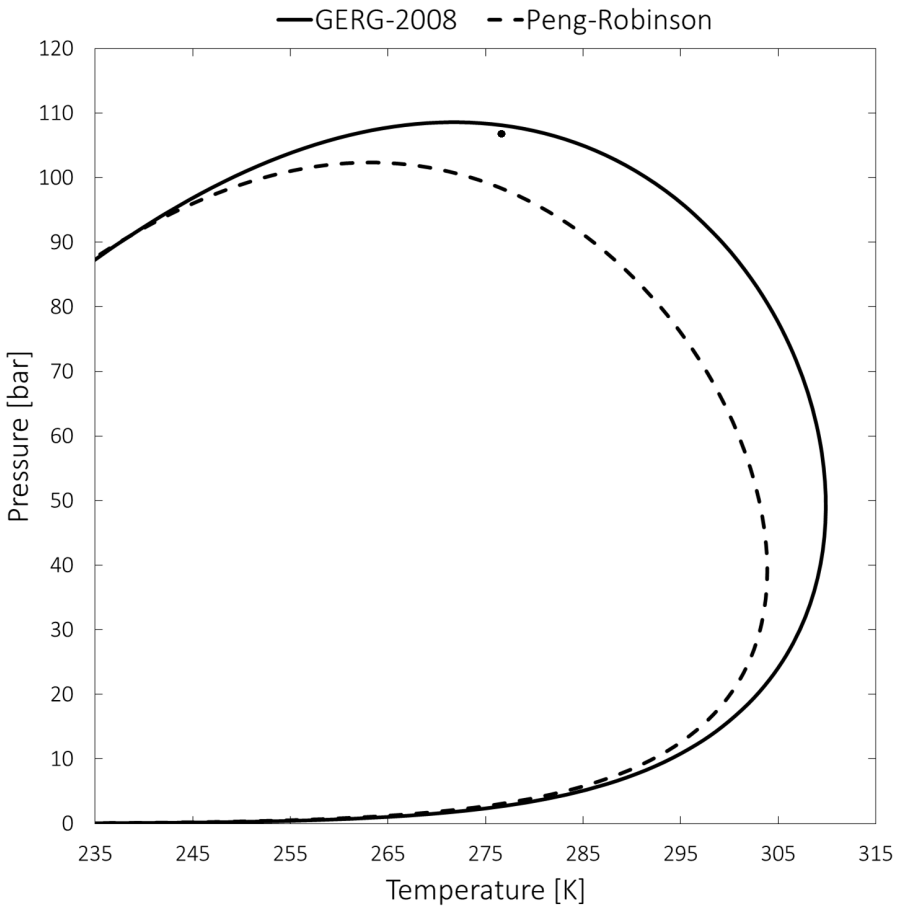

Figure 5.14: Predicted phase envelope of the mixture at the terminal in the *Condensation* case study, using the Peng-Robinson EoS and the GERG-2008 EoS. The operating conditions are depicted by the point. Source: Multiflash™.

In conclusion, the developed flow assurance application has some limits. In fact, using the Peng-Robinson EoS might lead to a failure in the prediction of condensation, which is the main threat for the network, so the most accurate GERG-2008 EoS has to be used. However, as one can see from Table 5.4, the computational time of the Step 2 simulation (the one to be run during normal operation) using the GERG-2008 EoS and discretisation Scheme A (the less detailed one) is about 1.5 hours. This would basically mean that the flow assurance application cannot be considered as properly online. In fact, the data collection is done each 30 minutes, and within that time interval it would be needed to analyse the results of the latest simulation (making 30 minutes the maximum allowed computational time for the simulation to be considered as online). Furthermore, the less detailed discretisation would lead to numerical dispersion, so to higher inaccuracy of the results (mainly in terms of compositions).

These limits can be overcome by 'mixing' the two approaches. In ProcessBuilder it is possible to modify a flowsheet in order to call different thermodynamic models when required. Due to the similarity of the results in terms of pressure, flowrate and composition using the Peng-Robinson and the GERG-2008 EoSs, the former one can be used for the whole simulation, having the positive aspect of a small computational time and making it possible to use a more detailed discretisation. Then, the GERG-2008 EoS can be called to perform an accurate flash calculation to predict the possible condensation of the gas only at the terminal, the unit which would be more affected by the formation of liquid. This task has not been done because it is not simple, and it has been considered as not part of the project.

Conclusions

Natural gas has been gaining an always larger share of the hydrocarbon market, but many of the reservoirs from which it can be extracted are located deep under the seabed. Usually, the gas coming from each offshore platform is sent to an onshore processing facility (in which it is treated) through a pipeline network. In this case, the direct control of the pipelines through measurements is not feasible, and one needs to rely on simulations to achieve an adequate *flow assurance*, which consists in maintaining the desired flow of gas in the network. For this reason, modelling properly the flow of the fluid inside the pipelines, as well as its thermodynamic properties, is paramount to predict the arrival conditions at the processing facility, thus reducing safety risk, reaching the required productivity and extending the network life.

Because of these strong motivations, it has been decided to develop an efficient flow assurance application for subsea pipeline networks, with the particular aim to predict the possible condensation of natural gas, hence ensuring a stable and safe operation. Furthermore, the application to be developed should be viable online, in order to monitor what is happening in the network and predict what could happen in the near future, all in a considerably short period of time. In fact, it is common industrial approach to collect the input data of the model with a constant frequency (30 minutes in the analysed case study) and within this time gap the results of the previous simulation have to be obtained and analysed. Therefore, to be considered as effectively online, the simulation must take at most 30 minutes.

The software used in the project was gPROMS® ProcessBuilder, developed by *Process Systems Enterprise Ltd*, which has proven adequate for the desired application. Amongst the models in the ProcessBuilder library, the *Pipeline single-phase gML* model has been chosen because it is distributed on the axial direction and it can be simulated dynamically, hence allowing to account for the continuous fluctuations of the fluid properties in each part of the network. The use of the flexible Multiflash™ package for modelling the thermodynamic properties allowed to compare different Equations of State, assessing their accuracy and their effect on dynamic simulations (mainly in terms of computational time).

Some difficulties have been found on the discretisation approach of the *Pipeline single-phase gML* model, which if combined with step changes in the input specifications led to unpredictable failure due to backflow. This problem has been by-passed modifying the flowsheet in order to simulate ramp changes instead of step changes (which bring more stability to the system and are even more realistic as properties change continuously, not discretely). However, some limits remained, such as the impossibility to simulate sources whose flowrate is zero or

a small value. This problem, which is intrinsic to the model, leads to inaccuracy. A solution to the zero flowrate problem could be to develop a feature which basically 'switches off' the sources that are not delivering fluid in the network, making them virtually disappear from the flowsheet and equations, but allowing the user to easily connect them back when they are put again into work. The problem of small flowrates is more difficult to solve as it would be needed to modify the forward discretisation approach of the *Pipeline single-phase gML* model.

Another intrinsic problem linked to the pipeline discretisation is numerical dispersion, a phenomenon which smooths the profiles and leads to the impossibility to simulate and predict sudden peaks in the measured values even when using an extremely detailed discretisation of the pipelines. It has to be specified, though, that each measured quantity might be wrong to due to measurement errors or missing information (such as the situation analysed in the case study). However, numerical dispersion is impossible to eliminate completely.

Despite all the difficulties and limits, the application showed a remarkable accuracy, basically due to its model-based nature. The *Pipeline single-phase gML* model proved adequate for the desired objectives, and its dynamic behaviour has been deeply analysed and compared with other software and models. The validation of the results performed against plant data coming from an actual network showed that the real profiles are followed by the simulations. Therefore, one can assume that, even when used as a predictive application, the model is trustworthy. Furthermore, the thermodynamic validation showed that the condensation is well predicted by the GERG-2008 EoS, while the Peng-Robinson EoS is less accurate and might fail to predict it, so the latter should not be used if the aim of the application is to predict condensation, which is usually the main threat for a natural gas pipeline network (both in terms of safety and economical operation of the plant). However, using the GERG-2008 Equation of State leads to higher computational time. Therefore, in order for the application to be considered as online, a trade-off between the accuracy (mainly linked to the discretisation of the pipeline and the thermodynamic model) and the computational time must be performed.

With the aim of considering the application as online, the computational time has been decreased by performing a wide set of sensitivity analyses and using some useful gPROMS® tools, first and foremost the *Save* and *Restore* tasks. However, it is still too high for the application to be online and have a good accuracy of the thermodynamic and physical properties. As a solution, it may be accepted that the operators do not analyse the results of the latest simulation to be run, but previous ones only. In fact, it would still be possible to act on the network in order to prevent potential hazardous situation, as the residence times in pipeline networks are usually very large. The choice whether this is tolerable or not is case-dependent.

Otherwise, the model could be simplified even more, trying not to lose much accuracy or details of interest. For example, one could customise the model at a coding level (thanks to the gPROMS® ModelBuilder structure) in order to disregard the temperature and each property linked to it (e.g. heat transfer coefficients, enthalpies and so on), thus alleviating the computational burden. This would not lead to a significant loss of accuracy because the temperature of the fluid is always constant and equal to the sea temperature, apart from the first portions of the

pipelines near the platforms (usually the extracted gas is warmer than the sea).

Another possible modification of the model could be made to use the GERG-2008 EoS only at the processing facility, where the possible condensation of the gas would lead to the biggest problems, and the Peng-Robinson EoS elsewhere. In fact, the only difference between the two thermodynamic models is visible in the calculation of the phase envelope, so on the prediction of condensation phenomena, not in the calculation of physical properties unless the flow is thoroughly multi-phase (in the case of liquid fractions close to zero there is no visible effect). Calculating the physical properties along the network with the Peng-Robinson EoS and the phase envelope only at the terminal with the GERG-2008 EoS would lead to a strong reduction of the computational time and to the possibility to use a more detailed discretisation, increasing the accuracy of the results. One needs to keep in mind that usually the operating conditions of natural gas networks exceed the validity range of the pressure of the GERG-2008 EoS, therefore even this EoS might be not perfectly accurate, thus leading to the possibility of unpredicted condensation. The only feasible approach to by-pass this problem is to use corrective factors to overestimate the phase envelope in order to obtain conservative predictions instead of non-conservative ones in terms of condensation.

A fundamental achievement of this project has been to understand how to properly run dynamic simulations in order to obtain meaningful results, which can also be used for validation and predicting purposes. The so-called *packing*, which corresponds to the operation of 'filling' a pipeline network (from a simulation point of view) with a fluid which is not affected by the unreasonable steady-state initial conditions assumption, is a key but time-consuming procedure, and it does not have to be done every time one has to run a simulation. In fact, just the last set of specifications needs to be run, thus drastically reducing the computational time, thanks to the *Save* and *Restore* tasks. Then, if the application is intended as a predictive tool, the system must be given enough time to settle to a new steady-state. This is based on the assumption that the last set of specifications is constant, which is physically untrue but the only feasible approach.

Eventually, the results of the single-phase model could be compared to the results of a multi-phase one. In fact, if a really small fraction of gas condenses, the disperse flow regime (drops of liquid dragged by the gas flowing) could not represent a threat for the processing facility. Instead, serious problems are encountered if one or more *slug* of coalescent liquid reach the facility. Slugging regime usually happens with a high fraction of liquid and under specific fluid velocities. Even if using a multi-phase simulator for an online application would surely prove impossible, as the higher number of calculations leads to an increase of the computational time, the comparison might still be useful to find information on single-phase simulation (e.g. a liquid fraction tolerated by the facility).

Bibliography

Abd Majid M.A. and Woldeyohannes A.D. (2011), Simulation model for natural gas transmission pipeline network system, *Simulation Modelling Practice and Theory*, **19**, 196-212.

Aspen Technology, Inc. (2015), *An Integrated Approach to Modeling Pipeline Hydraulics in a Gathering and Production System*, Bedford, MA (USA).

Avila S., Blanco S.T., Velasco I., Rauzy E. and Otin S. (2002), Thermodynamic Properties of Synthetic Natural Gases. 1. Dew-Point Curves of Synthetic Natural Gases and Their Mixtures with Water and Methanol. Measurement and Correlation, *Ind. Eng. Chem. Res.*, **41**, 3714-3721.

Bai Y. and Bai Q. (2005), *Subsea pipelines and risers*, Elsevier, Kidlington, Oxford (UK).

Bird R.B., Stewart W.E. and Lightfoot E.N. (2007), *Transport phenomena*, Wiley, Madison (USA).

BP P.L.C. (2016), *BP Statistical Review of World Energy*, 65^{th} Edition, London (UK).

Bratland O. (2013), *Pipe Flow 1*, Dr. Ove Bratland Flow Assurance Consulting, Bang Lamung (Thailand).

CEDIGAZ (2015), *Medium and Long Term Natural Gas Outlook 2015*, Rueil-Malmaison (France).

CEDIGAZ (2016), *Natural Gas in The World 2016*, Rueil-Malmaison (France).

CEDIGAZ (2016), *Medium and Long Term Natural Gas Outlook 2016*, Rueil-Malmaison (France).

Cengel Y.A. (2007), *Heat and Mass Transfer: A Practical Approach*, McGraw-Hill, New York, NY (USA).

Chaczykowski M. (2009), Sensitivity of pipeline gas flow model to the selection of the equation of state, *Chem. Eng. Research and Design*, **87**, 1596-1603.

Chaczykowski M. (2010), Transient flow in natural gas pipeline - The effect of pipeline thermal model, *Applied Mathematical Modelling*, **34**, 1051-1067.

Churchill S.W. and Bernstein M. (1977), A correlating equation for forced convection from gases and liquids to a circular cylinder in cross flow, *J. Heat Transfer*, **99**, 300.

Colebrook C.F. (1939), Turbulent Flow in Pipes with Particular reference to the Transition Region between the Smooth and Rough Pipe Laws, *Inst. Civ. Eng. J.*, **11**, 133-156.

Cornot-Gandolphe S., Appert O., Dickel R., Chabrelie M. and Rojey A. (2003), The challenges of further cost reductions for new supply options (pipeline, LNG, GTL), *22nd World Gas Conference*, Tokyo (Japan).

Dittus F.W. and Bölter L.M.K. (1930), Heat Transfer in Automobile Radiators of the Tubular Type, *Publications in Engineering*, **2**, 443.

Gato L.M.C. and Henriques J.C.C. (2005), Dynamic behaviour of high-pressure natural-gas flow in pipelines, *Int. J. Heat and Fluid Flow*, **26**, 817–825.

Gnielinski V. (1976), New Equations for Heat and Mass Transfer in Turbulent Pipe and Channel Flow, *Int. Chem. Eng.*, **16**, 10.

Haaland S.E. (1983), Simple and Explicit Formulas for The Friction Factor in Pipe Flow, *J. Fluids Eng.*, **105**, 89-90.

Hawley A.G. and George D.L. (2012), Use of equations of state and equation of state software packages, *American School of Gas Measurement Technology.*

Häring H.W. (2008), *Industrial gases processing*, Wiley, Munich (Germany).

Herran-Gonzalez A., De La Cruz J.M., De Andres-Toro B. and Risco-Martin J.L. (2009), Modeling and simulation of a gas distribution pipeline network, *Applied Mathematical Modelling*, **33**, 1584-1600.

Hilpert R. (1933), Heat Transfer from Cylinders, *Forsch. Geb. Ingenieurwes*, **4**, 215.

Kidnay A.J. and Parrish W.R. (2006), *Fundamentals of natural gas processing*, Taylor and Francis Group, Boca Raton, FL (USA).

Kok J.B.W. and van der Wal S.(1996), Mixing in T-junctions, *Applied Mathematical Modelling*, **20**, 232-243.

Kunz O., Klimeck R., Wagner W. and Jaeschke M. (2007), The GERG-2004 Wide-Range Equation of State for Natural Gases and Other Mixtures, *GERG Technical Monograph 15.*

Kunz O. and Wagner W. (2012), The GERG-2008 Wide-Range Equation of State for Natural Gases and Other Mixtures: An Expansion of GERG-2004, *J. Chem. Eng. Data*, **57**, 3032–3091

Liu H. (2005), *Pipeline Engineering*, Lewis Publishers, Boca Raton, FL (USA).

Matkoa D., Geigerb G. and Gregoritza W. (2000), Pipeline simulation techniques, *Mathematics and Computers in Simulation*, **52**, 211-230.

Mayeaux M. (2011), Use of Equation of State (EOS) Software, *American School of Gas Measurement Technology*.

Manohar K. and Ramroop K. (2010), A Comparison of Correlations for Heat Transfer from Inclined Pipes, *Int. J. Eng.*, **4**, 268 .

Moniz E. et al. (2011), *The Future of Natural Gas*, Massachusetts Institute of Technology, Cambridge, MA (USA).

Morch O., Nasrifar K., Bolland O., Solbraa E., Fredheim A.O. and Gjertsen L.H. (2006), Measurement and modeling of hydrocarbon dew points for five synthetic natural gas mixtures, *Fluid Phase Equilibria*, **239**, 138–145.

Nasrifar K. and Bolland O. (2006), Prediction of thermodynamic properties of natural gas mixtures using 10 equations of state including a new cubic two-constant equation of state, *J. Petr. Sci. and Eng.*, **51**, 253–266.

Pantelides C.C., Nauta M. and Matzopoulos M. (2015), Equation-oriented process modelling technology: Recent advances and current perspectives, *5th annual TRC Idemitsu workshop*, Abu Dhabi (UAE).

Peng D.Y. and Robinson D.B. (1976), A New Two-Constant Equation of State, *Industrial and Engineering Chemistry Research Fundamentals*, **15**, 59-64.

Redlich O. and Kwong J.N.S. (1949), On the Thermodynamics of Solutions. V. An Equation of State. Fugacities of Gaseous Solutions, *Chem. Rev.*, **44**, 233-244.

Schoutena J.A., Janssen-van Rosmalenb R. and Michelsa J.P.J. (2005), Condensation in gas transmission pipelines. Phase behavior of mixtures of hydrogen with natural gas, *Int. J. Hydrogen Energy*, **30**, 661-668.

Soave G. (1972), Equilibrium Constants from a Modified Redlich-Kwong Equation of State, *Chem. Eng. Sci.*, **27**, 1197-1203.

Voulgaris M. (1995), *Prediction and Verification of Hydrocarbon Liquid Drop Out of Lean Natural Gas*, Ph.D. Thesis, Delft University of Technology (Netherlands).

Voulgaris M., Peters C.J. and de Swaan Arons J. (1995), On the Retrograde Condensation Behavior of Lean Natural Gas, *Int. J. Thermophysics*, **16**, 629-642.

Voulgaris M., Peters C.J. and de Swaan Arons J. (1998), Prediction of the Condensation Behavior of Natural Gas: A Comparative Study of the Peng-Robinson and the Simplified-Perturbed-Hard-Chain Theory Equations of State, *Ind. Eng. Chem. Res.*, **37**, 1696-1706.

Wagner W. and Kretzschmar H.J. (2007), *International Steam Tables*, Springer, Berlin (Germany).

Wang X. and Economides M. (2009), *Advanced Natural Gas Engineering*, Gulf Publishing Company, Houston, TX (USA).

Wood D., Mokhatab S. and Economides M.J. (2007), Offshore Natural Gas Liquefaction Process and Development Issues, *SPEPFC*, 1-7.

Zhu G.Y., Henson M.A. and Megan L. (2001), Dynamic modeling and linear model predictive control of gas pipeline networks, *J. Process Control*, **11**, 129-148.

Acknowledgments

My deep gratitude goes to my academic tutor Prof. Bezzo for giving me the possibility to make this wonderful experience, and for the consistent technical support during the entire period of the internship, and beyond.

My thankfulness goes to PSE Managing Director Prof. Pantelides for assigning me this project, and for giving me the possibility to learn a lot about the gPROMS® platform.

I would like to express my gratitude to my supervisors Dr. Giovanoglou and Dr. Rodriguez for sharing with me their deep scientific and technical expertise. I have been honoured working with such passionate and helpful persons like you.

A special thanks goes to Head of Oil & Gas Business Unit Dr. Marriott for the wise suggestions and lessons on how to manage an engineering project also from a commercial point of view.

Finally, I would like to thank all the people at PSE (not forgetting my fellow interns), my family and my friends, always willing to support me and walk by my side on this important path of my life.